Babes-Bolyai University Cluj-Napoca
Faculty of Environmental Science and Engineering
Doctoral School of Environmental Science

GEOGENIC METHANE IN PETROLIFEROUS AND GEOTHERMAL AREAS IN ROMANIA: ORIGIN AND EMISSION TO THE ATMOSPHERE

-PhD Thesis-

Scientific coordinator:
prof. dr. Calin Baciu

PhD student:
Artur Ionescu

CLUJ-NAPOCA 2015

Acknowledgements

This thesis was realized with the support of Project ***PN-II-ID-PCE-2011-3-0537*** of the Romanian National Research Council; and by the financial support of the Sectorial Operational Program for Human Resources Development 2007-2013, co-financed by the European Social Fund, under the project ***POSDRU/159/1.5/S/133391*** - "**Doctoral and postdoctoral excellence programs for training highly qualified human resources for research in the fields of Life Sciences, Environment and Earth**".

I would like to express my gratitude to my scientific advisor **prof. dr. Calin Baciu** for the continuous support of my Ph.D. study and research, for his implication and patience, and being always available for my questions.

I would like to express my sincere thanks to my mentor **dr. Giuseppe Etiope**, who from the beginning shaped my understanding on gas geochemistry and seepages; and always had time for teaching me his thoughts and know-who on gas geochemistry. I am also deeply grateful also for offering me the internship opportunities in Rome, at the Istituto Nazionale di Geofisica e Vulcanologia (INGV), for making possible to realize valuable analysis for this research and helping me in data interpretation. I also would like to thank dr. Etiope for critical reviewing of my thesis.

I would like to acknowledge the help from: **dr. Roberto Basili** (INGV) for guiding me in the use of MapInfo software; **Pierfrancesco Burrato** for teaching me the use of GIS (INGV); **dr. Cristian Malos** for helpful comments regarding the evaluation of the geospatial analysis (UBB); and **dr. Giancarlo Ciotoli** (CNR-IGAG) for reviewing the spatial analysis chapter of my thesis; **dr. Mircea Moldovan** (UBB) for performing the radionuclide analysis on the water samples; **dr. Peter Sauer** (Indiana University) for isotopic analysis on the extracted gases

from the springs; **Dr. Michael J. Whiticar** (University of Victoria, Canada) for isotopic analysis on the Pausa sample and valuable discussions on gas geochemistry; I would like to thank also **dr. Cosma Constantin** (UBB), **dr. Dario Tedesco** (Second University of Naples); **dr. Giorgos Papatheodorou** (Patras University) for their useful comments and ideas given during my research, **dr. Pop Cristian** (UBB) for crucial contribution during field work, and **Luigi Inocennzi** (INGV) for video editing.

I would like to thank also my guidance committee for their useful comments thought out my PhD. research, namely: **dr. Nicoleta Brisan**, **dr. Dan Costin**, **dr. Dumitru Ristoiu**.

My sincere thanks goes to **dr. Laszlo Kekedy-Nagy** who in the first years of the faculty thought me the meaning of scientific research, and guided me in my first steps on becoming a researcher; and having until the present, the time and patience to discuss my newest works and results.

I specially thank **Ioana-Cristina Pistea** (UBB) and **Stavroula Kordella** (University of Patras) for supporting me during my PhD, and I also appreciate all the kind people who helped me during these years, from the staff of the *Faculty of Environmental Science and Engineering UBB* and *INGV Rome*.

The referees: **Prof. Dr. Dumitru Ristoiu**, **Dr. Giuseppe Etiope**, and **Assoc. Prof. Mihai Popa**, are greatly acknowledged for thoroughly analyzing this thesis.

Last but not the least, I would like to thank my parents, **Margit-Julianna Ionescu** and **Cornel-Constantin Ionescu** for supporting me during these years and not letting me give up.

Contents

KEY WORDS

- seeps
- spatial analysis
- flux
- molecular composition
- isotopic composition
- post-genetic alteration
- source rock
- reservoir
- radioactivity
- Petroleum Seepage System

1. INTRODUCTION AND OBJECTIVES

According to the 2013 BP Statistical Review of World Energy (BP, 2014), Romania is one of largest petroleum producers in Europe, with proved resources of oil and natural gas (0.6 thousand million barrels of oil and 0.1 trillion cubic meters of gas reserves). At least 18 petroleum systems and 8 petroleum basin provinces were assessed (Popescu 1995; Pawlewicz 2005, 2007). Due to intense tectonics, caused by the Carpathian orogenesis and post-orogenetic basin uplift (e.g., Transylvania basin), numerous hydrocarbon seepage systems (as defined by Abrams 2005) developed, making Romania one of the countries in the world with the largest numbers of surface hydrocarbon seeps. They include gas seeps, sometimes forming eternal fires, mud volcanoes, oil seeps, gas-bearing springs and solid seeps (asphalt, bitumen, and tar). Seeps are an important tool for petroleum exploration, because they can provide useful information about the source rock maturity, quality of the reservoir, and secondary alterations (Etiope et al. 2009a). Seeps are also a natural source of greenhouse gas (methane) and photochemical pollutants (ethane and propane) for the atmosphere (Etiope & Ciccioli, 2009).

This thesis entitled: "Geogenic methane in petroliferous and geothermal areas in Romania: origin and emission to the atmosphere" aims to account for a better insight into origin of gas seeping in Romania, and related geochemical processes. The data will mainly refer to methane, subordinately and in some cases to other gaseous hydrocarbons like ethane and propane.

The main objectives of the present thesis are to:

1. to assess the geographical distribution and mapping of the main hydrocarbon seeping areas with GIS;

2. to find possible relationships between seepage and geological features (fault, lithology etc.);

3. to evaluate the geological emissions to the atmosphere of methane, and the associated hydrocarbons (ethane and propane) from the main petroliferous areas, and some selected geothermal provinces in Romania;

4. to assess the origin of gas and post-genetic alterations via molecular and isotopic analysis;

5. to verify links between surface gas seepage and hydrocarbon reservoirs that may represent energy resources in the possibly future;

6. to investigate possible links between radioactivity and gas.

The first part of the thesis consists of a **theoretical** overview, summarising the fundamental notions of gas/hydrocarbon seepage, the origin of geogenic hydrocarbons (including abiotic methane) and the state of the art in Romania and worldwide. A brief chapter on the history of seepage documentation in Romania is also provided.

The second part of the thesis describes the **experimental** work: the investigated areas (including geological background), methodology and the interpretive techniques. The methodology contains the following main points: (a) site census, (b) flux measurements and estimation, (c) gas and water sampling, (d) molecular and isotopic analyses, and (e) determination of dissolved gaseous

hydrocarbons in water. Radionuclide measurements (radon and radium) were also performed in some springs to verify possible radioactivity related to seepage.

The second part of the thesis consists of the results and data interpretations. The first subchapter describes the database of seeps in Romania, named HYSED-RO, specifically developed in this thesis. Using this database, seep distribution was assessed, followed by geo-statistical evaluation of the seep occurrences. The following subchapters discuss the gas flux of the seeps. By sampling of the seep gases, molecular and isotopic compositions were determined in order to assess gas origin and secondary alteration. Two specific subchapters will focus on the relationship between seep geochemistry and reservoir geochemistry; in order to see if seeps can be used as natural "boreholes" for subsurface investigations; and for the first time the source rock maturity will be discussed using gas geochemical data for the Romanian seeps. The following subchapter discusses the dissolved methane content, and its origin, in springs. The last subchapter focuses on the possible relationship between hydrocarbons and radionuclides in the springs. Finally using all geochemical data a proposed geochemical map or model will be presented for the Romanian gases.

2. THEORETICAL PART

2.1. Notion of seepage

Gas manifestations are the surface expression of the flow of gases from a subsurface reservoir to the surface. The term "seepage" in *sensu stricto* (in petroleum geology) is the upward flow of hydrocarbon-rich gases from a subsurface reservoir. This gas is mainly composed of methane (CH_4) and other light hydrocarbons, like ethane, propane and butane. Other gases are also associated with the hydrocarbon-rich component: CO_2, N_2, He and H_2S. Geothermal and volcanic CO_2-rich gases, where hydrocarbons are at low concentration are not considered seeps: the term seep and seepage refers only to hydrocarbon-rich systems, typically in sedimentary basins. Natural CO_2 emissions increase towards volcanic/geothermal areas, while CH_4 emissions increase towards hydrocarbon prone sedimentary areas (Fig 1.).

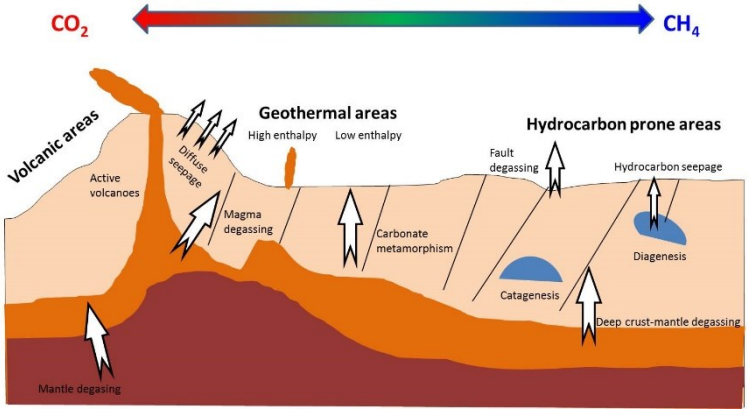

Figure 1 Sketch illustrating the various sources of geogenic methane degassing. Figure modified from Etiope & Klusman 2002 and Morner & Etiope 2002.

There are some cases where the gas composition in the seeps is composed mainly of non-hydrocarbon gases (CO_2, N_2). These manifestation can be still be considered seeps if the origin of hydrocarbons is from organic-rich sediments. A typical example is the Homorod mud volcano, a seep located in Romania where the major component is nitrogen and CH_4 is only a minor component (Etiope et al. 2011a). Another special case of seeps is that of abiotic gas, released in serpentinised ultramafic rocks (Etiope & Schoell 2014). These abiotic gas seeps have not been documented in Romania, yet.

Seeps can be classified based on the surface manifestation and fluid typology (Etiope 2015). The term macro seepage is usually defined as a visible emission of gas (in this case CH_4), which perturbs the soil condition and the surface morphology. Macro seeps can be of different types: gas seeps, oil seeps, gas-bearing springs and mud volcanoes.

Miniseepage is the invisible, diffuse exhalation of gas surrounding a macro seep, or between individual macro seeps. In a seepage area minisepage area gradually decreases towards the outer part of the seepage area (Etiope 2015).

Microseepage is the slow, continuous loss of methane and other light hydrocarbons in sedimentary basin, which contain hydrocarbon reservoirs. Microseepage is independent of the macroseepage area. In normal conditions dry soil is a sink for methane, due to methanotrophic bacterial activity (Figure 5). It means that methanothopic bacteria consume the methane flowing from the atmosphere towards the soil. In microseepage areas we have an emission of methane (and other light hydrocarbons) towards the atmosphere, which is higher than the bacterial activity of the soil. (Etiope & Klusman 2010).

2.2. Gas origin

Methane can have two origins: biotic and abiotic. Biotic methane is formed from the decomposition of organic material. The causes of the decomposition can be two: microbial (degradation by microorganisms, specifically Archaea) and thermogenic (degradation due to temperature) (Figure 6.). These two origins can be distinguished in a stable carbon vs hydrogen isotope diagram, as shown in Fig. 6.

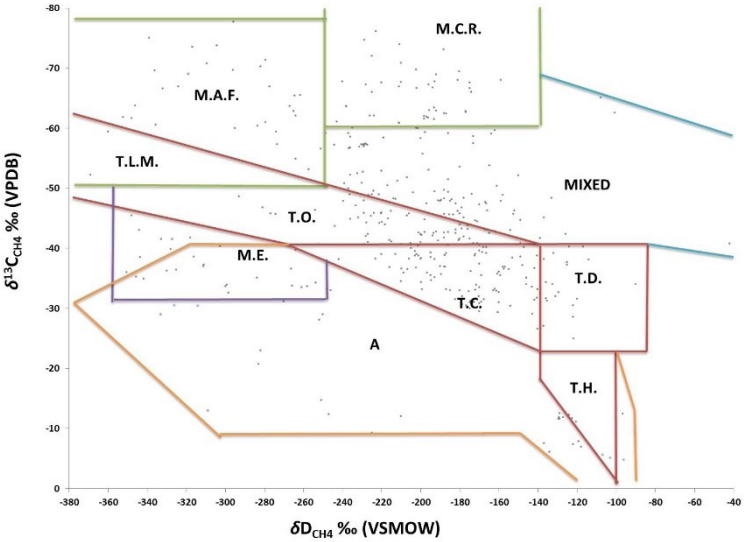

Figure 2 Carbon and hydrogen isotope diagram (Schoell-plot) modified after Etiope et al. 2013a and Etiope & Sherwood Lollar 2013; M.A.F.: microbial acetate fermentation; M.C.R.: microbial carbonate reduction; T.L.M.: thermogenic low maturity; T.O.: thermogenic with oil; T.C.: thermogenic with condensate; T.D.: dry thermogenic; T.H.: thermogenic high temperature; M.E.: microbial evaporitic; A.: abiotic; small grey dots represent data from a global seep database (GLOGOS, GasConsult Inc.).

The formation of microbial methane can be from two pathways (Whiticar 1999). The first one, acetate fermentation, follows the general reaction:

$$CH_3COOH \rightarrow CH_4 + CO_2 \quad (1.)$$

The second, carbonate reduction, has the general reaction:

$$CO_2 + 8H^+ + 8e^- \rightarrow CH_4 + 2H_2O \quad (2.)$$

Besides the two pathways described above, there is another pathway for methanogenesis, in so called hypersaline environments. Microorganisms produce methane through a series of complex pathways (McGenity 2010). In this specific environment the values of $\delta^{13}C$ ranges between -30‰ to -50‰; and $\delta^{2}H$ range between -250‰ to -350‰ (Tazaz et al. 2012).

Thermogenic methane can be of five types (see Fig. 6): thermogenic low maturity ($\delta^{13}C$ from -65‰ to -45‰, $\delta^{2}H$ from -400‰ to -250‰); thermogenic oil ($\delta^{13}C$ -45‰ to -40; $\delta^{2}H$ from -350‰ to -100‰); thermogenic condensate ($\delta^{13}C$ from -40‰ to -20‰; $\delta^{2}H$ from -250‰ to -150‰); thermogenic dry ($\delta^{13}C$ from -40‰ to -20‰, $\delta^{2}H$ from -150‰ to -100‰), and in extreme cases thermogenic high-temperature ($\delta^{13}C$ from -20‰ to -15‰ and $\delta^{2}H$ from -150‰ to -100‰).

Abiotic methane is formed due to inorganic chemical reactions that occur in different environments. Etiope & Sherwood Lollar 2013 summarized all the processes that can produce abiotic methane.

The Fischer-Tropsch Type (FTT) reactions are the most widely invoked mechanism, for abiotic methane generation, mainly in serpentinized ultramafic rocks (Etiope et al. 2011b). Serpentinization is the hydration of the olivine/pyroxene

mineral during which the serpentinite mineral and free hydrogen is formed. The free H_2 may react with CO_2 or CO to form CH_4. The FTT process may be independent from serpentinization, H_2 being produced from other sources.

These reactions are catalysed by transition metals or by platinum-group elements. A wide range of temperatures have been reported in the literature: above 200 °C (McCollom & Seewald 2007; Taran et al. 2007), but also at low temperatures below 100 °C (Thampi et al. 1987; Etiope & Ionescu 2014).

Etiope & Schoell 2014 and Etiope 2015 classified abiotic methane by the different systems in which they are formed. Based on their classification we have 5 classes: crystalline shields, volcanic-geothermal systems, alkaline rock inclusions, mid-ocean ridge (MOR) serpentinization and land-based serpentinization or MSP – Methane in land-based Serpentinized Periodites (Figure 7).

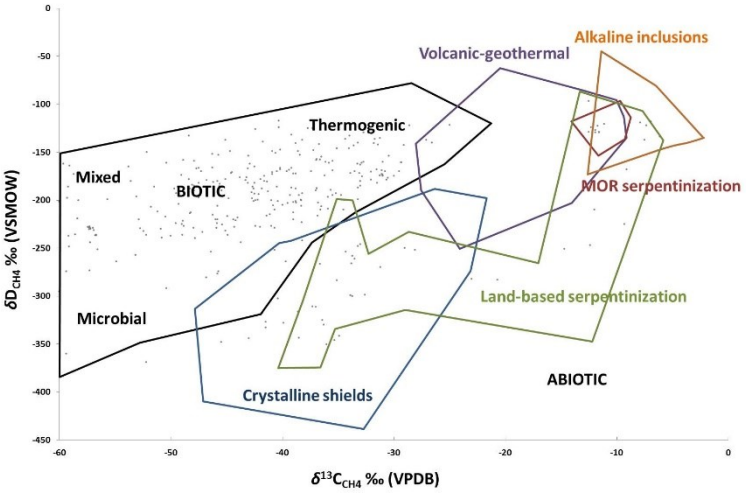

Figure 3 "Extended Schoell-plot" for biotic and abiotic methane, modified after Whiticar & Etiope 2014

The generation of methane trough abiotic processes in the ophioitic rocks, is of practical (new source of methane), but also of scientific interest. These sites are a modality to verify the conditions in which the Fisher-Tropsch type reaction, and other linked reaction pathways produce methane on other celestial bodies, like Mars (Etiope et al. 2011b).

Secondary microbial methane is formed due to biodegradation and secondary methanogenesis. This is a 3 phase reaction process. The process starts at the petroleum accumulation where anaerobic oxidation and hydrolysis removes C_{3+} molecules, producing water and carbon-dioxide. This is called the biodegradation phase. Methanogene microorganism feed on the released carbon-dioxide producing microbial methane and some residual carbon dioxide. This phase is called the secondary methanogenesis. In the final stage a mixing phase occurs between the primary thermogenic and the secondary microbial methane.

2.3. State of the art in Romania and worldwide

At national level there are quite few gas geochemical data published. A systematic approach towards a comprehensive characterization of gases was initiated after the year 2000 through collaboration between UBB-INGV. For Romania 11 isotopic and molecular data were available. Out of these 11 data only 9 are published (Baciu et al. 2008, Etiope et al. 2009b and Etiope et al. 2011a). The other two sites are unpublished data from Baciu & Etiope. Rowland et al. 2010 investigated a large number springs in the Pannonian region, and measured the dissolved hydrocarbon concentrations, and also measuring $\delta^{13}C\text{-}CH_4$ in some samples.

Based on the GLOGOS database Europe is the most abundant continent regarding seeps. This could be that European seeps are more widely documented and/or studied then other sites on other continents. In Europe the countries with the most catalogued seeps are Italy, Azerbaijan and Romania. The Romanian seep catalogued will be discussed in more detail in the following chapters.

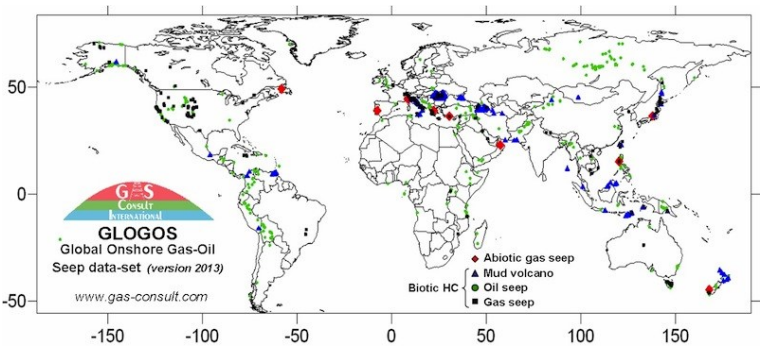

Figure 4 Map of seeps catalogued in GLOGOS, version 2013

3. EXPERIMENTAL PART

The experimental work of the thesis includes the following subchapters:

(a) census of seeps in Romania;
(b) geological background, with the description of the investigated areas
(c) methodology, which includes: flux measurements and estimation, gas and water sampling, molecular and isotopic analysis, determinations of the dissolved hydrocarbons, and radionuclide measurements in water.

In the thesis the first step was the census of the seeps in Romania. This was done first by a literature survey and then by direct field investigations/explorations. A seep database was then developed for Romania. Based on the database a selection of areas was made, for field investigation, and a total of 141 sites were investigated across Romania.

Out of these 141 sites, on 39 sites flux measurements were performed. For those sites were the flux was high also gas samples were collected (12 gas samples). Out of these 12 gas samples, molecular and isotopic analysis was performed on all samples. Out of the 141 sites, 97 water samples were collected, from which we performed 96 measurements for determining the light hydrocarbon concentrations in the water samples, 63 molecular analyses and 59 isotopic analyses were performed on the extracted gas from selected water samples, and also radionuclide activity determination was done for 95 samples.

In addition to the 141 investigated sites collaboration was started with researchers from the Department of Molecular Biology and Biotechnology, Babes-Bolyai University in order to measure the dissolved methane concentrations and origin in Transylvanian hypersaline lakes which originate from the bottom of the lakes. Preliminary results show that the dissolved gases are of microbial origin. Further studies are conducted in order to verify if the microbial methane is modern or geological, i.e. derived from seepage (Andrei et al. 2015, The ISME Journal, in press).

The following scheme summarises objectives and activities performed in the experimental work.

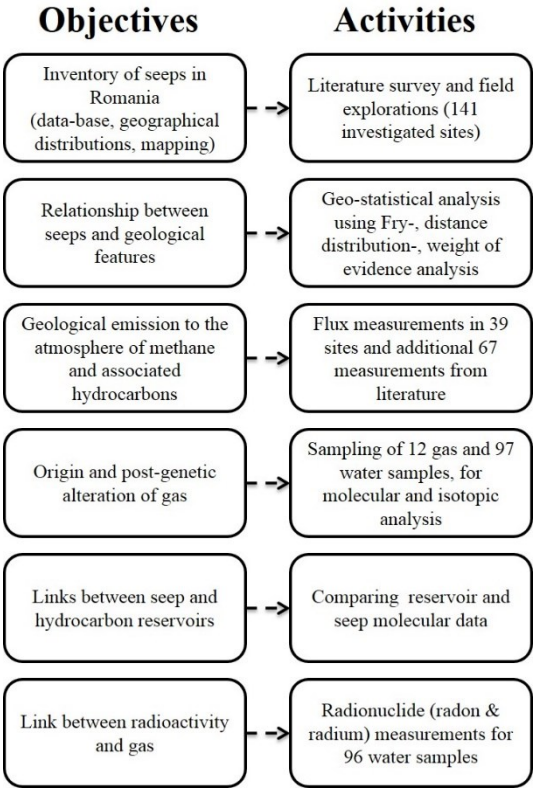

Figure 5 Box plot summarizing the objectives and activities of the thesis

3.1. Census of seep sites: development of the HYSED-RO database

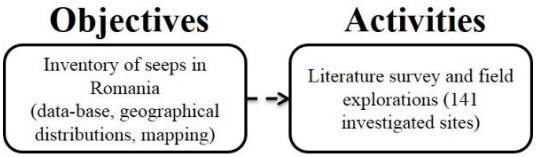

In order to have a clear view about the seeps and the number of seeps in Romania a detailed literature survey was carried out. A wide variety of scientific literature can be found, which describe based on the publishing years scientific knowledge about "seeps" or more widely termed "gas manifestations". The literature from which the seepage location were taken have a wide range of years, the oldest being from 1853 (Andrae) until the present.

Field explorations (search and visit to several seepage sites) were then conducted to check the information reported in the literature and also to look for new undocumented seeps. With all information acquired, a database was then created. The database is organized in a tabular form, with attributes. Each column, or field, of the table is an attribute. Each row, or record, of the table is uniquely linked to a seepage site. Each field representing an attribute is treated as one variable, which can be defined as: "*Char (n)*" – a text string of n characters, or "*Decimal (n,m)*" – a real number of n total digits (including decimal separator) and m decimal places. The content/structure for the main table is presented in the following table:

Table 1 Structure of the HYSED-RO database

Nr.	Field	Variable	Description
1.	ID	Char (n)	Identification number for each individual seep.
2.	Name	Char (n)	The name of the seep or the name of the nearest settlement.
3.	Province	Char (n)	Refers to one of the five petroleum provinces occurring in Romania, in which seeps are found, as defined by the USGS. The four petroleum provinces are: *Carpathian-Balkanian Basin Province*, *North Carpathian Basin Province, Pannonian Basin Province*, *Transylvanian Basin Province* and *Ukrainian Shield Basin Province.*
4.	Type	Char (n)	Refers to the type of manifestation: *gas seeps, mud volcanoes, oil seeps, gas-bearing springs, solid seeps* and *unknown manifestations*.
5.	Status	Char (n)	Refers to the activity of the seep, which can be: *active*, *inactive* or *uncertain*.
6.	Latitude	Dec (n,m)	Refers to the GPS location, in decimal degrees.
7.	Longitude	Dec (n,m)	

Items (1) to (7) are available for all seeps. If one item is missing the entry in the database does not exist. The ID (identification number) is a unique code given for each individual seep in the database. In the database the ID is composed of 11 characters, in the following format:

$$CC - PPP - TTT - \#\#\# \quad (7.)$$

where:

- CC is a two-character ISO 3166-1 code for names of officially recognized countries (http://www.iso.org/iso/country_codes/iso_3166_code_lists.htm)
- PPP is the abbreviation of petroleum provinces identified by the USGS (United States Geological Survey) that can be found on the territory of the country: Carpathian-Balkanian Basin Province (*CBB*), Pannonian Basin Province (*PBP*), Transylvanian Basin Province (*TBP*), Ukrainian Shield Basin Province (*USB*) and the North Carpathian Basin Province (NCB);
- TTT is the type of manifestation gas seep – *GAS*, mud volcano – *MUD*, oil seep – *OIL*, gas-bearing spring – *SPR*, solid seep – SOL and unknown manifestation – *UNK;*
- ### is an alphanumerical number ranging from 001 to 999.

As mentioned earlier (chap. Notion of seepage), we added only those locations that can be considered seep in *sensu stricto*.

3.2. Geological settings and investigated areas

3.2.1. General geological setting

In this part a short overview of the main geological and structural features is presented, together with the hydrocarbon potential.

The Romanian territory overlaps a large portion of the Carpathian Orogene and parts of the East European, Scythian, and Moesian Platforms (Sandulescu, 1984). The conventional hydrocarbon resources are mainly located in six areas (Krezsek 2011): External Carpathians (1), Getic Basin (2), Foreland of the Carpathians and the undeformed parts of the East European Margin (3), basins developed on top of the Inner Carpathians, Pannonian Basin (4), Transylvanian Basin (5) and the Black Sea (6). According to Popescu (1995), about 30% of the Romanian territory is covered by 18 petroleum systems, ranging from Palaeozoic to Pliocene in age.

Relatively little information on the Romanian unconventional hydrocarbon plays is available at this time. At a worldwide scale, the main areas with shale gas potential are assessed in a report released by EIA (2013). The Carpathian Foreland and the Moesian Platform are the main units with significant prospective of unconventional oil and gas resources. Exploration works are currently conducted on the Carpathian Foreland.

The US Geological Survey has defined several Total Petroleum Systems (TPS) covering the hydrocarbon-bearing areas in Romania (Pawlewicz 2007), mainly:

- the Moesian Platform Composite TPS,
- the Dysodile Schist – Tertiary TPS
- the Transylvanian Composite TPS, and
- part of the Greater Hungarian Plane Neogene TPS (Dolton 2006).

In a broader sense, the first two systems belong to the Carpathian Balkanian Basin Province (Pawlewicz 2007), extending in northern Bulgaria and southern and eastern Romania.

Figure 11 presents the general geological map of Romania, with the major faults and lithological units.

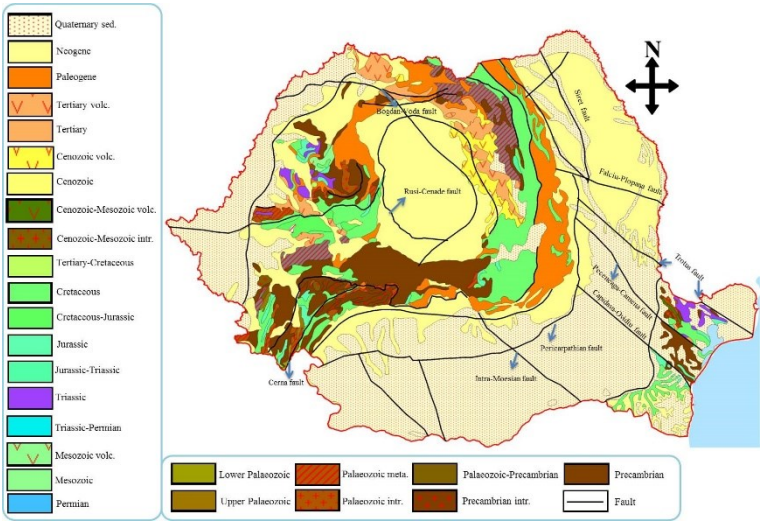

Figure 6 General geological map of Romania, showing the main faults. Modified after: USGS 2002, Filipescu & Huma 1979, Knapp et al. 2005, Molin et al. 2012 and Krezsek et al. 2010

3.2.2. Investigated areas

In the present study a total of 141 sites where investigated from the following areas: from the Transylvanian Basin 34 sites, Paleogene Flysch 29 sites, Herculane tectonic graben 22 sites, Carpathian Foredeep 41 sites, the Pannonian Basin 12 sites and finally the Moldavian Platform 3 sites.

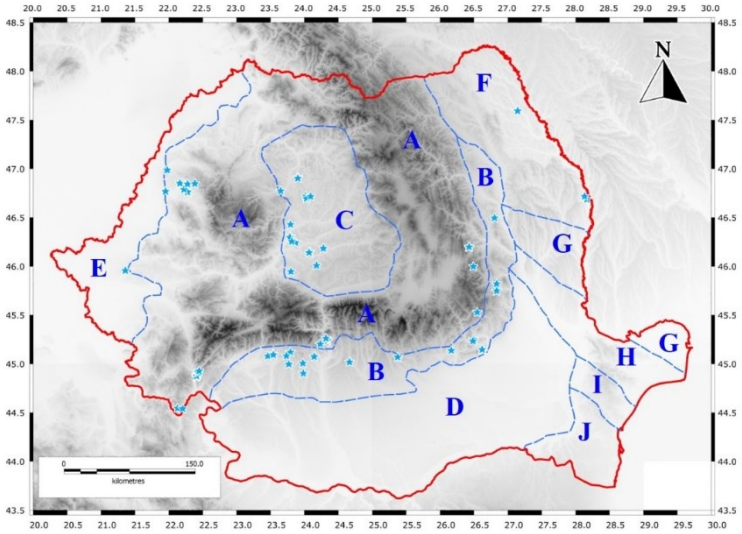

Figure 7 Map showing the investigated sites during 2012-2014. Letters indicate the petroleum systems of Romania modified after Krezsek 2011: A – Carpathian Massif, B – Carpathian Foredeep, C – Transylvanian Basin, D – Moesian Platform, E – Eastern Pannonian Basin, F – Moldavian Patform, G – Scynthian Platform, H – North-Dobrogean Orogen, I – Central-Dobrogean Massif, J – South-Dobrogean Platform

3.3. Methodology and field work

3.3.1. Flux measurements and estimations

3.3.1.1. Direct measurements

Methane and carbon dioxide fluxes were measured at 39 sites using the closed chamber method. The Instrumental package (West System, Pontedera, Italy) is equipped with a CH_4 and CO_2 sensors and wireless data communication to a palm-top computer. The fluxes are automatically calculated using a linear regression of the gas concentration build-up in the chamber. The methane sensor includes semiconductor (range 0-2000 ppmv; lower detection limit of 1 ppmv; resolution 1 ppmv), catalytic (range 2000 ppmv – 3% v/v) and thermal conductivity (range 3% - 100 % v/v) detectors. The CO_2 detector is a double beam infrared sensor (LI-COR, with a range of 0 – 20000 ppmv, accuracy of 2% and a repeatability of ±5 ppmv) (Popita et al. 2014). The accumulation chamber was equipped with a Nafion drying tube (Perma Pure, USA) for humidity removal. In the case of bubbling pools a funnel was used instead of the accumulation chamber. In order to remove the excess humidity of the free gas on the bubbling springs a Drierite drying unit was added before the West Systems instrumentation package. Also if needed, a floating collar can be attached to the accumulation chamber.

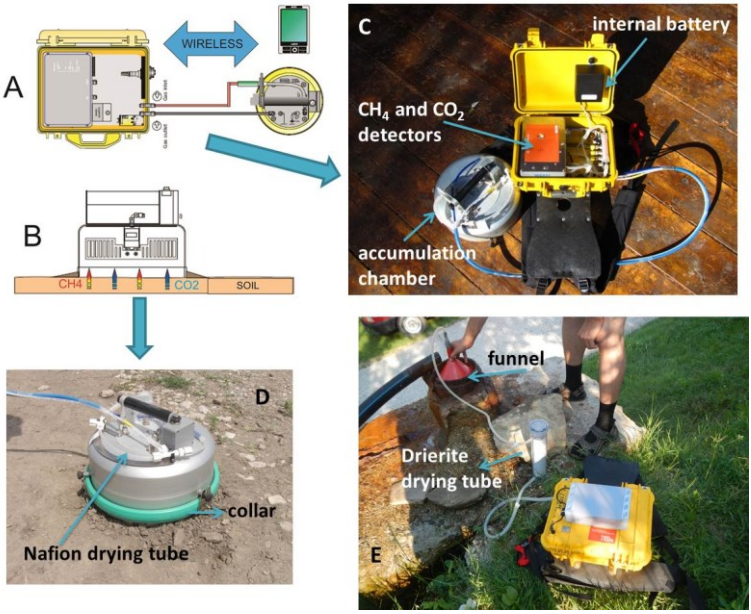

Figure 8 Methodology of flux measurements: A – sketch of the West Systems fluxmeter; B – sketch of the deployments of the accumulation chamber on soil; C – individual parts of the fluxmeter; D – close up of the accumulation chamber during measurement; E – measuring springs using funnel and a Drierite drying tube.

The gas flux for CH_4 and CO_2 was calculated using the linear regression method, if the rate of increase of the gas concentration in the chamber is constant (F):

$$F = \frac{V_c}{A_c} * \frac{c_2 - c_1}{t_2 - t_1} \qquad (8.)$$

where V_c is the volume of the chamber, A_c is the footprint area of the chamber, c_1 and c_2 are the gas concentrations at time t_1 and t_2 respectively.

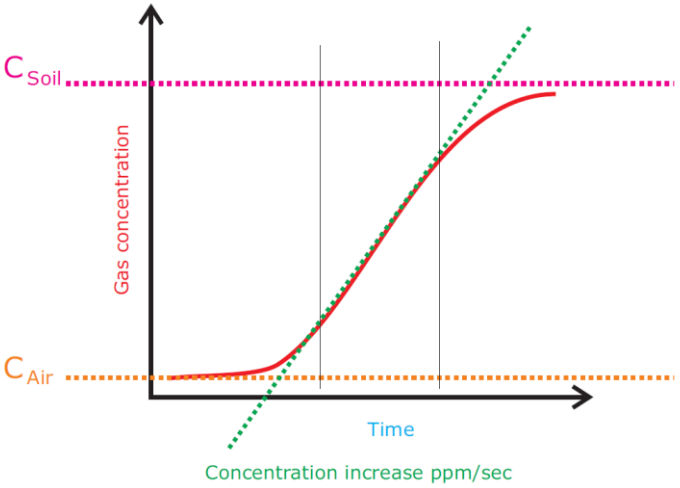

Figure 9 Method for selecting the optimum slope (concentration increase ppm/sec) for the flux individual flux measurements.

The flux is calculated using the closed chamber technique via the following formula:

$$F = \frac{86400 * P * V}{10^6 * R * A * (T+237)} * M * 1000 * a \qquad (9.)$$

where, F is the flux of methane or carbon dioxide [mg·m^{-2}·day^{-1} for CH_4 and g·m^{-2}·day^{-1} for CO_2]; P is the barometric pressure [mBar]; R is the universal gas constant, 0.08314510 [(bar·L)/K]/mol; V is the volume of the accumulation chamber; A is the area of the accumulation chamber; T is the temperature in K; a is the angular coefficient [ppm/sec] or slope, and M is the molecular weight of the gas.

The total emission of the seepage area is estimated by the sum of the emission from the different zones and the individual vents. The two interpolation methods were performed by using the Surfer 10 software package developed by GoldenSoftware Ltd.

For some seeps we also know the molecular concentrations of ethane and propane. Based on this, if we assume that the concentration of the two gases does not change considerably throughout the seepage area, we can calculate the flux and total emission for ethane and propane. In the case of the ethane and propane, the flux (F_n) is calculated using the following equation:

$$F_n = \frac{C_{CH_4}}{C_n} * F_{CH_4} * moll.corr_n \qquad (10.)$$

where, C_{CH4} is the concentration of methane, C_n the concentration of ethane or propane, F_{CH4} is the flux of methane at the sampling point, and "mol.corr." is the molecular correction (for ethane 1.875, respectively 2.75 for propane). This equation can be used only if we presume that the concentration of either gas does not change significantly in the measured area (Etiope & Ciccioli 2009).

3.3.1.2. *Indirect measurement*

In case of burning seeps that cannot be extinguished or bubbling pools that are inaccessible with the instrumentation, we can use indirect measurements for evaluating the gas emissions. For burning seeps it is possible to estimate the order of magnitude of the gas flux by visual examination of the flames (Hosgormez et al. 2008, Etiope et al. 2011b). The method developed by Delichathsios 1990, considers that flame size is proportional to the gas flow (g/s), via the following equation:

$$F = Q/H_c \qquad (11.)$$

where F = flux, Q = the heat release rate (kW or kJ/s), H_c is the heat of the combustion (kJ/g). Q can be calculated with the following relation:

$$Q = (Z_f/0.052)^{3/2} * P \quad (12.)$$

where Z_f is the flame height, and P is the flame perimeter ($P = 4D$, d is the estimated base of the flame). The method has some uncertainties when the flame is turbulent, or it is affected by cross winds. Even if there is an uncertainty during the visuals examination of the flames, due to external conditions, the method can give us an estimate on the order of magnitude of the flux. For example in order to have an output of 15 kg/day a flame must be approximately 50 cm high and having a diameter above 10 cm.

For bubbling pools (with bubble trains or plumes) the flux can be estimated by observing bubble size and bursting frequency. The method was developed by Etiope and published in 2004 (Etiope et al. 2004). The original model published by Etiope et al. 2004 had a bubble diameter range from 1 to 30 cm, and output from 1 to 10 tons/year and a frequency of 0.01 until 2 bubbles per second. In order to have a wider range we created several plots with higher ranges.

We started from the following assumption: let's have a 1 cm diameter bubble with a frequency of 1 bubble/second. We know that the bubble volume (cm^3) is derived from:

$$V_{bub} = (D^3 * \pi)/6 \quad (18.)$$

In order to have the volume in L we divide V_{bub} with 1000. If we know that 1 mole of methane is 16 g, and 1 mole of methane has a volume of 22.4 l. So 22.4 L

has a 16 g of pure methane. If we know the volume of the bubble we can calculate the gram of methane/second:

$$F = (V_{bub} * 16)/22.4 \quad (19.)$$

If we have a frequency lower or higher than 1 bubble per second we multiply or divide the frequency accordingly.

3.3.2. Molecular and isotopic analysis

Five gas samples (Andreiasu-, Lopatari-, Raiuti-, Lepsa eternal flames and Andreiasu mud volcano) were analyzed, at Isothech Labs Inc. (Illionois, USA) for molecular composition (C_1-C_6 alkanes, ethylene, H_2, CO_2, N_2, H_2S, He and Ar) by gas chromatography (Shimadzu 2010 TCD-FID, accuracy 2%), and for isotopic composition of C_1-C_3 and CO_2 by Isotope Ratio Mass Spectrometry (IRMS, Finnigan Delta Plus XL, precision ±0.1‰ ^{13}C, ±2‰ for ^{2}H and ±0.3‰ for ^{15}N).

The other seven gas samples were analysed at INGV Rome. The molecular analysis was performed with: a Fourier Transform InfraRed spectrometer (FTIR Gasmet DX-4030, Gasmet, Finland) with a standard spectra library for rapid, semi-quantitative (with accuracy from 10-20%) and simultaneous determination of 14 gases (CH_4, CO_2, H_2O, CO, C_2H_6, C_2H_4, C_3H_8, n-C_4H_{10}, i-C_4H_{10}, n-C_5H_{12}, i-C_5H_{12}, C_6H_6, SO_2 and COS) with typical detection limits of; and also with a West System instrument packed (WestSystems ver.2), equipped with a TDLAS for CH_4 (tuneable diode laser absorption spectroscopy; range 0.1 ppmv – 100%v/v; repeatability, 0.1

ppmv) and a double-beam infrared CO_2 sensor (IR-Licor; range 0–20000 ppmv with an accuracy of 2% and a repeatability of ±5 ppmv).

For isotopic analysis ~50-100 mL of gas were collected in a Teflon bag and analysed within a few minutes, using a Cavity Ring-Down Spectroscopy (CRDS) methane carbon analyser (Picarro G2112-I, Picarro Inc., California; precision <0.7% at 1.8 ppmv CH_4 5 min., 1σ, and <0.4% at 20 ppmv CH_4, 5 min., 1σ). The detector was equipped with a soda lime pallet tub, for extracting CO_2 content, which can affect the measurements. A semiconductor detector (Hydrotech Huberg, Italy; detection limit of 5 ppmv) was used to detect H_2 in the gas samples that were analysed and INGV Rome.

Before each set of samples a standard was injected into the analyser (Isometric Instruments H-iso1, 2500 ppmv, $\delta^{13}C$ = -23.9‰ ± 0.2‰). A diluted sample was added into a sampling bag. For a 12 ppm sample of the standard the CRDS measured a value of $\delta^{13}C$ = -24.8‰. Figure 42 illustrates the analysis procedure.

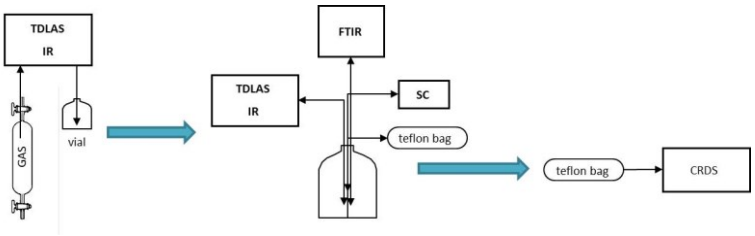

Figure 10Work-flow of the gas analysis from gas samples, performed at INGV Rome. TDLAS – tunable diode laser absorption spectroscopy; IR – infrared detector; FTIR - Fourier Transform InfraRed spectrometer; SC – semi-conductor; CRDS - Cavity Ring-Down Spectroscopy

A duplicate sample from Pausa spring was sent to the Biogeochemistry Facility (School of Earth & Ocean Sciences, Victoria University, Canada) for isotopic analysis ($\delta^{13}C_1$, $\delta^{13}C_2$, $\delta^{13}C_{CO2}$). The analyses were performed using Mat 253 mass spectrometer, with a Conflo IV interface,

The seven gas samples were extracted from water samples, and were sent to Indiana University for $\delta D\text{-}CH_4$ measurements, using a ThermoFinnigan Delta Plus XP ±4‰, equipped with GCC interface IU designed methane pre-concentrator (Miller et al. 2002). Figure 46 illustrates the analysis procedure used.

For 3 samples also the H_2S concentration was determined using a RAE pump and colorimetric tubes.

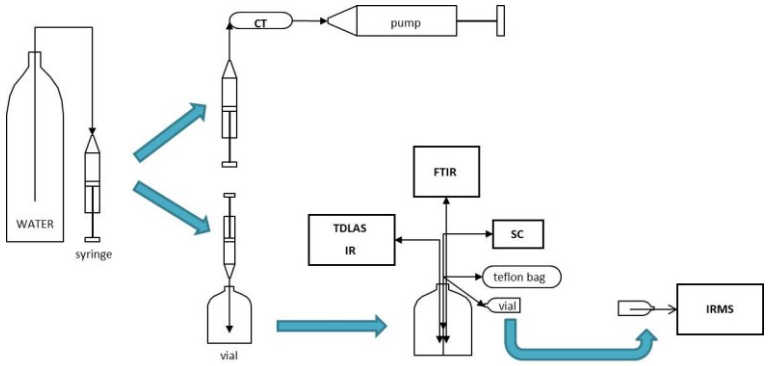

Figure 11 Work flow of the gas analysis of dissolved gases from water samples, INGV Rome. CT – colorimetric tube, IRMS – Isotope Ratio Mass Spectrometry.

For calculating the dissolved concentration of hydrocarbons from the water samples we use the following equation:

$$C_L = C_G * \left(\beta + \frac{V_G}{V_L}\right) - C_A * \left(\frac{V_G}{V_L}\right) \qquad (15.)$$

where C_L is the dissolved gas concentration in mL/L; C_G is the concentration of gas in mL/L (if we have the concentration in ppmv we divide it with 1000); β is the Bunsen coefficient (L/L); V_G is the volume of the gas (headspace) (L); V_L is the volume of the water (L); C_A is the atmospheric concentration (mL/L). The Bunsen coefficient for methane is 0.025, for ethane 0.052 and for propane 0.039. The atmospheric concentration for methane is 2 ppm. After we have the concentration in mL/L, we transform in order to have µg/L, via the following equation:

$$C = \frac{C_L * 106 * m.w.}{24500} \qquad (16.)$$

where *m.w.* is the molecular weight of the gas.

3.3.3. Radionuclide measurements in water samples

In this study we only analysed radon (radon-222) and radium (radium-226) from the waters samples. For the measurements of the radon in the water samples we used the LUK-VR system which consist a LUK-3C device and a scrubber. The device works on the scintillation method using Lucas-cells. The method works on the following principle that the water having a certain radon concentration is placed in the scrubber, leaving a known headspace above the water. After a certain period of time, equilibrium is established between the concentration of radon in the water and the air volume above it, so that the total radon concentration is divided between the two (Cosma et al. 2008). The relationship can be written as:

$$\alpha = \left(\frac{A_w}{A}\right) * \left(\frac{V_a}{V}\right) \qquad (19.)$$

where α is the coefficient of solubility of radon-222; A_w is the activity of radon in the water; A is the total activity; V_a is the volume of the headspace and V is the total volume of the scrubber. By substituting A_w with $A - A_a$, we get the following relationship:

$$Aa = \frac{A}{\alpha} * \left\{ \frac{\left[\frac{V_a}{V_w}\right]}{[1+V_a(\alpha * V_w)]} \right\} \quad (20.)$$

The measuring procedure is the following: 300 ml of water sample is put in the scrubber, which is closed tightly and shaken well for about 1 minute. The headspace is then transferred in the Lucas cell. The transfer process is based on using a Janet syringe with a volume of 150 ml of distilled water, into the water sample in the scrubber; thereby the increasing water volume pushes out the volume of air above it, in order to fill the Lucas cell. The Lucas cell is prior of this is evacuated of air using a pump. The solubility coefficient of radon is affected by the temperature of the water, via the following relationship:

$$\alpha = 0.105 + 0.405 * e^{-0.0502T} \quad (21.)$$

where T is the water temperature. The waters where analyzed within a maximum of 12 hours from the sampling time. Correction of the sampling time is done using the following equation:

$$A_{(0)} = A * e^{\lambda * \Delta t} \quad (22.)$$

where $A_{(0)}$ represents the initial activity of radon (at the time of the sampling), A is the measured activity, Δt is the elapsed time between the sampling and the

measurement; $\lambda = ln2/T$ is the radioactive constant of radon (T = 3.82 days, half-life of radon). Based on the counts that the detector measures via the scintillation effect of the Lucas cell, the activity is equal to:

$$A\left(\frac{Bg}{L}\right) = 9.85 * N\left(\frac{c}{s}\right) \quad (23.)$$

Before each measurement the Lucas cell is replaced from the system and the background activity is measured. The detection limit is 0.2 Bq/L (Cosma et al. 2008).

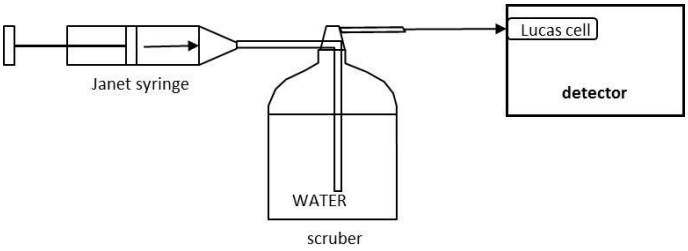

Figure 12 Sketch of measuring radionuclide activity, from water samples.

The radon and radium measurements are linked. The radon activity is equal to the radium activity, after a period of 30 days, when radium can be considered in secular equilibrium with radon. This happens due to radium-226 α-decays into radon-222 and an alpha-particle. For radium concentration measurements the same method was applied, after a period 30 days after sampling (Moldovan et al. 2009).

3.4. Results

The experimental work described so far is summarized in figure 54, as a flowchart. As we can see we have 6 major packages that were the direct results of the PhD thesis. The first major package is the direct results of the literature survey, from which the HYSED-RO database was created. The HYSED-RO (Hydrocarbon SEppage Database – Romania) is a repository of hydrocarbon seepages in Romania. Based on the HYSED-RO database the seep distribution was evaluated based on GIS and geo-statistical methods, which is the second package. The third and fourth major packages were the quantification of the flux to the atmosphere the evaluation of gas origin. Based on these two results the post-genetic alterations were described based on gas geochemistry. The sixth package contains the description of the radionuclide activity and link with gas geochemistry. Combining all the packages, we tried to create a preliminary gas geochemical model for Romania.

All the raw data that were used in creating the different packages can be divided in two parts: the first is the field investigations carried out in the period of the PhD thesis, the second being gas geochemical data already published by different authors and also unpublished data by Baciu and Etiope.

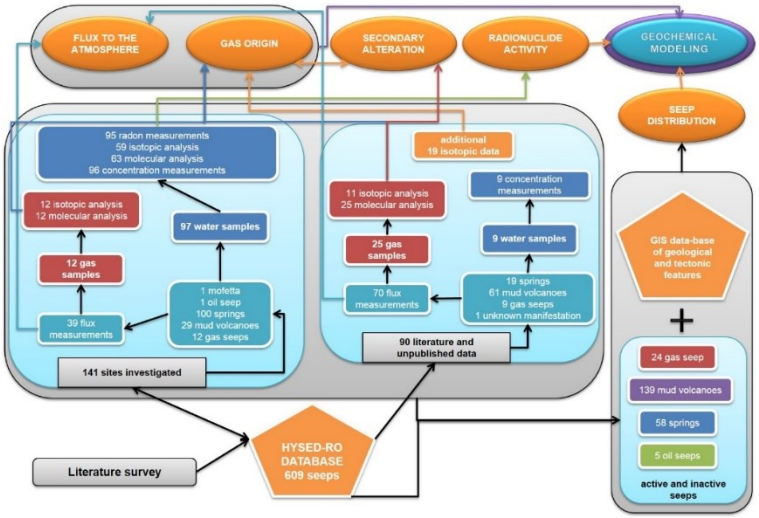

Figure 13 Flow chart describing the research data and the link between each result package

3.4.1. The database

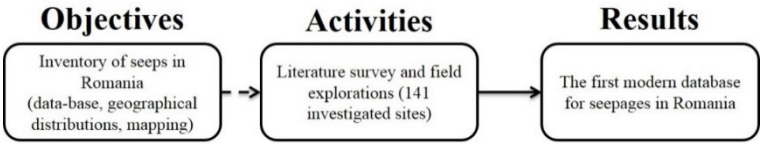

The first catalogue of gas and petroleum manifestations in Romania was creted by Tonescu in 1953. The catalogue contained a total of 1000 points with seepages. It is worth mentioning that in Tonescu's catalogue 73% represents "oil springs", while the rest of 27% are gas emanations including mud volcanoes (Paraschiv 1984). Although the database would be of high importance, for geochemical exploration, it got lost due to unknown reasons (Baciu personal communication). Paraschiv 1984 describe the seepage distribution by the state-of-

the-art for that period (based on the Tonescu database), and also created a synthesis map of the hydrocarbon occurrences.

The Hydrocarbon Seep Database for Romania (HYSED-RO) is a repository of geogenic hydrocarbon seepages, for the Romanian territory. The Database highlights the research work from the past 15 years, and the observations of hydrocarbon related gas manifestations of the past century.

The HYSED-RO is the first country wide database for Romania, which supplies a fresh and unified view on methane seepage sites for the whole territory of Romania. The database is the first attempt to catalogue all hydrocarbon seeps in Romania, not only there locations but also, the data concerning these manifestations: molecular and isotopic analysis (gas, water), flux data, water analysis, GPS locations, references for individual seeps etc. (Ionescu et al. 2014).

The database was planned and designed in such a way, that it can be an interface between data providers (geochemist, environmental scientist) and the users from different research areas: environmental sciences, geology, geochemistry, hydrocarbon exploration and other Earth scientist.

The data-base contains 609 seeps, distinguished in the following six categories: gas seeps, mud volcanoes, gas-bearing springs, oil seeps, solid seeps and unknown manifestations.

The database contains all the locations reported in the scientific literature, but also on personal observation. From the HYSED-RO database, 51% of seeps are

mud volcanoes, 21% are gas-bearing seeps, 11% are oil seeps, 10% are gas seeps, 4% solid seeps and the rest of 4% unknown manifestations. The following table summarizes the statistics of the database, based on the activity of the seeps and reference type (investigated or literature data).

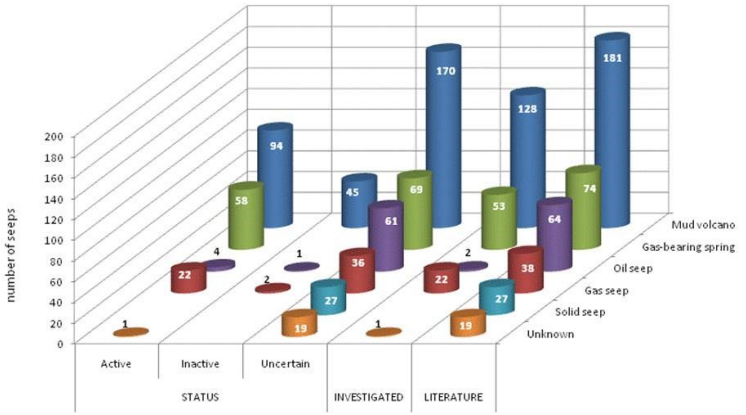

Figure 14 Column chart showing the number of the different seep types, activity and investigation status.

3.4.2. Seep distribution and mapping

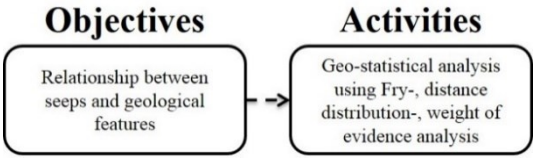

In order to understand the occurrences of the seeps we added the HYSED-RO in a GIS interface, using MapInfo Professional Ver. 11, for evaluating the geological framework of appearances. The layers used in the evaluation of seep

occurrences are: geological map of Romania, a DEM of Romania, hydrocarbon systems of Romania, geothermal map of Romania, petroleum reservoirs.

Seeps have been stored in the GIS geo-database and categorized according to their type and status. The layers were created from existing geological data and maps. The maps were digitized and geo-referenced in WGS84 Latitude and Longitude projection.

A geodatabase has been constructed in a GIS environment to store, manage and analyse all geographical data. In particular, the following base layers are included:

- geology: Generalized Geology of Europe (USGS 2002)
- tectonics: Faults of Europe (USGS 2002), Filipescu and Huma 1979, Knapp et al. 2005, Molin et al. 2012 and Krezsek et al. 2010,
- heat flow: Demetrescu 1982, Demetrescu & Polonic 1989, Demetrescu & Andreescu 1994, Andreescu et al. 1989,
- petroleum reservoirs: Beca & Prodan 1981 and Borcos et al. 1983,
- petroleum systems: Krezsek 2011, Popescu 1995, Geological provinces of Europe (USGS 2002)

3.4.2.1. The Transylvanian Basin

The main border between the Carpathian Orogen and the Transylvanian basin consist in the West by the so-called Rusi-Cenade fault, and in the East by the main Transylvanian Fault (which starts from the Southern part of the basin and continues NE, then NW meeting with the Bodgan-Voda fault in the northern part of the basin). In the Basin the average geothermal gradient ranges from the centre of the basin until the outer rim concentrically, from 30 mW/m^2 to 60 mW/m^2.

Among the 609 inventoried seeps of Romania, 40% occur in the Transylvanian basin (244 seeps); they include 157 mud volcanoes, 38 gas-bearing springs and 27 gas seeps. Based on the historical literature some oil and solid seeps also occur in the region (early 19th century). Popescu (1995) proposed that in the basin the deeper thermogenic reservoir system could be found in the western part of the basin. Although it is a speculative system, first proposed by Popescu, one might consider having this system based on the historical descriptions of oil and asphalt seep. Among the 244 catalogued seeps 88 are active, 24 are inactive and rest (132) are uncertain. Gas seeps are found mainly in the central part of the basin, and their distribution is elongated in a SW-NE direction. Mud volcanoes can be found all over the basin mainly clustered in the centre or along the borders of the reservoirs. Oil and asphalt seeps, based on the old scientific literature, are found mainly in the south-eastern part of the basin.

3.4.2.2. Carpathian Orogen

The geothermal gradient in the Carpathian Orogen is quite complex. Geographically from the Transylvanian Basin until the Neogene Volcanism the gradient rises up to a maximum of about 120 mW/m^2 in the central part of the volcanic area, then slowly decreases towards 40 mW/m^2 towards the east. This area is well known for its high CO_2 content in gases, mofettas, carbonated mineral waters, etc. In the Southern Carpathians, from the border of the southern part of the Transylvanian basin towards the Foredeep, the geothermal gradient shows a small increase from 60 up to 70 mW/m^2, and then again decreasing to 40 mW/m^2 towards the east. In the Southern Carpathians two geothermal areas can be distinguished: the first occurs in the Olt-valley sector (Caciulata-Calimanesti and Olanesti), and the second at Baile Herculane. The Herculane geothermal area is a special case because the high geothermal gradient is due to a granitic intrusion hosted in the area, and enriched in uranium minerals. The gas-bearing springs in this area are located parallel to the Cerna-fault that cuts the granitic intrusion (Wynn et al. 2010). In the north-western sector of the area the geothermal gradient is quite constant ranging between 60-70 mW/m^2, whereas in the south-western area the gradient values increase towards the Pannonian Basin from 60 to 90 mW/m^2.

Among the catalogued seeps, in the Carpathian Orogen (Paleogene Flysch and Herculane tectonic graben) 27.8% (169) of the seeps occur in the orogen. These seeps consist of 58 gas-bearing springs, 36 oil seeps, 29 mud volcanoes, 19 gas seeps, further 19 seeps are probably asphalt pits, and 8 are unknown manifestations. Based on their status 39 seeps are active, 3 inactive and 127 are uncertain

manifestations. The gas and oil seeps are mainly located in the Eastern Carpathians, whereas the mud volcanoes are clustered in the northern sector of the Apuseni Mountains (together with asphalt-pits) and Eastern Carpathians. Gas-bearing springs with methane content occurs in the Neogene volcanism, in the geothermal areas of Herculane and in the Olt-valley, as well as in the reservoirs found in the flysch-part of the Eastern Carpathians. The oil seeps and asphalt pits are located between the Apuseni Mountains and the northern part of the Eastern Carpathian; and in the outer rim of the Eastern Carpathians.

The seeps found in the Foredeep represent 17.2% (105) of the total catalogued seeps. The seeps are mainly mud volcanoes (38) and gas-bearing springs (28). These seeps include 25 active, 5 inactive and 75 are uncertain. Although in this area only 25 active seeps occur, this is one of the highest emitting areas, based on its greenhouse gas output (Baciu et al. 2007, Frunzeti et al. 2012a).

3.4.2.3. *The Moldavian and Scythian Platforms*

The East European Platform is represented in Romania only by its south-western part, the Moldavian Platform. Few conventional hydrocarbon deposits have been identified, and are confined to the Miocene formations. A limited portion of the Scythian Platform is located on the Romanian territory, between the Moesian and the East European Platforms. Hydrocarbon deposits are located in the Paleozoic and Neogene formations. Exploration works for unconventional gas are planned, mainly focusing on the Silurian sediments.

The geothermal gradient of the two platforms is about 40 mW/m^2. Only a slight increase can be found near the eastern margin of 50-60 mW/m^2. In the two

platforms, no major oil/gas reservoirs occur. Only one-two small reservoirs are located near the Carpathian Foredeep.

The seeps found in this area represent the 13.8% of the total database. They are mainly composed of mud volcanoes (80), of which 24 are active, 16 inactive and 40 uncertain. The rest of the seeps consist of 1 uncertain gas seep, and 3 springs (1 active and 2 uncertain).

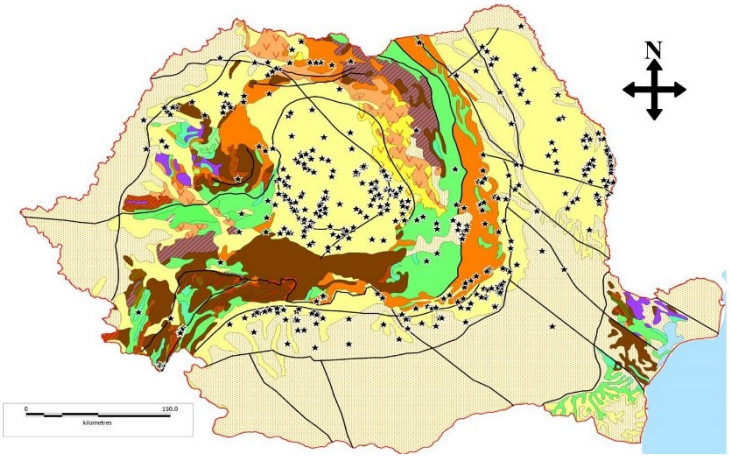

Figure 15 Map showing the general geology of Romania and the seepage locations. Stars represent data points from HYSED-RO. For legend of the background geological map see figure 11.

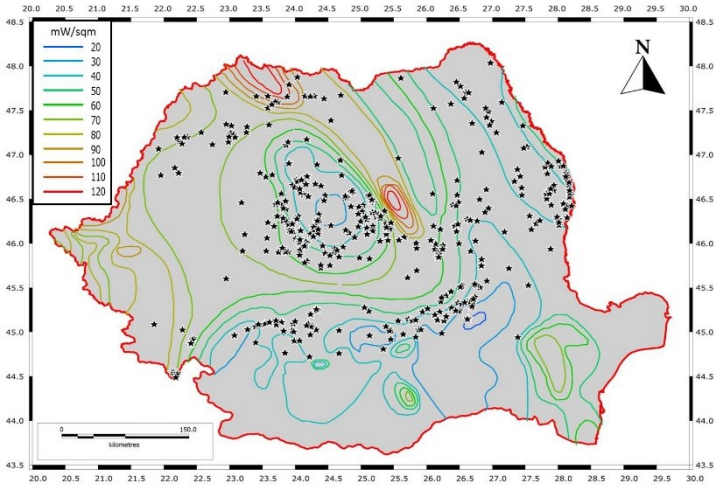

Figure 16 Map showing the heat flow (modified after Demetrescu 1982, Demetrescu & Polonic 1989, Demetrescu & Andreescu 1994, Andreescu et al. 1989) of Romania and the catalogued seeps from HYSED-RO

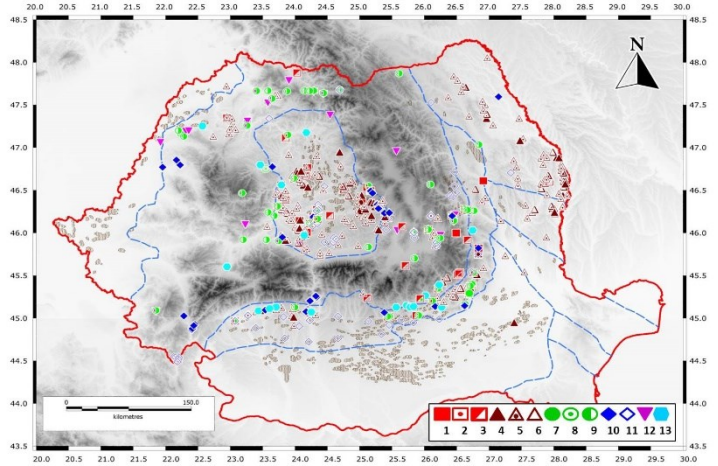

Figure 17 Map showing the different types of seeps on the Romanian territory: 1 – active gas seep; 2 – inactive gas seep; 3 – uncertain gas seep; 4 – active mud volcano; 5 – uncertain mud volcanoes; 6 – inactive mud volcanoes; 7 – active oil seep; 8 – inactive oil seep; 9 – uncertain oil seep; 10 – gas-bearing spring; 11 – uncertain gas-bearing spring; 12 – solid seep; 13 – unknown manifestation

3.4.3. Spatial analysis of the seep pattern distribution

In order to evaluate the statistical occurrences of the seeps and their relationship to geological features; four kinds of spatial analysis were performed: Fry-analysis, the distance distribution method (DDM), the weight of evidence (WofE) and the frequency ratio (FR).

3.4.3.1. The Fry-analysis

Fry-analysis was used for investigating the spatial pattern of seep occurrences. Fry analysis (Fry 1979) is a graphical method of spatial autocorrelation analysis of point object. The method translates data points into so called Fry-plots. A map of data points is marked with parallel (N-S and E-W) reference lines. For an n number of data points, there are n^2-n translations called Fry points. Fry analysis not only reveals major trends but also enhances subtle trends in a set of points. It allows the recording of distances and trends between every pair of Fry points, which can be used to visualize trends in a point set. Fry-analysis is used in a variety of different fields: mineral assessment (Carranza 2009), geomorphology (Ghosh & Carranza 2010), archaeology (Dirks & Berger 2013) and also the first time in hydrocarbon exploration (Salati et al. 2013).

For analysis of regional trends of seeps in Romania we only selected those seeps from the HYSED-RO database that are active or inactive. Before the creation of the Fry-points and Fry-plots the seeps GPS coordinates were re-projected in a UTM 34-35T WGS84 reference frame.

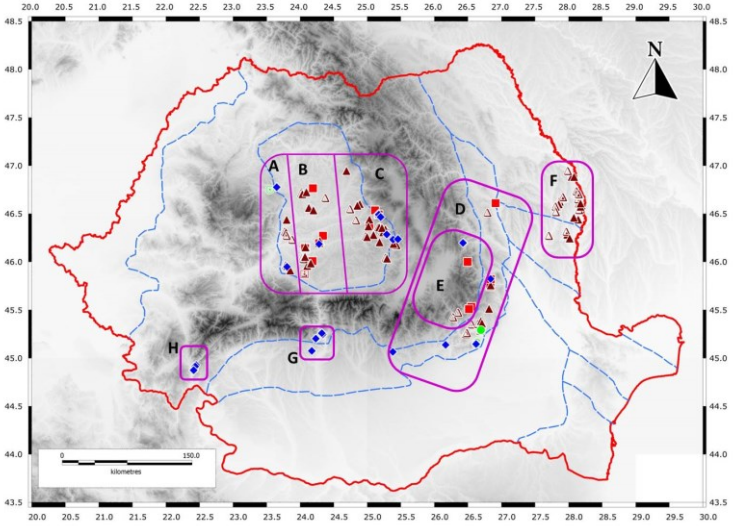

Figure 18 Map showing the points used for the Fry-analysis, and the different individual areas: A – Transylvania 1; B – Transylvania 2; C – Transylvania 3; D – Carpathian Foredeep; E – Paleogene Flysch; F – Moldavian and Scythian Platforms; G – Olt-Valley and H – Herculane graben.

After each Fry-analysis of the regions, we added all the translations into one map. For each subset of Fry-points we deleted those that where outside the geological frame work of each area.

3.4.3.1.1. The Transylvanian Basin

Fry-analysis was used for those seeps in the Transylvanian basin which are active or inactive. Three main clusters can be found in the basin for the active/inactive seeps: 1. a SE cluster; 2. an east-centre one; and 3. a Western cluster.

Based on the rose diagram for all translations the first cluster has a strict NS orientation. If we create the rose diagram for only does 2nd order neighbours that

have an average distance below 6235 m from each other, the seeps have a NW-SE orientation with a secondary N-S trend. The orientation of the first cluster coincides with the orientation of the Rusi-Cenade fault. The centre main cluster has a major W-E orientation with a circular secondary trend for all other directions. Out of these secondary trends the majority of the seeps have an orientation between NNW-SSE and NNE-SSW. The distribution of the seeps found in the lower part of the centre cluster coincides with the orientation and location of the Cenade-Rusi faults NW-SE orientation.

The third cluster is situated close to the Neogene Volcanism. The majority of the seeps are located almost parallel to the Gurghiu-Harghita volcanic mountains. There major orientation is a NW-SE one.

Based on the Fry-analysis we can evaluate the areas that could hold new resources (reservoirs). To evaluate the possibility of new hydrocarbon reservoirs in the Transylvanian Basin, a new map was created, by adding in a single map the Fry-points from the 3 investigated areas; another class of Fry-points generated using all the Transylvanian Basin seeps; the uncertain seeps from the HYSED-RO database; a dataset with the locations and contours of the petroleum reservoirs. The Fry-points which were outside the geological frame work were not taken into consideration Based on the overlapping point classes and reservoir locations, one might say that the areas of the basin that could hold new sources of hydrocarbons would be SE and also the mid-westerns and SW part of the basin.

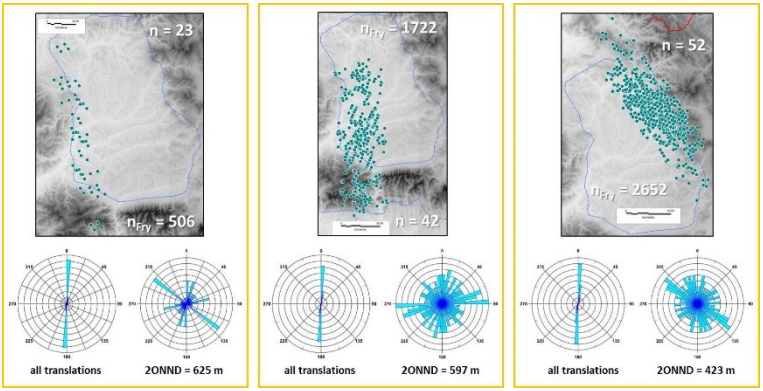

Figure 19 Fry-plots for the Transylvanian seeps (left – Transylvania 1; middle – Transylvania 2; right – Transylvania 3), rose diagram show the orientation of the Fry-points for all translations but also for the 2nd order neighbours. 2ONND denotes mean 2nd order nearest neighbour distance; n = number of original points; n_{Fry} = number of Fry-points created.

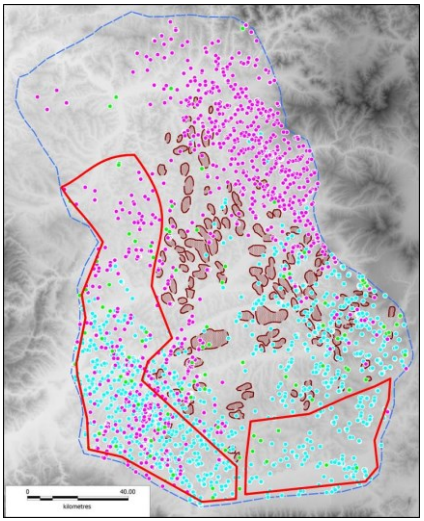

Figure 20 Map showing the probability of unexplored hydrocarbon reservoirs in the Transylvanian Basin. Point colours: violet – Fry-plot of the individual areas, azure – translations of all the Transylvanian point together; green – uncertain seeps. Brown areas are the known hydrocarbon reservoirs, and red border area represents the area which could hold new unexplored hydrocarbons resources.

3.4.3.1.2. The Carpathian Orogen

In the case of the Carpathian Orogen, seeps are divided in four groups: seeps in the Paleogene Flysch, seeps in the Foredeep, the Herculane graben and seeps in the Olt Valley.

Seeps located in the Paleogene Flysch highlight a main N/NNE – S/SSW orientation, and are oriented almost parallel to the border of the Foredeep. On the other hand, seeps in the Foredeep have a main NE-SW trend with a minor W-E trend. The Fry-points from this area are in close relation to the orientation of the Foredeep. The Herculane-cluster shows a main NNE-SSW orientation, the seeps being parallel to the Cerna-fault and the Cerna-graben. The spring from the Olt-valley geothermal region have the same orientation as the Herculane seeps, moving along the Olt Valley.

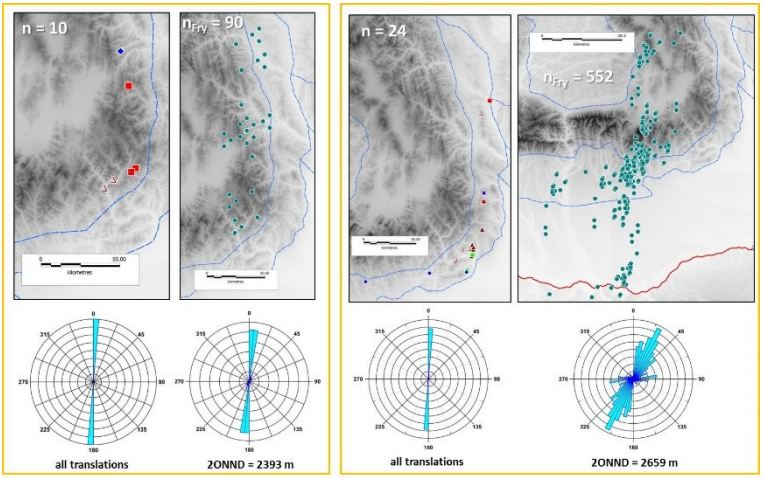

Figure 21 Fry-plots and rose-diagrams for: Left - the Paleogene Flysch seeps, Right – Carpathian Foredeep seeps

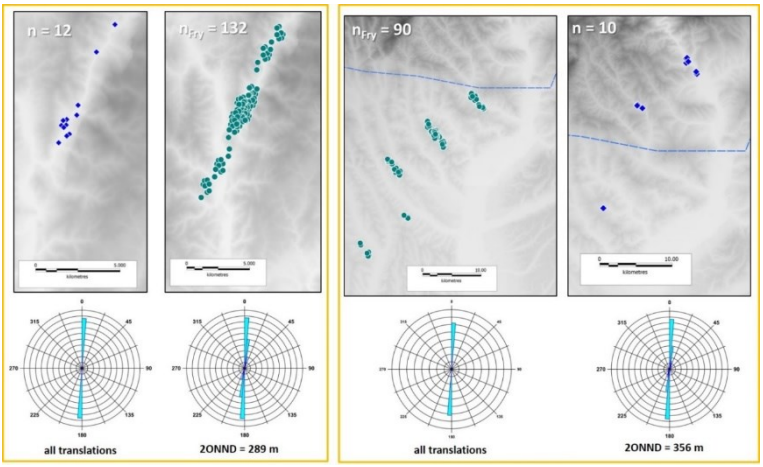

Figure 22 Fry-plots and rose-diagrams for: Left - the Herculane spa, Right – Olt-Valley

3.4.3.1.3. The Moldavian and Scythian Platforms

Fry-analysis was also performed on a cluster of seeps almost parallel to the Prut Valley/River, between the Moldavian and the Scythian Platform. Fry-plot clearly shows the so called "imaginary corridors" of the Fry-points (Carranza 2009). These are the imaginary lines where the Fry-points have the highest probability to appear. The corridors are almost parallel, having an average distance between each other of about 20-25 km. The major orientations is a NW-SE one, with a secondary being the trend of the corridors.

Based on the Fry-points distribution and orientation other seeps could exist in the Moldavian/Scythian Platforms. In the Moldavian Platform it would be the mid-south, south-eastern part of the Platform, with a high possibility of seep occurrences in the central part of the region. This area should continue through the Scythian platform, up to the Trotus fault, and possible in the western part of the North-Dobrogean Orogen.

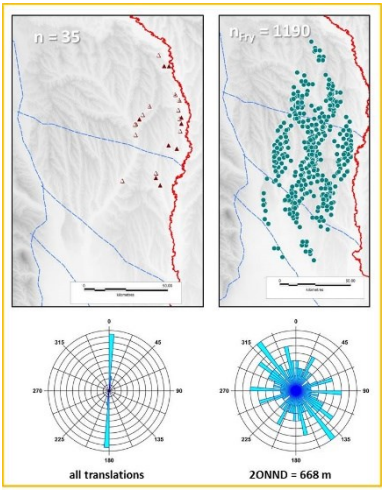

Figure 23 Fry-plots and rose-diagrams for the Moldavian and Scythian Platforms.

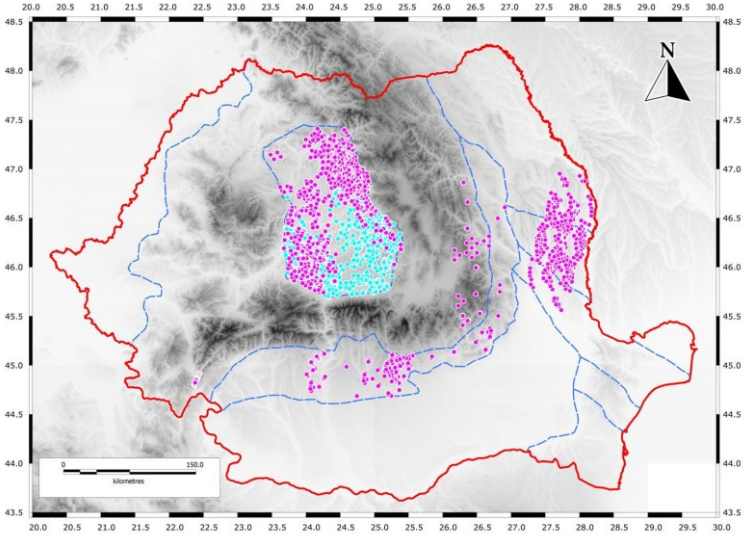

Figure 24 Map showing the revised Fry-points created for the whole Romania territory. Violet points – Fry-points from individual areas; Azure points – Fry-points of all the Transylvanian seeps taken as one area.

3.4.3.2. The distance distribution analysis

Berman (1977) demonstrated that spatial association between a set of point objects and another set of objects with particular geometry can be quantified. This method is known as the distance distribution analysis or the distance distribution method (DDM).

The DDM involves comparing a cumulative relative frequency distribution of distances from a set of geological features to seep locations (denoted as $D_{(M)}$), and a cumulative relative frequency distribution of distances from a set of non-seep locations (denoted as $D_{(N)}$). $D_{(M)}$ is a non-random probability while $D_{(N)}$ is a random probability distribution. The graph of $D_{(M)}$ is compared with the graph of $D_{(N)}$ by calculating the Kolmogorov-Smirnov statistic to test the null hypothesis that locations of points of interest and the geological features are spatially independent (Berman 1977, 1986):

$$D = D_{(M)} - D_{(N)} \qquad (24.)$$

If $D=0$, then the seep location and the set of geological features are spatially independent. If D is positive, than there is a positive spatial association between the seeps and the geological features. If D is negative, then there is a negative spatial association between the seeps and the set of geological features. A positive association indicates that there is a set of plausible geological controls affecting seeps occurrences. In order to statistically determine if $D_{(M)}$ is significantly greater than $D_{(N)}$, an upper confidence band for the $D_{(N)}$ is calculated:

$$uD_{(N)} = D_{(N)} + \sqrt{9.21(N+M) / 4NM} \qquad (25.)$$

where M is the number of seeps used to estimate $D(M)$, while N is the number of random objects use to estimate $D(N)$ and 9.21 is the tabulated critical χ^2 value for 2 degree of freedom and a significance level of $\alpha = 0.01$.

The distance from the geological feature with the highest positive D value, is also very important. It indicates the optimal distance from the geological feature at which there is a significant higher proportion of occurrences of seeps, then would be expected due to chance. The distance in which the positive D value is the highest can be calculated through a test of significance of positive spatial association by calculating the beta statistics (β):

$$\beta = \frac{4D^2NM}{(N+M)} \qquad (31.)$$

DDM has been applied to quantify the spatial associations of seeps with faults and folds. For the locations of the seeps we used the same locations as in the Fry-analysis (HYSED-RO database). The random objects were generated using the following criteria, to have 10 times the number of random points then the seeps in an investigated area. The locations of the faults and folds where digitized from the 1:200000 Geological Map of Romania. DDM analysis was performed on 3 areas: the Carpathian Foredeep together with the Carpathian Paleogene Flysch; the Transylvanian basin and the Herculane Spa area. Map from figure 69 shows the selected regions and table 10 shows the results of the DDM analysis.

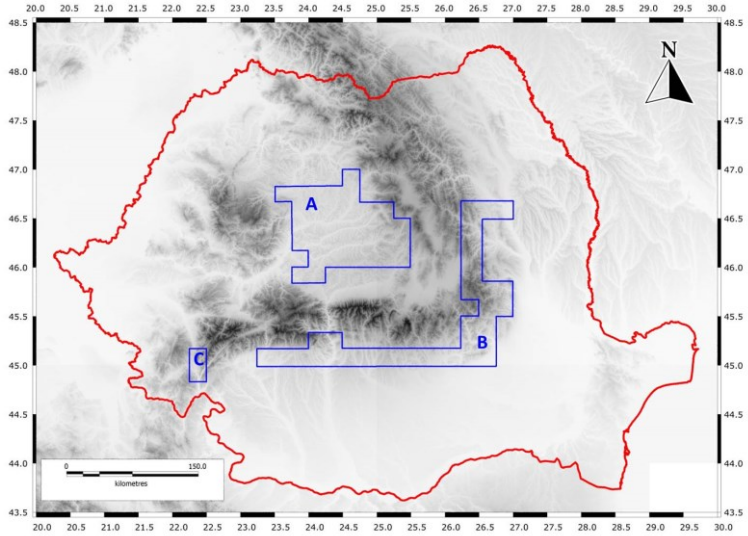

Figure 25 Map showing the selected areas for DDM: A – Transylvania Basin; B – Carpathian Foredeep and Paleogene Flysch, C – Herculane graben

Table 2 Results of the DDM analysis

Area	Type	d	DM	DN	DM/DN
Transylvania	anticline	1.5	0.8	0.31	**2.58**
	syncline	6	0.78	0.65	1.20
	fault	0.5	0.15	0.15	1.00
Foredeep	anticline	1	0.95	0.37	**2.57**
	fault	7.4	1	0.94	1.06
	revers fault	1.2	0.9	0.66	1.36
Herculane	normal and revers fault	0.4	1	0.3	**3.33**

d – optimal distance; DM – seep distribution probability, DN – random object distribution probability;
DM:DN – ratio of seep vs random object probability.

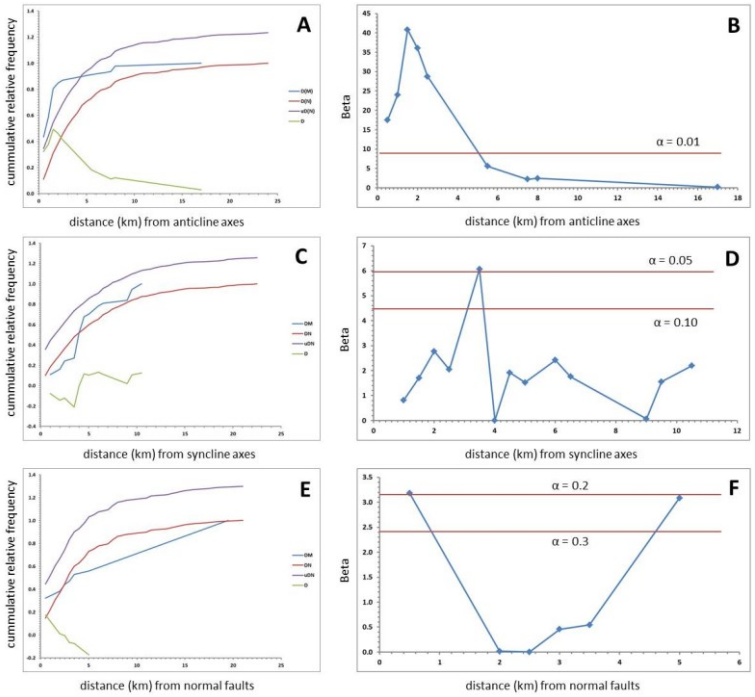

Figure 26 Graphs showing the DDM results for the Transylvanian Basin. The left columns represent the cumulative relative frequency curves of distances at seep locations (DM) and random objects (DN), with D representing spatial association of seeps with structures and uDN representing the confidence band for α = 0.01. Graphs at right column show the β-statistics of the differences (D) between cumulative relative frequency curves.

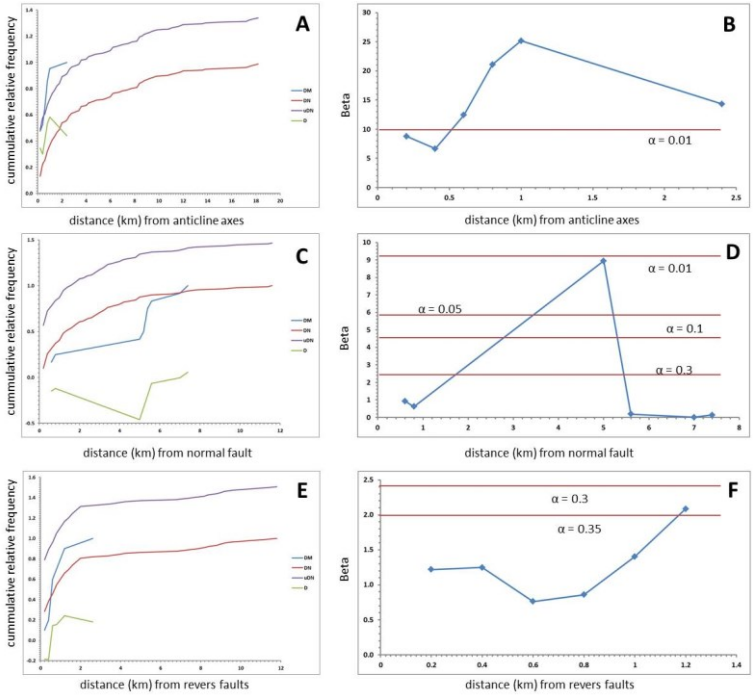

Figure 27 Graphs showing the DDM results for the Carpathian Foredeep and Paleogene Flysch

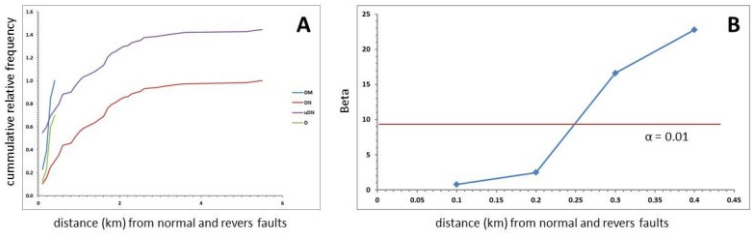

Figure 28 Graphs showing the DDM results for the Herculane graben

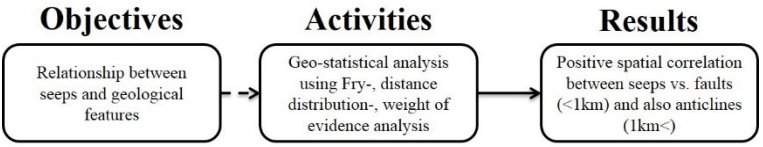

3.4.3.3. The weight of evidence analysis

The weight of evidence analysis (WofE) uses a log-linear derivation of Bayesian probability to quantify spatial association between a dependent variable (a predictive factor) and an independent variable (a geo-object). The WofE method is based on the idea that several binary patterns can be combined to predict another binary pattern (Bonham-Carter et al. 1989). The method calculates the weight for the presence or absence of each geo-objects predictive factor's class based on the presence or absence of a geo-object within the study area. In this method a positive weight (W^+) and a negative weight (W^-) represent, a positive and a negative spatial association of geo-object with a predictive factor, respectively. The W^+ and W^- are calculated as:

$$W^+ = log_e \left[\frac{P\left(\frac{F}{O}\right)}{P\left(\frac{F}{O^*}\right)} \right] \qquad (27.)$$

$$W^+ = log_e \left[\frac{P\left(\frac{F^*}{O}\right)}{P\left(\frac{F^*}{O^*}\right)} \right] \qquad (28.)$$

where P is the probability, F and O are the presence of the predictive factor and the object of interest, and F^* and O^* are the absence of the predictive factor and the object of interest.

The weights contrast (C) is the measure of the spatial association between the geo-object and the predictive factors is calculated as:

$$C = (W^+) - (W^-) \qquad (29.)$$

A contrast value equal to zero indicates that the considered factor is not significant for the analysis; a positive value indicates a positive spatial correlation while a negative a negative spatial correlation. We also used studentized contrast (sig_C) to measure the certainty with which a contrast is known (Bonham-Carter et al. 1989). It is calculated as the ratio of the contrast divided by its standard deviation:

$$sig_C = C \frac{C}{\sqrt{s^2(W^+) + s^2(W^-)}} \quad (30.)$$

A sig_C greater than 2 suggest a statistical significant spatial correlation.

In order to calculate the probability we used the method of Barbieri & Cambuli (2009):

$$P = exp(\sum W^+) + \ln Pp(s) \qquad (31.)$$

where P is the posterior probability and $Pp(s)$ is the prior probability.

For using the WofE method several different factors that could influence the presence of seeps in an area, were digitized several layers. Using the 1:200000 Geological Map of Romania, the faults and lithological units were digitized, and also a shape file with the petroleum reservoirs of Romania was added. For each investigated area a 500 x 500 m grid was created over the individual shape files.

In the study case the equations for the positive and the negative weight were used as follows:

$$W^+ = ln\left\{\frac{\left(\frac{a}{b}\right)}{\left[\frac{c-a}{d-b}\right]}\right\} \quad (32.)$$

$$W^- = ln\left\{\frac{\left(\frac{e}{b}\right)}{\left[\frac{f-e}{d-b}\right]}\right\} \quad (33.)$$

where: a is the number of seeps in a class; b is the total number of seeps; c is the pixel number for each class; d is the pixel number of the study area; e is the total number of seeps – the seeps in the class; f is the number of pixels for the study area – the number of pixels of the class. The prior probability was calculated according to the following formula:

$$Pp(s) = \frac{total\ number\ of\ seeps}{total\ number\ of\ pixels\ of\ the\ study\ area} \quad (34.)$$

The term "class" we understand, indicates individual lithological unit from the study area. The WofE was performed on seeps and on the tectonic features and petroleum reservoirs. The intersection between these two last features is also evaluated. The weights for these features were also calculated: W_{tect} (weights of tectonic feature occurrence for a lithological unit) and W_{res} (weights of reservoir occurrences for a given lithological unit). Based on the calculated weight, Seep

Probability Index (SPI) was calculated in order to evaluate which lithological unit influences the majority of the seeps occurrences, according to the following equation:

$$SPI = W_{seep}^{+} + W_{tect}^{+} + W_{res}^{+} \qquad (35.)$$

The WofE was perforemd on 6 areas in Romania: the western (1) and eastern part of the Transylvanian Basin (2), E-SE part of the Carpathian Foredeep (3), the SW area of the Foredeep (4), the southern part of the Moldavian Platform together with the Scythian Platform (5) and the Herculane graben (6). The same raw data was used as in the previos methdos (HYSED-RO).

Three mentions must be made: 1. for those seep locations that overlap "Quaternary Holocene" sediments, are not classified in this "class", but in the "class" of the lithological unit that it intersects. This criterion was taken into consideration because: a. Holocene sediments are found in those areas were the river-beds were formed due to erosion (the rivers didn't just erode the lithological unit, but also performed sedimentation in parallel); b. the seeps found in these points do not have their origins in the newest sediment but in the underlying lithological layers; 2. The lithological units are not updated for the new nomenclature and unit names; 3. the Tortonian unit from the maps is changed to Badenian unit, but the abbreviation was kept.

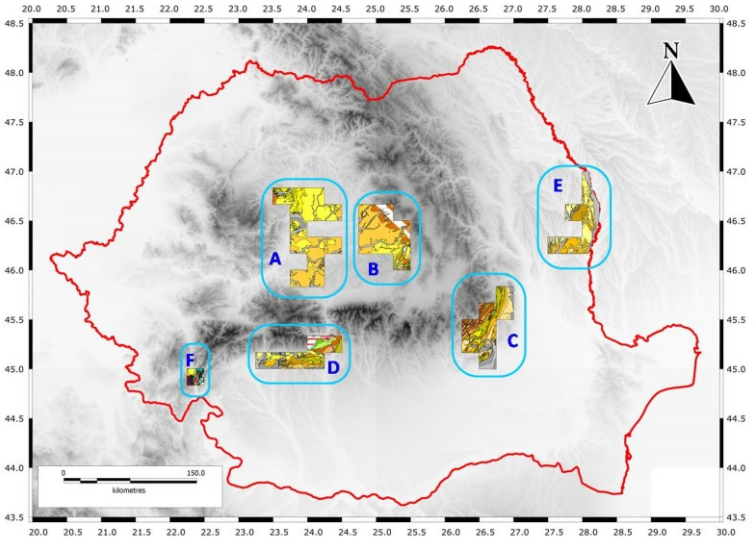

Figure 29 Map showing the selected areas used in WofE analysis: A – Transylvania 1; B – Transylvania 2; C – Carpathian Foredeep 1; D – Carpathian Foredeep 2; E –Moldavian and Scythian Platform; F – Herculane graben

3.4.3.3.1. The Transylvanian Basin

Based on the WofE analysis of the two investigated areas of the Transylvanian Basin the following conclusions can be defined:

- the western area has positive spatial association for Pannonian and Volhynian units, more significant is the Pannonian unit (sig_C = 4.88 and P = 0.0058).
- no correlation/association was found for lithologic units and tectonic features for the above mentioned units, but a positive association of petroleum reservoirs with the Volhynian unit found.

- based on the P value (4.8849) of the Pannonian unit and the SPI value (0.4874) of the Volhynian unit, it is probable that these two units have a positive spatial association of the seep occurrences.
- in the eastern part of the Transylvanian Basin, besides the Pannonian and the Volhynian unit a positive spatial association also with the Badenian unit. In this case the most significant units are the Badenian and Volhynian units.
- also for these two units positive spatial association with tectonic features (faults or/and folds) was found.
- from the three units, mentioned above the Badenian has the highest probability for seep occurrences, followed by Volhynian and Pannonian, based on the SPI values.

3.4.3.3.2. The Carpathian Foredeep

The first investigated areas of the Carpathian Foredeep, a positive spatial correlation, for seep occurrences in Badenian, Maeotian and Pontian units was calcualted. The Badenian unit results the most important and shows the highest probability (P = 0.0083) followed by Maeotian (P = 0.0058) and Pontian (P = 0.0045). Any positive association of the lithologic units with tectonic feature and petroleum reservoirs was observed.

For the second investigated area of the Carpathian Foredeep, a more complex association was highlighted. A spatial association for seep occurrences was calculated for the following units: Bessarabian, Maeotian, Eocene, Santonian,

Ypressian and areas with amphibolite. Significant association only results for the Eocene unit and the areas with amphibolite. A correlation with tectonic features and petroleum reservoirs was found for the Bessarabian unit, whereas for the Maeotian units a significant spatial association exist only with petroleum reservoirs. Calculated SPI values indicated the following probability order of seep occurrences: Eocene > Bessarabian > Maeotian > amphibolite areas > Santonian > Ypresian.

3.4.3.3.3. Other investigated areas

In the Moldavian Platform positive correlations with Bessarabian, Pleistocene and Chersonian units were found, and for the Pleistocene unit a significant correlation was found with petroleum reservoirs. Based on the calculated SPI values the most important lithologic unit is the Pleistocene (SPI = 3.7443) followed by Bessarabian and Chersonian units.

In the case of the Herculane graben area positive weights for the Albian unit, amphibole-, granite- and skarn areas were calculated. The highest contrast can be found for the amphibole areas ($sig_C = 5.3537$). For this area any spatial association with tectonic features was not found.

3.4.3.4. The frequency ratio method (FR)

The frequency ratio model is a simpler geospatial analysis tool compared to the WofE method. It is based on the same theoretical assumptions of the weight of evidence method; and can be expressed as a ratio that represents the quantitative relationship between seep occurrences and different causative parameters that affect seep occurrences (Oh et al. 2011). The calculation step is the following for a parameter that affects the seep occurrence:

$$FR = \frac{\left(\frac{A}{B}\right)}{\left(\frac{C}{D}\right)} \qquad (35.)$$

where A is the number of seeps in a class; B is the total number of seeps, C is the number of pixels for the class, and D is the number of total pixels of the study area. The FR method was used as the WofE method, for different lithological units, compared with seep occurrences, tectonic features and petroleum reservoirs. The same raw data as in the case WofE method was used. By calculating the ratio for each factor, the frequency of seep occurrence was evaluated using the Seep Occurrence Potential Index (SOPI), by sum of all FR values for a given lithology:

$$SOPI = \sum(FR)_i \quad (36.)$$

Tables 17-22 summarize the values for FR for the investigated areas. For most cases the calculated values show the same conclusions as the WofE. We have only two investigated areas were differences can be observed compared to the WofE. In the western part of the Transylvanian Basin, the Pleistocene appears, together with the Pannonian and Volhynian as the 3rd lithologic unit that could control the seep occurrences. The other site is eastern part of the Carpathian Foredeep where, another five lithologic units appear as controlling factors. Based on the FR values the lithological units can be ordered (from the most significant to the less significant): Badenian > Maeotian > Sarmatian > Pontian > Palaeocene > Lattorfian > Levantin > Helvetian.

3.4.4. Gas flux

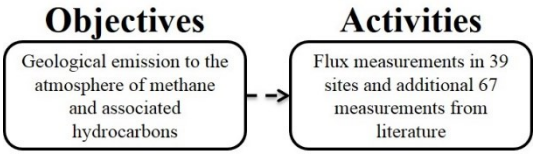

The summary of the total outputs (methane, ethane and propane) measured in the investigated sites can be seen in table 23. In order to have a complete comparison to other measured/estimated fluxes, we compared our data to other measurements performed in Romania. We used the data from: Etiope et al. 2004, Baciu et al. 2007, Baciu et al. 2008, Etiope et al. 2009b, Spulber et al. 2010, Spulber 2010, Etiope et al. 2011, Frunzeti et al. 2012a, Pop 2014 and Pop et al. 2015.

In the Transylvanian Basin the highest output of methane was measured/estimated at the Tauni craters, ranging between 0.45-194.12 t/y. The other smaller mud volcanoes have emissions in the order of 10^{-2} – 10^{-5} t/y.

For the Tauni seepage area we calculated the outputs based on the bubble visualization. We could only perform visual and also chamber measurements at one crater. But based on the measurements/estimates of that crater we can conclude that the two methods used have the same order of magnitude.

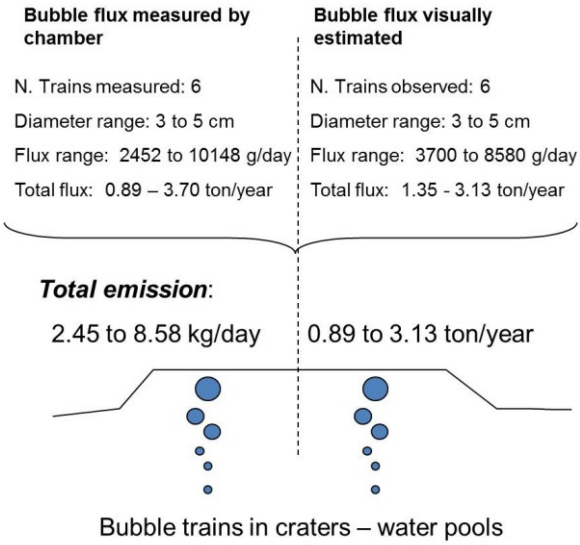

Figure 30 Sketch comparing direct vs. indirect flux measurements at Tauni Crater 1.

For the other craters the sum of the individual bubble train outputs was taken into consideration. The estimated total emission for the Tauni seepage area is about 452 t/y, out of which 14 t/y is the Tauni mud volcano (Pop 2014).

For the Transylvanian Basin the two highest emitting areas are Sarmasel and the Tauni seeps. These are followed by the Deleni > Praid and other higher emitting areas (1 t/year, like Boz, Cobatesti and Homorod). We can observe that in the western part we have low emitting areas, for example, Sic, Frata, Ocnisoara, and to the south of Boz the Veseud seeps. Between the high emitting areas and the middle range (10-$10^{1.5}$ t/m^2/year) we have a very low emitting area. These seeps are found, in a geographical view point, at the eastern part of the Transylvanian Plain. Between

the Transylvanian Plain and the Eastern Carpathian Neogene volcanoes we can find a few seeps that are linked to the salt diapirs found in the area, like the seeps from Corund and Praid.

In the Paleogene Flysch area the Lepsa and Lopatari eternal flames have a total output of 28.4 t/y. Lepsa having roughly ~1.5 t/y output. For the Lopatari seep we calculated a total emission of 26.9 t/y; using 14 measurement points, for an interpolated area of 35 sqm. The highest flux values were measured in two points, 5533 and 70570 g/m2/day. Possibly these are the "vents" of the seepage area.

Also in this area we visually estimated the Slanic-Moldova Nr. 2 spring using the method of Delichathios 1990. We estimated that the flame has a "height" of 20 cm and a flame diameter of 5 cm. Based on these parameters; we estimated a ~1.64 t/y output of methane.

In the Carpathian Foredeep the highest emissions where found at the Andreiasu eternal flames. The total output was estimated via direct measurement on the seepage area (31 measurements) and via visual estimation of a burning vent.

From the 31 measurement points 7 points had with 2 order of magnitude higher flux values then the mean flux. Based on these values these points were treated as vents (macroseepages). In order to calculate the total emission of the area, the miniseepage, a sort of "cut of the peak" was done for these seven points, in such a way that, the value didn't exceed one order of magnitude than the neighbouring flux value. Two variants were performed, a cut of the peak until 1000 $g/m^2/day$ and a second one until 10000 $g/m^2/day$. Based on these two variants we calculated the total output of the area using the kriging interpolations method. For the vents we just summed the individual values. The final output was calculated by adding to the

miniseepage the total output of the vents, and calculating an average from the two variants (minimum output of 33.8 t/y and a maximum of 57.5 t/y).

We estimated the emission of a burning vent using the same technique (Delichathios 1990), because we weren't able to put the chamber, due to the vent being right under the rock wall constructed around main seepage area. We estimated the flame had a height of 60 cm and a width of 5 cm, based on this we assumed that the total surface area of the flames was ~300 cm^2. We assumed that if the flame would burn "freely" without being effected by the wall geometry, based on our calculations we estimated a diameter of ~20 cm for the flame. Based on these parameters we calculated a 8.67 t/y output from the flame.

Via the measurements and the visual observation of the flame, a total of 54.3 t/y of methane and 27.6 t/y of carbon dioxide was estimated for an area of 264 sqm.

The mud volcano close to the eternal flames has a much lower emission in comparison with the eternal flames, having an estimated 3 t/y output of methane. The Raiuti eternal flames release 17.2 t/y of methane in to the atmosphere, while the sulphur springs close to the seeps release 1 kg/y or methane.

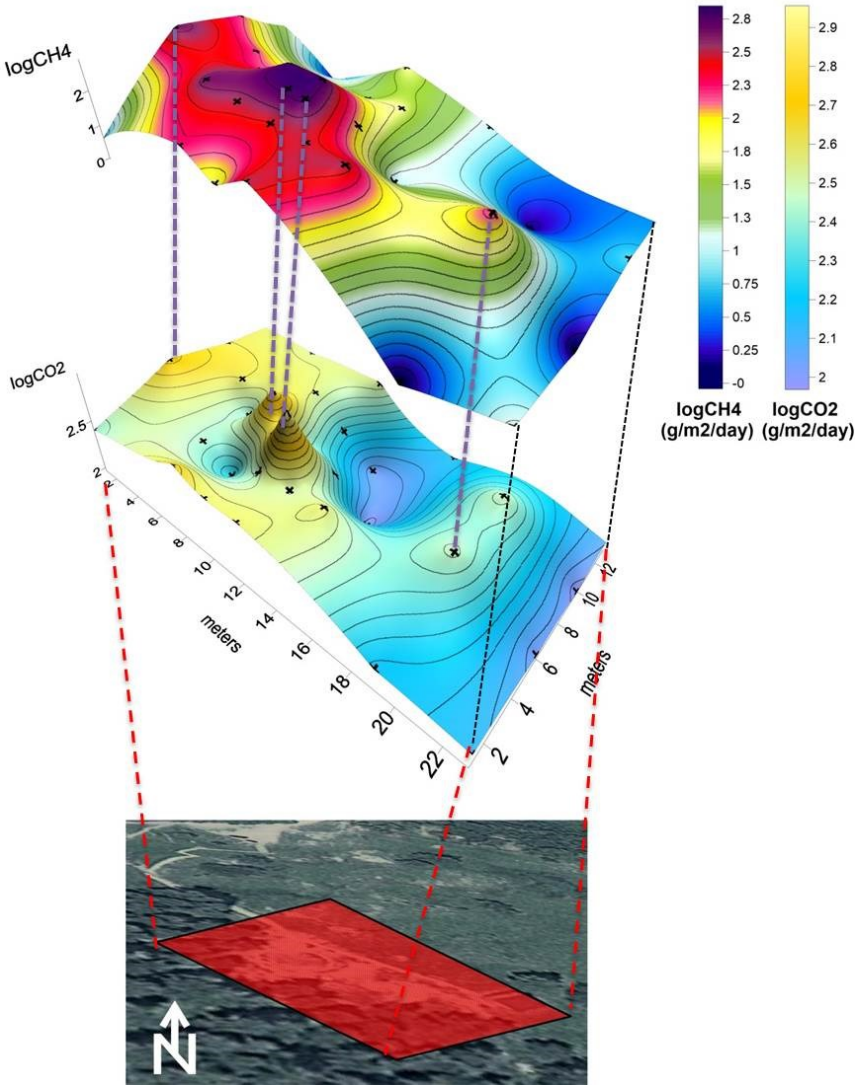

Figure 31 3D surface diagram of the Andreiasu eternal flames flux measurements, showing the variation of the flux. Crosses represent measurement points.

The biggest mud volcano investigated in the Carpathian Foredeep was the Alimpesti mud volcano, the estimated output is ~19.02 t/y of methane, by taking into consideration the whole area of the mud volcano. The other mud volcanoes investigated in the southern part of the Fordeep emit of the order of 10^{-3} – 10^{-4} t/y of methane. From the investigated gas-bearing springs Pausa has the highest output (5.03 t/y). Pausa is followed by the Ochi springs from Sacelu-Gorj, with 0.03 t/y of methane. The other springs investigated have methane measured at the spring outlet, of the order of 10^{-5} t/y.

In the Carpathian Foredeep, we have a very high emitting area in the south east, with the following seeps: the Paclele mud volcanoes, followed by Andreiasu seepage area. Witch continues to the north to Raiuti, and the Paleogene Flysch (Lopatari, Lepsa, Slanic-Moldova). The high-emitting areas are followed by the Sarata-Monteoru seepage, and Matita spring. A significant emission can be observed in the south western part of the Carpathian Foredeep (Alipesti mud volcano). Between Pausa and Alimpesti we have two low emission sites: the Caciulata-Calimanesti springs and the Ferdinand springs.

From the Moldavian Platform the highest emission was found at Hlipiceni gas-bearing spring (11.08 t/y), while for the Poganesti mud volcano we measured 0.61 t/y of methane. For the Herculane area, for the two springs were flux measurements were performed, the highest was found for the Scorillo spring (0.21 t/y of CH_4).

The Moldavian Platform has two very high emitting areas: the Bacau seepage and the Hlipiceni seep. These areas are followed by the seeps located close to the Prut River (Chersacosul, Stanilesti, Berezeni). Between these three positive flux areas we have a very low emitting zone, starting from the Leosti region until Vocotesti. These seeps located in this region have a very low flux, being almost inactive. In the Cotnari area we have a slight increase of flux, caused by an active mud volcano.

In the south east of Romania we can find a small flux at the Herculane springs, and another small flux at the north-west due to the Lesmir seep.

For the so called "Forocici" emission area in 2012 a preliminary survey was performed. Direct flux measurements of the flux and gas sampling were performed. Based on the flux measurements the crater has a total output of 0.5 t/y of methane and 466.7 t/y of carbon dioxide. The laboratory analysis, for the collected gas sample, was performed at ATOMKI Debrecen, using a Thermo Finnigan Delta plus XP type stable isotope mass spectrometer. Based on the measurements the major component is carbon dioxide 99.3%, followed by methane 0.5% and nitrogen 0.5%. The R/Ra ($(^3He/^4He)_{sample}$ / $(^3He/^4He)_{atmosphere}$) ratio was also measured, having a value of 3.73.

Based on the direct measurements and the laboratory analyses, it can be confirmed that the Foroici crater is not a mud volcanoas described by Uruioc et al. 2012! The flux measurements and also the laboratory analysis of the gas sample, show that this gas manifestation could be better called a mofetta rather than a mud volcano. The flux of CO_2 having a three order of magnitude higher flux then methane.

The ethane and propane flux was also estimated, for those seeps were molecular analysis of the gases were performed. As we can observe the ethane and propane fluxes are proportional with the methane fluxes. The highest outputs were estimated for: Andreiasu, Lopatari and Raiuti eternal flames and the Alimpesti mud volcano.

We performed the same exercise also for ethane and propane emissions for Romania as for methane. For ethane the highest emissions can be found at: Paclele, Andreaisu, Bacau, and Alimpesti. We have lower emissions in Pausa, followed by Lepsa and Raiuti areas. The lowest amount is released at: Saceu-Gorj (Ochi spring) and Poganesti 2. In the case of propane the magnitude of emission for the seeps remains the same, the maximums being found in the eastern side of the Foredeep.

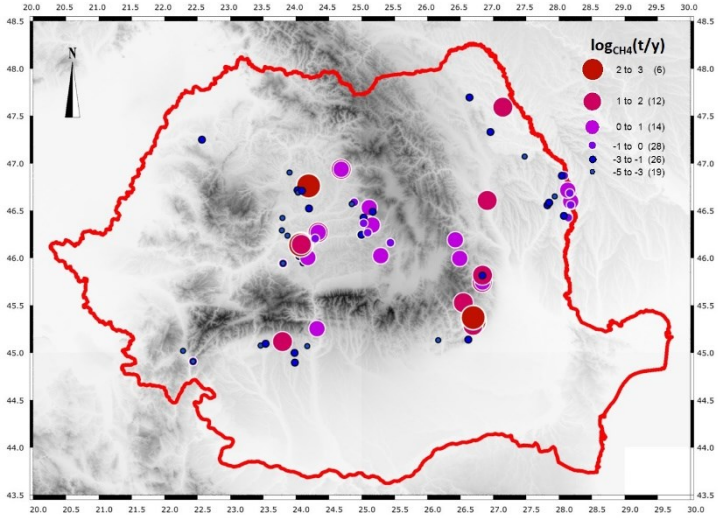

Figure 32 Dot-plot for the emission of methane, for the main Romanian seeps. In the legend the values are in tons/year logarithmic scale, values in brackets represent the number of seeps in each category.

The total geogenic methane output from the Romanian territory is estimated to be in the order of 2000-3000 t/y. Based on the National Inventory Report for 2014 (issued by the Ministry of Environment and Climate Change), Romania methane emission from fuel combustion is 47.89 Gg/y, from industrial processes its 0.68 Gg/y and for agricultural field burning its 3.87 Gg/y. The total methane emission, 2-3 Gg/y (1 Gg = 1000 tons) is comparable with these man-made sources. The photochemical pollutants have a total output of: 34.6 t/y ethane and 20.8 t/y of propane. These data should be considered in future national inventory reports.

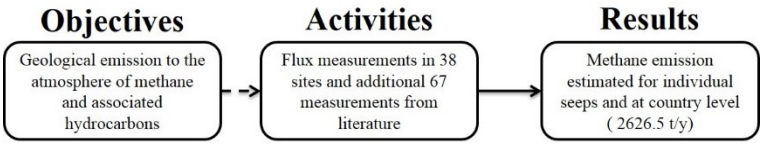

3.4.5. Origin of hydrocarbons in seeps

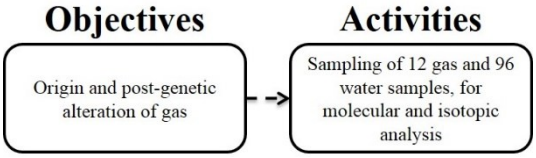

Table 25 and 26 contains all available molecular and isotopic data. By plotting the carbon ($\delta^{13}C$) and hydrogen (δD or $\delta^{2}H$) isotope plot for methane (Schoell-plot) we can distinguish between different origins of methane (fig 89). The plot is calibrated for vitrinite reflectance (an indicator of source rock maturity), according to Jenden et al. 1993. We observe two main groups of data. The first contains the microbial methane from the Transylvanian Basin, the second contains the dominantly thermogenic methane from the Carpathians (Paleogene Flysch and Foredeep).

The Transylvanian gases are very similar to one another mainly because of the similarities of the reservoirs in that area. The thermogenic gases can be divided in five smaller groups. These groups also indicate the rough maturity and also give a clustering based on the geographical/geological location of the seeps. The three everlasting fires from the Carpathians form one group. These have the highest vitrinite reflectance (highest maturity), using the calibrated Schoell-plot. These seeps are located in the Outer Foredeep, except the Lopatari which is in the Paleogene Flysch. We could also observe that there is no significant isotopic variation of the Andreiasu EF from 2007 until 2012 ($\delta^{13}C_1$: -34.48; -35.72 and δD:

-147.6; -151). The gas issuing from source rocks with the lowest maturity is found in the Paleogene Flysch (Lepsa sample). This petroleum system can host oil (located within "thermogenic with oil" area of Schoell-plot); that can be biodegraded as suggested by positive $\delta^{13}C\text{-}CO_2 = 5.03$). Bacau, the Andreiasu mud volcano and the Berca mud volcanoes are found between thermogenic with oil and thermogenic with condensate. We could say that they are in a transition zone between the low and the high maturity gases found in Romania. The maturities of the gases are, thus, of different degrees: the lowest 0.5% is found for Bacau, while the highest for the Beciu mud volcano.

The Pausa gas-bearing spring is similar to the Outer Foredeep, based on the isotopic data, but is more enriched in deuterium than all other gases (most δ^2H depleted is the Lepsa sample). The sample is shifted more to the middle part of the thermogenic dry area, which could be due to the spring being affected by the geothermal fluids of the area.

Praid has an isotopic composition different from the other ones. It is found between the thermogenic with condensate, and also having a much higher maturity, R_o >4.0%. The gas could be partially oxidized and/or the reservoir is located close to the Neogenic volcanic area of the Eastern Carpathians; accordingly, we cannot exclude that the reservoir could have had a minor addition of abiotic source (geothermal origin) of methane. Praid seep has also the second highest helium content in Romania (0.45%) after Homorod seep (1.5%; Etiope et al. 2011a)

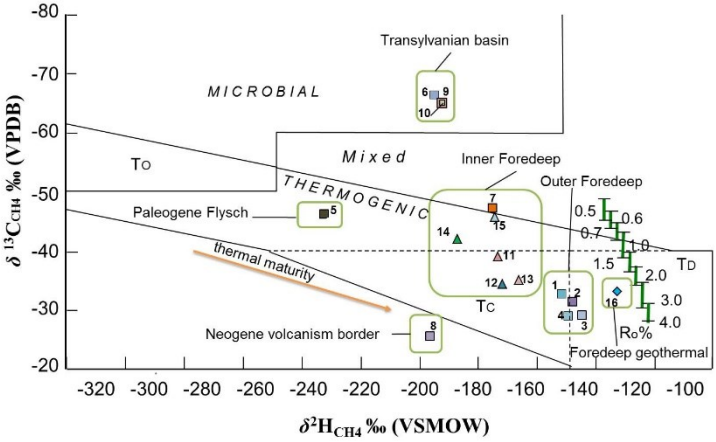

Figure 33 Isotopic composition of methane of seep gases from Romania. R_o: vitrinite reflectance index. The relationship between vitrinite reflectance and methane $\delta^{13}C$ is from Jenden et al. 1993. "Eternal flames": 1 – Andreiasu EF (eternal flame) 2012; 2 – Andreiasu EF 2007; 3 – Raiuti; 4 – Lopatari; 5 – Lepsa; 6 – Sarmasel; Gas seeps: 7 – Bacau-Gheraiesti; 8 – Praid; 9 – Deleni 1; 10 – Deleni 2; Mud volcanoes: 11 – Andreiasu MV (mud volcano); 12 – Beciu; 13 – Paclele Mari; 14 – Paclele Mici; 15 – Fierbatori; 16 – Pausa duplicate.

By ploting also the so called "Bernard-diagram" (Fig.90), it can be observed that the samples are grouped in six clusters. The first cluster contains the microbial gas of Transylvanian gases and Hlipiceni. Deleni 1 and 2 (numbered 9 respectively 10) have relatively the same $\delta^{13}C$ composition but different degree of molecular fractionation.

The second cluster contains Paclele Mici (14) and the Andreiasu MV (11). The third cluster contains Bacau-Gheraiesti (7), Lepsa (5), Fierbatori (15), Alimpesti (21) and Poganesti (22). The fourth cluster contains the other everlasting fires from

the Carpathian area, Paclele Mari and Beciu mud volcanoes and Scorillo spring, having almost the same fractionation interval. The fifth cluster contains the high maturity gases, namely Praid, Sacelu-Gorj and Pausa. The sixth cluster contains the Homorod samples. The majority of the samples are located in the thermoganic area, while one sample is outside the thermogenic range.

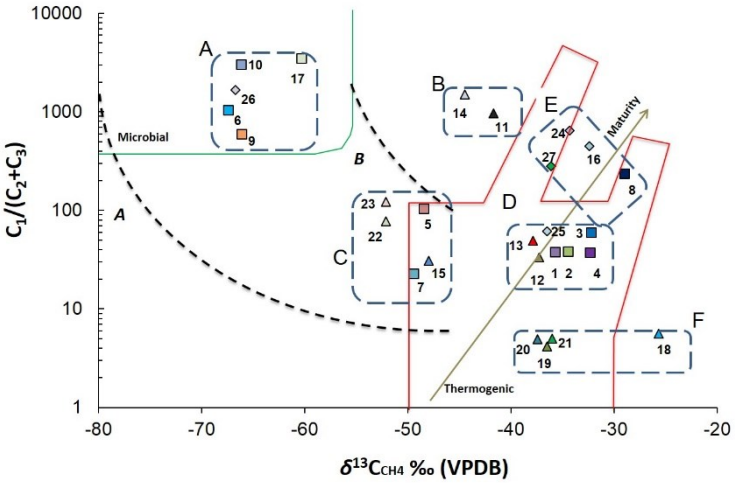

Figure 34 Natural gas interpretive ("Bernard") diagram (modified after Bernard et al. 1978) Line A and B are calculated mixing lines according to Whiticar 1999, for possible gas microbial and thermogenic end members. Numbers according to figure 89. Tauni gas seep - 17; Mud volcanoes: Homorod seep 3 – 18, Homorod seep 4 July 2009 – 19, Homorod seep 4 August 2009 – 20, Homorod seep 4 September 2009 – 21, Alimpesti – 22, Poganesti – 23, Bubbling springs: Sacelu-Gorj – 24, Pausa – 25, Hlipiceni – 26. Scorillo – 27.

We also performed the Schulz-Floury distribution (Floury, 1936) for a check of possible abiotic component in the gas. The Schulz-Floury distribution, is a molecular distribution of the hydrocarbon homologs that is controlled by chain growth probability factor for abiogenic stepwise polymerization where (C_n + $1/C_n$) is approximately constant (C_n is the concentration in mole units). Thermogenic gas

is typically characterized by a correlation coefficient r^2 <0.9, while r^2 is >0.9 for dominantly abiotic gas and >0.99 for quasi-pure abiotic gas (Etiope and Sherwood Lollar 2013).

The test concludes that all gases in Transylvania and the Carpathian basin, having value of r^2 <0.9, have no significant abiotic components; they are dominantly biotic, microbial (the Transylvanian ones) or thermogenic (the Carpathian basin ones). A very interesting observation, is that Transylvanian gases have measurable amounts of C_2-C_4 alkanes (up to 0.1%). C_2-C_4 hydrocarbons cannot be produced by microbes (except C_2-C_3 in very special cases and in extreme low amounts; Formolo 2010). Our data suggest that Transylvanian gases can have minor thermogenic components (Sarmasel, Deleni, Tauni). This would be consistent with the hypothesis of a deeper thermogenic petroleum system suggested by Popescu 1995. This hypothesis is further suggested by the molecular data of the Transylvanian reservoirs published by Filipescu & Huma (1979), but also from the historical literature describing oil seeps in the central part of the Transylvanian Basin.

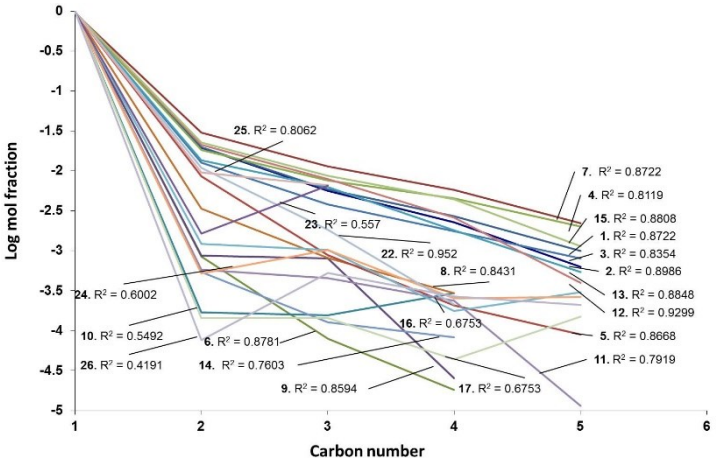

Figure 35 Evaluation of the Schulz-Floury distribution coefficient, r^2.

In order to see the origin of methane compared to the origin of ethane, the $\delta^{13}C$-C_1 vs. $\delta^{13}C$-C_2 diagram was plotted based on Milkov 2010. As we can observe, methane but also ethane in the Andreiasu EF 2012, Raiuti, Lopatari, Pausa, and the Homorod samples are pure thermogenic. Lepsa on the other hand, has a high amount of microbial input for the methane component with a thermogenic ethane component. This could be caused due to biodegradation, or secondary migration of the gas.

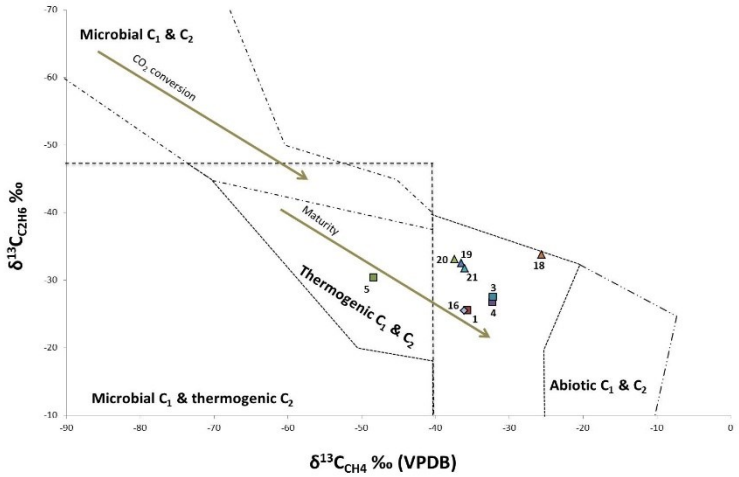

Figure 36 Relationship between stable carbon isotope composition ($\delta^{13}C$) of methane and ethane. Genetic fields modified after Milkov 2010.

3.4.5.1. Maturity and possible kerogen type

Popescu (1995) indicates that in Carpathian Paleogene Flysch the source rocks are shales of Oligo-Miocene formations, known as Dysodile and Menilite formations in Romania, and also in Ukraine and Poland. The kerogens are of type II and III, with a vitrinite reflectance between 1.10-1.15 $\%R_o$. Stable carbon isotopic composition of kerogen is known for the Menilite ($\delta^{13}C_{ker}$ of -26.6 ‰ for type II kerogen; -25.2 ‰ for type III; Kotarba et al. 2009) but not for Dysodile in Romania. Assuming Dysodile and Menilite have similar $\delta^{13}C_{ker}$ values and combining the maturity model by Berner and Faber (1996) and the thermogenic gas generation modelling by Tang et al (2000) it is possible to verify if the seep gas derives from the Dysidile source rocks.

Two plots ($\delta^{13}C_1$ vs $\delta^{13}C_2$ and $\delta^{13}C_2$ vs $\delta^{13}C_3$; Figs. 93-94) were drawn based on isotope modelling by Tang et al. 2000 (and conducted with GeoIsochem Corp. GOR Isotope software 1.94 for instantaneous generation of methane, ethane and propane from default Type I, II and III kerogen, with a heating rate of 5°C per 1 million of years).

The $\delta^{13}C_1$ vs $\delta^{13}C_2$ suggests that Andreiasu and Pausa gas was formed from type III or II kerogen, having a R_o of 1.5 to 2.0. Raiuti and Lopatari appear to be associated to higher R_o between 2.0 and 2.5. The Raiuti and Lopatari gases do not fit exactly with the GOR modelling, probably because they are a mixture of different methanes or the input parameters of the GOR modelling (for example the heating rate) are not optimal for the Carpathian basin. Lepsa is confirmed to derive from lower maturity kerogen (0.8-1.0 $\%R_o$) and is likely mixed with microbial gas.

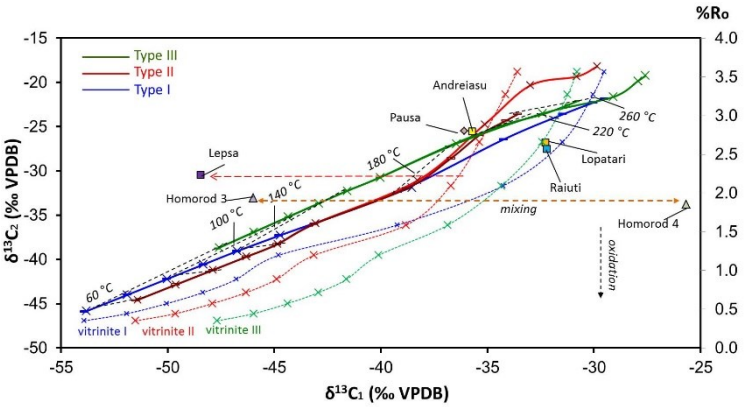

Figure 37 Thermogenic gas formation modeling from marine (Type I. and II.) and terrestrial (Type III) kerogen, calculated using GeoIsochem Corp. GOR software 1.94; heating rate of 5°C per million year (Tang et al. 2000, Etiope et al. 2013). Carbon-13 ratio for methane and ethane. Horizontal arrow indicates the biodegradation of the Lepsa sample assuming that the sample is derived from marine kerogen. Orange dashed line represent the mixing between the two sources of the Homorod seep.

The $\delta^{13}C_2$ vs $\delta^{13}C_3$ plot (Fig. 94) suggests Raiuti and Lopatari are formed from a type III kerogen, Andreiasu is more uncertain between Type II and III, but all are related to maturity between 1.5 and 2.0, as suggested by the $\delta^{13}C_1$ vs $\delta^{13}C_2$ plot. Based on the two GOR plots, the formation temperature of the three gases (Andreiasu, Raiuti and Lopatari) is possibly between 180-220 °C.

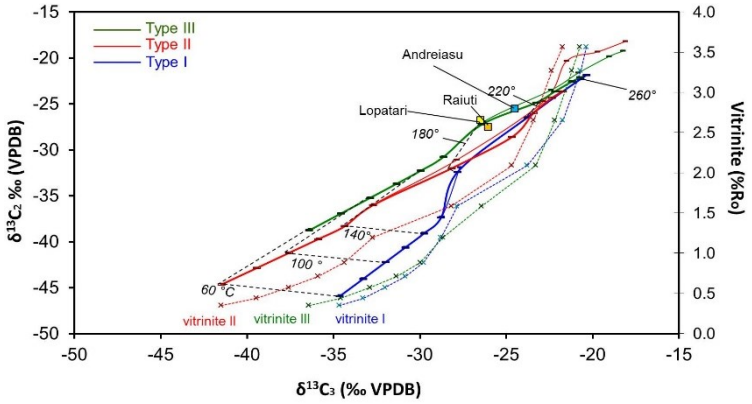

Figure 38 Thermogenic gas formation modelling from marine (Type I. and II) and terrestrial (Type III) kerogen, calculated using GeoIsochem Corp. GOR software 1.94; heating rate of 5°C per million years (Tang et al. 2000, Etiope et al. 2013). Carbon-13 ratio for ethane and propane used, and calibrated for vitrinite reflectance.

The $\delta^{13}C_1$ vs $\delta^{13}C_2$ maturity plot (Fig. 95) generated for Type II and III kerogen with a range of $\delta^{13}C_{ker}$ from -23 to -29 ‰ suggest that Lopatari and Raiuti derive from Type III kerogen. In order to fit the vitrinite values indicated by Popescu (1995; 1.1 to 1.2 $\%R_o$), the $\delta^{13}C_{ker}$ should be between -26‰. Andreiasu and Pausa appears closer to Type II kerogen, and would fit vitrinite 1.1-1.2 $\%R_o$ for $\delta^{13}C_{ker}$ -25

to -24‰. Lepsa clearly derives from lower maturity kerogen and it likely includes a microbial component.

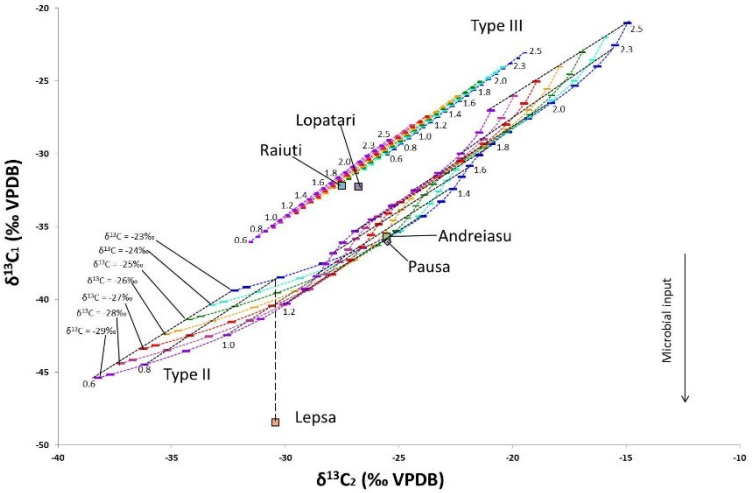

Figure 39 Maturity plot using carbon-13 ratio of ethane vs. methane based on Berner and Farber 1996. Values used for kerogen carbon isotopic ratio between -23 to -29 ‰, for type II and III kerogen.

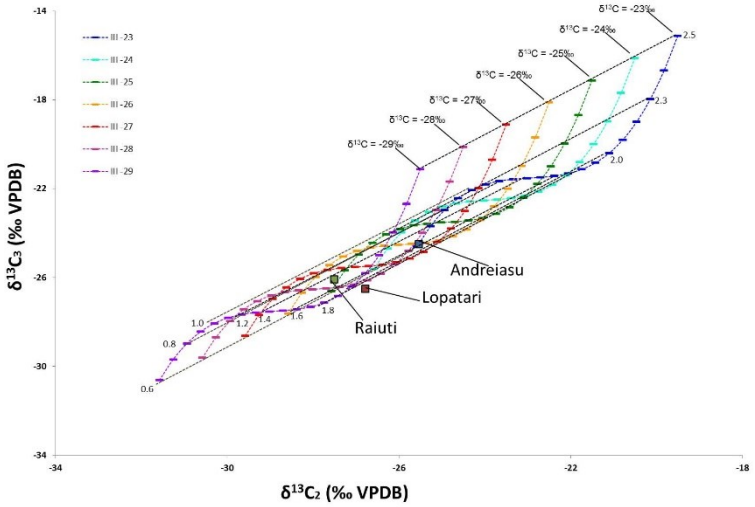

Figure 40 Maturity plot using carbon-13 ratio of ethane vs. propane based on Berner and Farber 1996. Values used for kerogen carbon isotopic ratio between -23 to -29‰, for type III kerogen.

The $\delta^{13}C_2$ vs $\delta^{13}C_3$ maturity plot (Fig. 96), less effective in distinguish the kerogen types, suggest, that Lopatari, Raiuti and Andreiasu have a higher vitrinite between 1.4 to 1.6 $\%R_o$ for $\delta^{13}C_{ker} = -28‰$.

Berner-Faber (using the Kotarba- and Popescu-data) and GOR-model are consistent in order of magnitude, and both indicate that the Lopatari and Raiuti gases are of type III kerogen. While Andreiasu and Pausa are of type II/III, and Lepsa is of low maturity type II kerogen.

In conclusion we can say that Lopatari and Raiuti are of type III kerogen, having a maturity of 1.0 to 1.6 $\%R_o$ for $\delta^{13}C_{ker}$ -26‰ (Fig. 95) and 1.4 to1.6 $\%R_o$ for

$\delta^{13}C_{ker}$ -28‰ (Fig. 96). The Andreiasu gas is more uncertain, being probably a mix between type II/III of higher maturity; for the Popescu (1995) R_o data it would have a $\delta^{13}C_{ker}$ of -25 to -24‰ for type II, or a type III with a maturity of 1.4 to 1.6 %Ro, and an initial $\delta^{13}C_{ker}$ of -28. Lepsa, is a type II (excluding the type I probability, based on Popescu 1995), of lower maturity, and it is probably mixed with microbial gas. The Lepsa seep is more distant geographically from the others, and it is a more internal seep of the Carpathian Paleogene petroleum system. Pausa on first impression resembles Andreiasu in isotopic composition, but further data are needed to better understand its origin.

The above mentioned conclusions are only of hypothetical assumptions, based on the present scientific literature. In order to better understand source rocks of the seeping gases, direct measurements of $\delta^{13}C_{ker}$ of Dysidile formations are needed in Romania, which would help deciphering the actual source rocks of the seeping gases.

3.4.5.2. *Post-genetic processes*

Three specific post-genetic processes are evaluated in the analysed gas samples:

(a) the molecular fractionation (loss of C_2-C_3 during gas migration to the surface);
(b) biodegradation followed by secondary methanogenesis (typically indicated by positive $\delta^{13}C$-CO_2 values). Both processes (a) and (b) are briefly explained in the theoretical part of the thesis.
(c) Addition or enrichment of non-hydrocarbon gases, such as N_2 and He.

3.4.5.2.1. Molecular fractionation

Figure 97 shows a diagram of the macro-flux vs. the Bernard-ratio for the thermogenic gases. The plot as described by Etiope et al. 2011c shows that the Romanian data are consistent with the following hypothesis: the higher the gas flux the lower the molecular fractionation of the gas (higher the amounts of C_{2+} seeping to the surface together with C_1). Also the Bernard ratio can increase if biodegradation is present. This is why Lepsa is further away from the other everlasting fires.

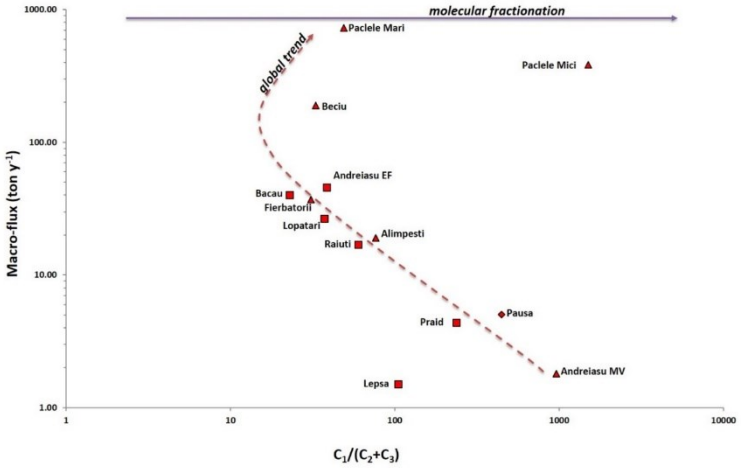

Figure 41 Diagram of macro-flux vs. Bernard-ratio ($C_1/(C_2+C_3)$) for the Romanian seeps., after Etiope et al. 2011. Dashed line represent the origin of methane: green – microbial origin, red – thermogenic origin, blue – mixing between thermogenic and microbial, violet – Homorod special case.

It can be observed that: Paclele Mici appears farther away from the global trend due to the high molecular fractionation; Andreiasu MV is different from the eternal flame because of the lower flux and higher molecular fractionation; Praid and

Pausa are roughly in the same “area” both being over-mature gases; Lepsa shifts away from the main cluster being biodegraded.

3.4.5.2.2. Biodegradation and secondary methanogenesis

Figure 98 represents the relation of $\delta^{13}C\text{-}CO_2$ vs. C_{CO2}. Samples from Pausa, Homorod 4a, 4c show a classic CO_2 origin related to decarboxylation, that is the main, typical origin of CO_2 in petroleum systems. Samples from Andreiasu, Raiuti and Lepsa show positive $\delta^{13}C\text{-}CO_2$ values, suggesting biodegradation of hydrocarbons, typically occurring in shallow reservoirs. Biodegradation is generally followed by secondary microbial methane (the reason for the ^{13}C enriched CO_2) that however has not the typical $\delta^{13}C\text{-}CH_4$ values of microbial gas. Secondary microbial methane has an isotopic character similar to thermogenic methane, as discussed by Brown (2011), so it cannot be distinguished from primary thermogenic methane.

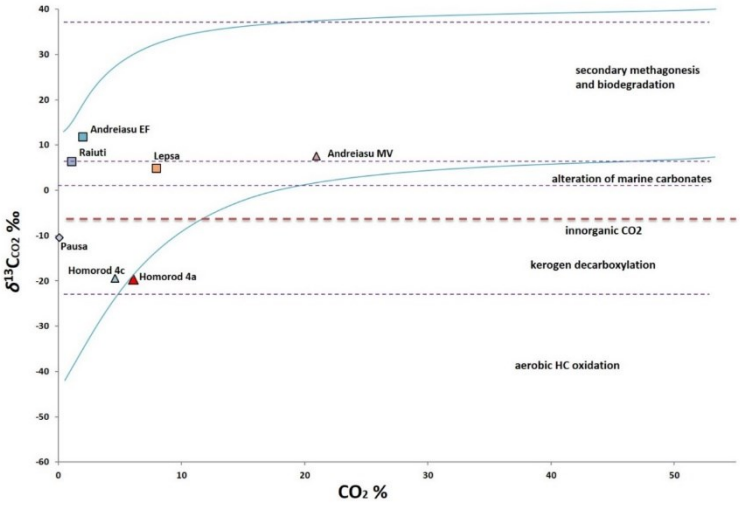

Figure 42 Plot for the relationship of $\delta^{13}C$ of CO_2 and CO_2 concentration. Classification of sources after Jenden et al. 1993. Curves are mixing lines of possible end-members after Jeffrey et al. 1991.

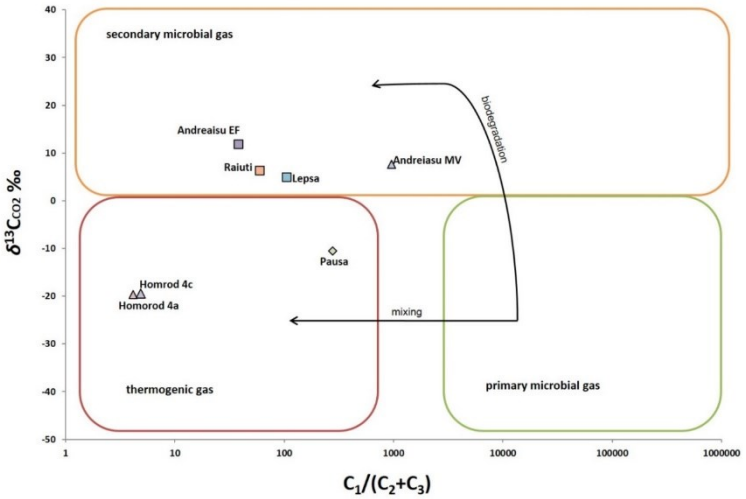

Figure 43 $\delta^{13}C$ of CO_2 vs. dryness $C_1/(C_2+C_3)$. Genetic fields after Milkov 2011

We also plotted the $\delta^{13}C$-CO_2 vs. Bernard ratio, after Milkov 2011. We can observe that again the methane from the Homorod samples and of Pausa are of thermogenic origin, while Andreiasu, Raiuti and Lepsa seeps have input from secondary microbial methane.

The so called natural gas plot or the Chung plot was plotted to evaluate the degree of biodegradation. We could do this for only 3 fires (Andreiasu, Raiuti and Lopatari). We know that based on other plots Andreiasu and Raiuti have a very high positive value for $\delta^{13}C$-CO_2. The shift due to biodegradation effect is very small, almost not visible. The positive $\delta^{13}C$-CO_2 values could be due to biodegradation or to secondary migration of the gases (from the primary to a secondary reservoir).

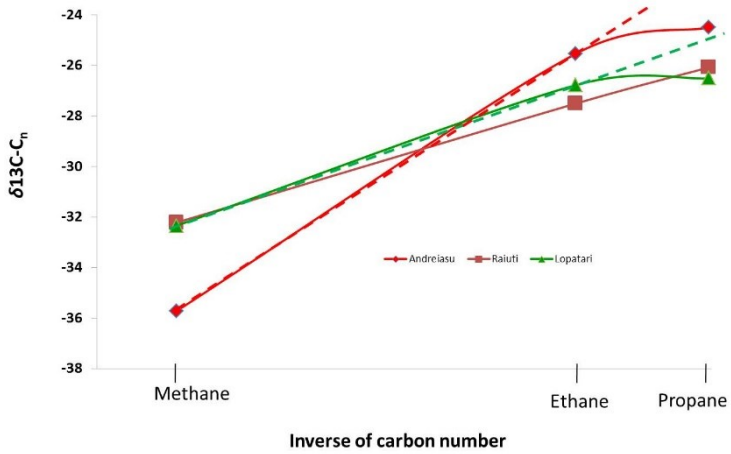

Figure 44 Natural gas plot (Chung-model) after Chung et al. 1988, with methane, ethane and propane isotopic data for 3 "eternal flames".

3.4.5.3. Presence of helium and nitrogen

The following map shows the concentration of helium in the free gases from the different seeps in Romania. The highest concentrations were found at was measured at the Mehadica geothermal springs by Mastan 1987 (2.22%). Also high values are found at Homorod (1.44%), followed by the Herculane gas-bearing springs (0.69% to 1.36%) and Praid seep (0.45%). The other seeps have very low concentrations of helium (<0.06%).

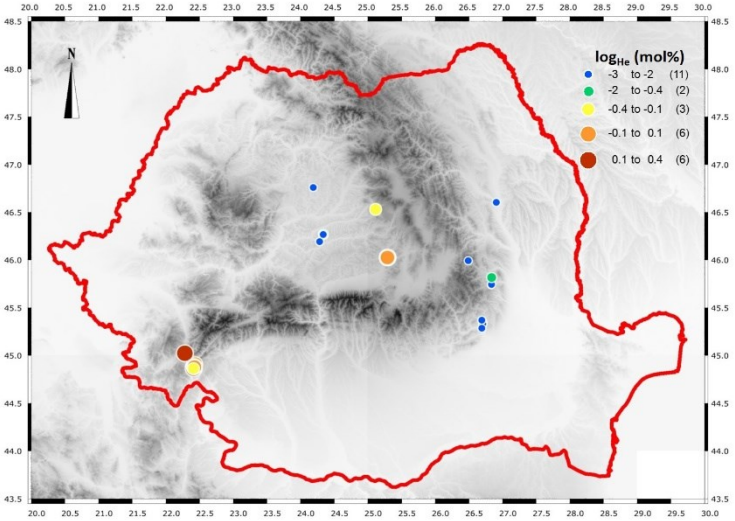

Figure 45 Dot-plot for the helium concentration in free-gas from Romanian seeps. The legend the values are in values in brackets represent the number of seeps in each category.

For the Homorod and the Deleni samples we plotted the $\delta^{15}N$ vs. N_2 concentration relationship, to understand the origin of nitrogen, following the genetic zonation of Zhu et al. (2000). In both seeps N_2 origin is not unequivocal: it can be from atmosphere, crust or mantle. While atmospheric source is more plausible for the Transylvanian microbial gas of Deleni, deep crust or mantle source are possible for Homorod that is close to a Neogene volcanic system, seems to have a deep crust or mantle origin

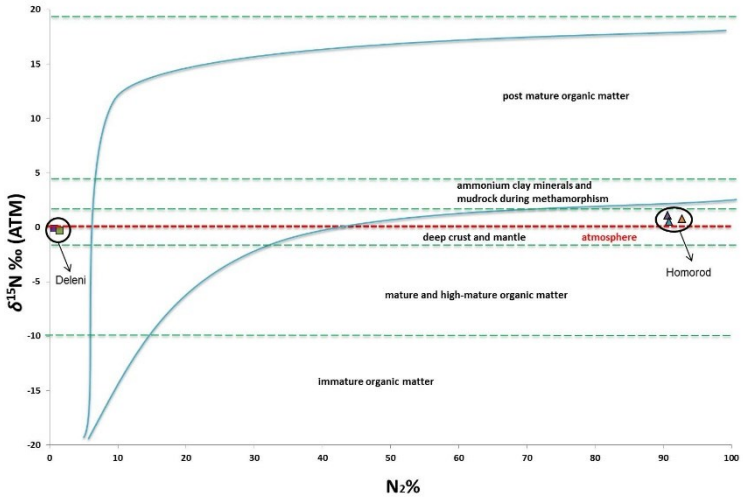

Figure 46 Plot for the relationship of $\delta^{15}N$ and N_2 concentration. Classification of sources after Zhu et al. 2000. Curves are mixing lines of possible end-members modified after Jenden et al. 1988.

3.4.5.4. Distribution of isotopic ratios in the free gases

By creating a dot-plot map for the isotopic composition of the methane for carbon-13 ($\delta^{13}C$) but also for deuterium ($\delta^{2}H$) we can clearly differentiate the regions which are more enriched or depleted regarding there isotopic abundance in the case of methane. For this we used data from other sites as well. Based on the article of Etiope et al. 2011a, we made a correction regarding the values of the Homorod gases, we taken into consideration the original values, estimated by Etiope et al. using Raigley-fractionation model.

For $\delta^{13}C$-CH_4 the most enriched values can be found at: Sacelu-Ochi, Pausa, Praid, Homord (original value) and the "eternal" fires from the Carpathians. Depleted values are present in the microbial areas, but also at Paclele, Lepsa and Alimpesti. More depleted deuterium isotopic ratios are present in the Transylvanian Basin, but also at Lepsa (being the most depleted in deuterium, -228‰). More enriched values are present in the Foredeep (Andreaisu, Lopatari and Pausa), while the Paclele gases are more depleted in deuterium in comparison to the fires.

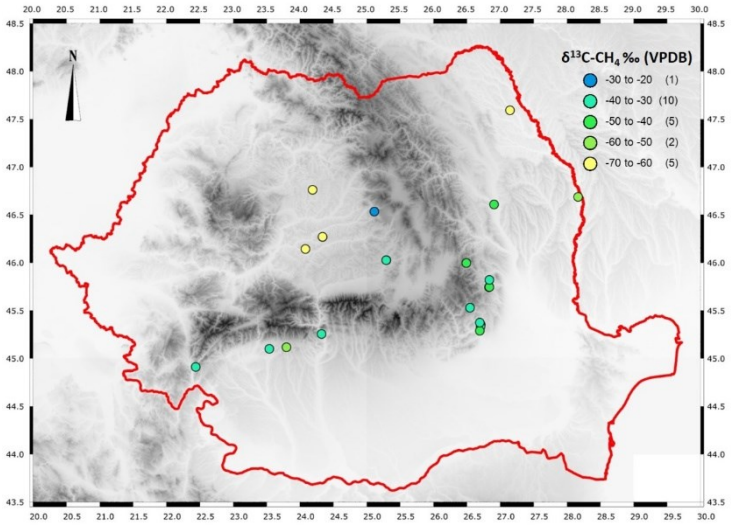

Figure 47 Dot-plot for the $\delta^{13}C$ (‰, VPDB) of methane in free-gas samples from Romania.

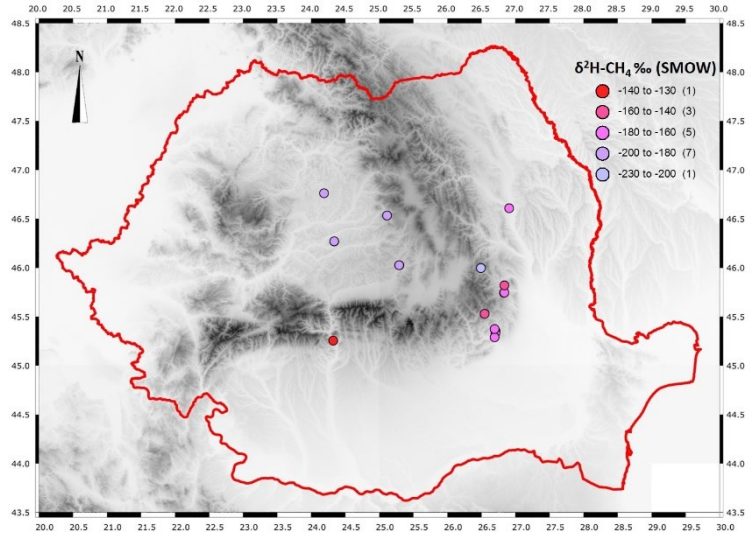

Figure 48 Dot-plot for the hydrogen isotope composition (δ^2H, ‰ VSMOW) in methane in free-gas samples from Romania.

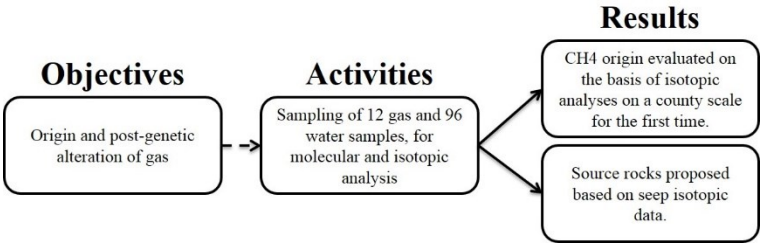

3.4.6. Dissolved methane and other light hydrocarbon in springs

In addition to gas seeps and mud volcanoes, 100 water springs have been investigated in order to verify if they carry significant amounts of methane, and those thus they may be considered as seeping systems (gas-bearing springs according to Etiope 2015).

From the total of 100 springs investigated, we collected a total of 96 water samples. Molecular analyses of the dissolved gases were performed for all 96 waters amples. The dissolved gases were extracted using the methodology described in the previous chapters. The following table summarizes the raw data of the analysis.

Based on these raw data we calculated the dissolved concentrations of light hydrocarbons, from methane until propane for some samples. From samples where we have multiple techniques, we used the data from the FTIR or the WestSystem portable detector from INGV facility.

Very high values, exceeding 10000 γg CH_4/L were measured in: Olanesti 3 (11820.33 µg/L), Hlipiceni (12771.53 µg/L) and Slanic-Moldova 2 (16359.72 µg/L). For the dot-plot we also used data from Kis 2013.

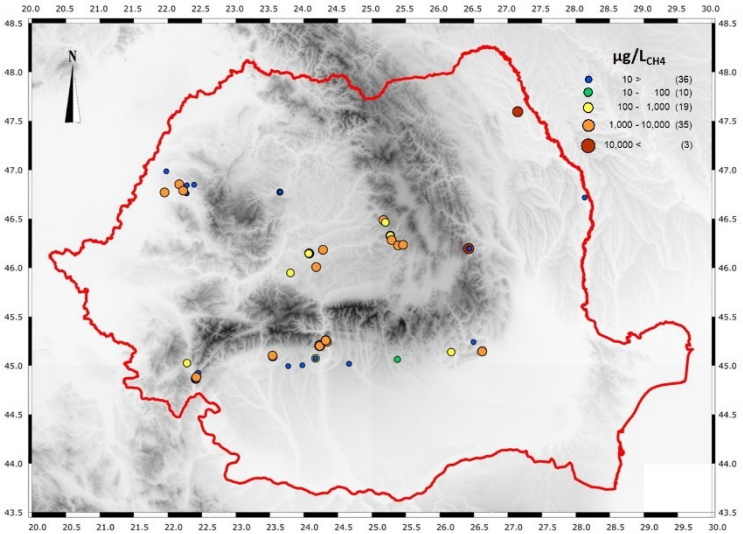

Figure 49 Dot-plot for the order of magnitude of dissolved methane concentrations for the Romanian investigated gas-bearing springs. In the legend the values are in µg CH_4 / L logarithmic scale, values in brackets represent the number of seeps in each category.

Ethane was detected in the 30 samples, ranging between 1.67 – 62.56 µg/L. The highest values can be found in Cozia, Decebal, Venera 2 and Neptun II.

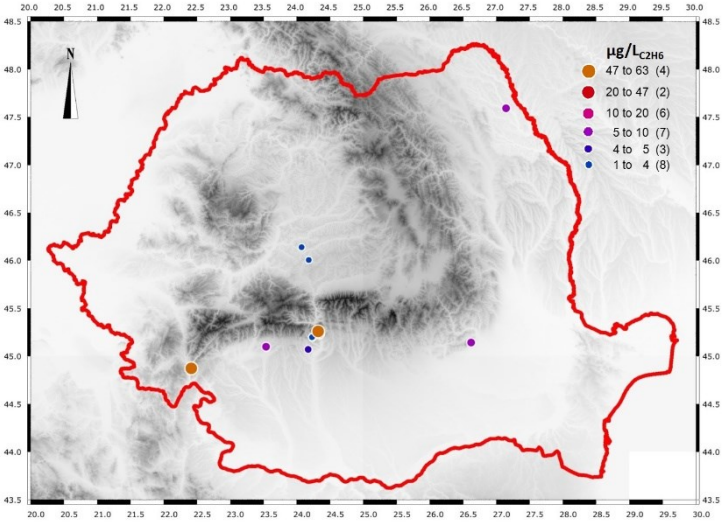

Figure 50 Dot-plot for the dissolved ethane concentrations for the Romanian investigated gas-bearing springs. In the legend the values are in µg CH_4 / L logarithmic scale, values in brackets represent the number of seeps in each category.

If we compare the data of the dissolved methane concentration in groundwater in petroleum systems in the USA (Warner et al. 2013, Molofsky et al. 2013), it appears that Romanian springs have generally high CH_4 concentrations. The average value of the data reported by Warner et al. 2013 is 0.9 µg CH4 /L. In the Molofsky dataset (1701 water samples) 3.4% of the samples contain over 7000 µg/L of methane. In the Romanian samples 35% have values below 1000 µg/L, 18% have values between 1000-5000 µg/L and 3.5% have values above 10000 µg/L.

3.4.6.1. Isotopic composition of dissolved gases

Table 29 summarizes all the available data for the $\delta^{13}C\text{-}CH_4$ composition of the dissolved methane in the spring waters.

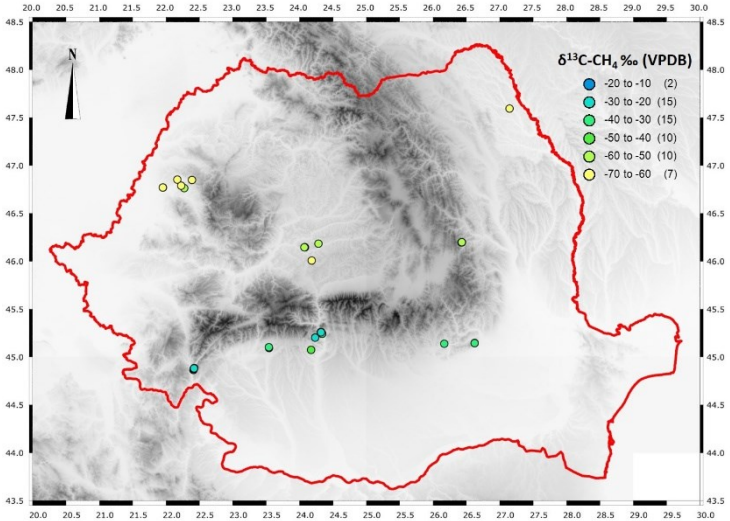

Figure 51 Dot-plot for the $\delta^{13}C$ (‰, VPDB) from dissolved methane in gas-bearing springs.

From the figure it can be observed that in the Foredeep and the Caciulata-Calimanesti geothermal area we have more enriched values $\delta^{13}C\text{-}CH_4$. The rest of the areas are more depleted in $\delta^{13}C\text{-}CH_4$. We can clearly see four areas with much depleted values. These are: the samples from the Transylvanian Plain, Slanic-Moldova, a few samples from Sarata-Monteoru and the Caciulata samples. The highest enriched values can be found at Diana III spring ($\delta^{13}C\text{-}CH_4$ = -18.1‰) and

in Calimanesti 7 ($\delta^{13}C\text{-}CH_4$ = -16.9‰), while the highest depleted values can be found in Damis ($\delta^{13}C\text{-}CH_4$ = -66.1‰) and Hlipiceni ($\delta^{13}C\text{-}CH_4$ = -67.8‰).

3.4.6.2. Origin of dissolved hydrocarbons

In order to evaluate the origin of the dissolved gases we used several interpretive techniques. First we added all the available carbon isotopic values in a Bernard-diagram, developed by Bernard et al. (Figure 108).

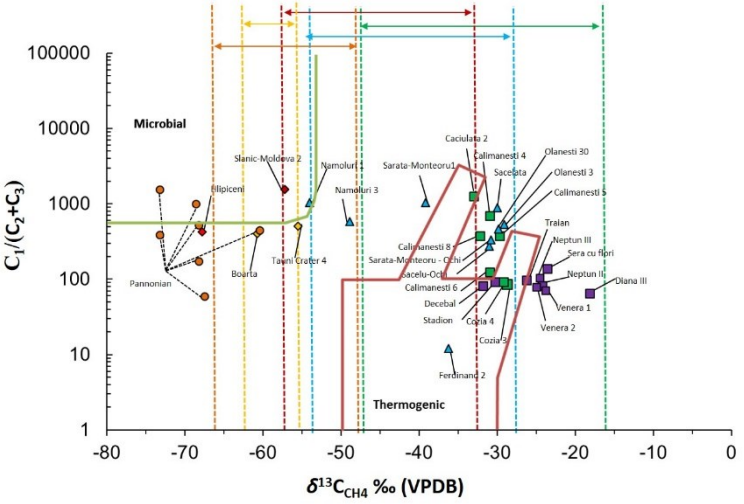

Figure 52 Bernard-diagram for water samples. Dashed lines represent range of carbon-13 from methane: green – Caciulata-Calimanesti, blue – Foredeep, red – Slanic-Moldova, yellow – Transylvania, orange – Pannonian basin (Rowland et al. 2011)

We can see from the following Bernard-diagram for the water samples that the Tauni Crater 4 and Boarta samples are of microbial origin, which is common for the Transylvanian basin. The dashed yellow lines indicate the isotopic range of the Transylvanian samples, but for which we couldn't calculate the Bernard-ratio

($C_1/(C_2+C_3)$). The values of $\delta^{13}C$ vary between -56 and -63‰. Also pure microbial are the Hlipiceni sample and the Slanic-Moldova 2 sample. The other Slanic-Moldova $\delta^{13}C$ values have a range between -32 and -57‰.

The Carpathian Foredeep dissolved gases have $\delta^{13}C$-CH_4 ranging from -54 to -28‰. The Ferdinand sample contains pure thermogenic of origin. While the origin of the Sacelu-Gorj and the Olanesti samples are clustered in a very narrow range.

The Caciulata-Calimanesti samples have δ13C values between -47 and -17‰. They appear to be mainly thermogenic of origin. Two clusters can be observed a more fractioned, similar to the Sacelu-Gorj samples and a second one, less fractioned, resembling the Herculane samples. The Herculane samples Bernard-ratio is almost identical, only with slight variations.

The data reported by Rowland et al. 2011 show, that the dissolved gases from the Romanian part of the Pannonian Basin, have a wide range of $\delta^{13}C$ values between -98 and -32‰. Based on the isotopic analysis the majority of the gases are of microbial origin, possibly having some small amount of thermogenic gas, due to the Pannonian Basin being a petroliferous but also a geothermal area.

The δ^2H of methane was analysed for 8 samples: Calimanesti 5, Cozia 4, Decebal, Neptun II and III, Pausa, Sacelu-Ochi and Sacelata. The most enriched values are found for the Neptun samples (δD = -68 – -92‰). By plotting the data in a Schoell-diagram, we can observe, that the Sacelata sample is found in the thermogenic with condensate range, while the Sacelu-Ochi sample is outside the

typical thermogenic range. The other samples can be found in the thermogenic dry area, except Neptun II which is outside the thermogenic range. We know that in the Schoell-plot the abiotic and the thermogenic range overalp each other slightly. Based on this we would say that the Sacelu-Ochi and Neptun II gases could be of possible abiotic origin.

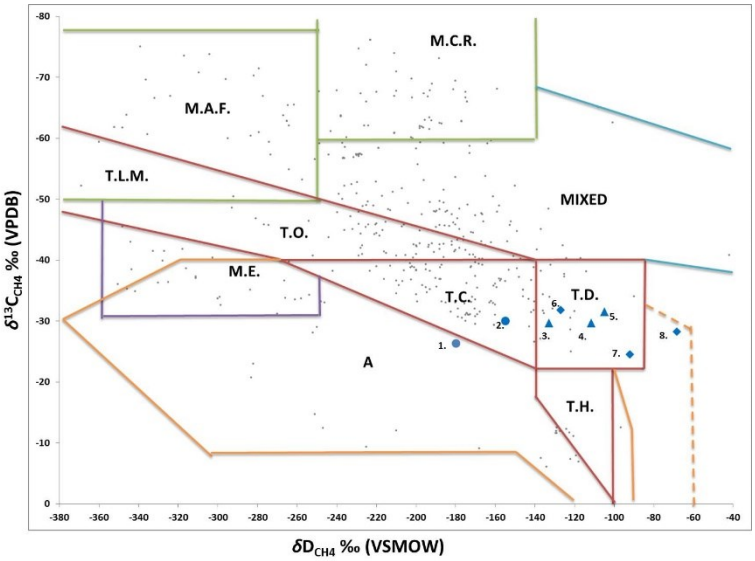

Figure 53 Schoell-plot showing the isotopic composition of methane in the sampled springs. Numbers represent: 1 – Ochi spring, 2 – Sacelata spring, 3 – Calimanesti 5, 4 – Pausa, 5 – Cozia, 6 – Decebal, 7 – Neptun III, 8 – Neptun II.

Again by plotting the data in the updated-Schoell plot (Whiticar & Etiope 2014), it can be observed that: Sacelu-Ochi appears in the volcanic-geothermal region, and the Neptun samples are outside the typical biotic range. Neptun II is closer to the volcanic-geothermal gases. By knowing the geological background of the spring areas, and also the isotopic values, it is possible that the gases are of mixed

origin. The ones being in the biotic range having a predominant biotic origin (thermogenic), while those outside the biotic range having various mixing ratios between biotic/abiotic gases.

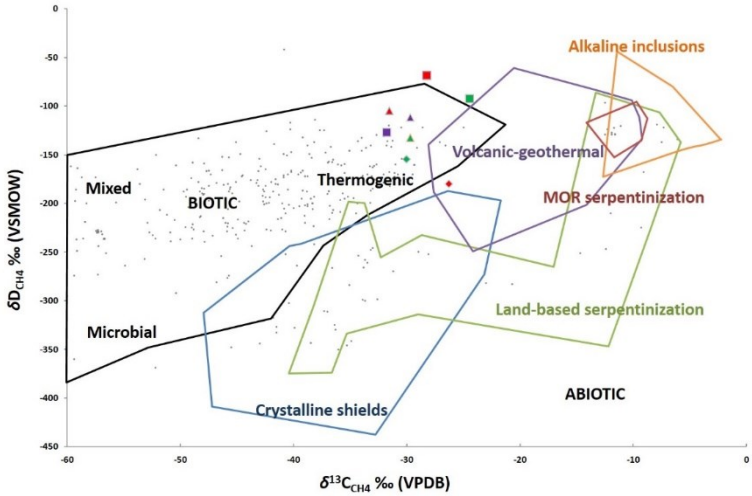

Figure 54 Updated Schoell-plot with investigated water samples: red diamond – Ochi; green diamond – Sacelat; green triangle – Calimanesti 5; violet triangle – Pausa; red triangle – Cozia 3; violet square – Decebal; green square – Neptun III; red square – Neptun II.

In the Herculane geothermal springs (having the most radioactive waters from Romania), an interesting geochemical systems is found. Based on the isotopic data the gases could be a mix between thermogenic/abiotic methane. Also in the area based on Mastan et al. 1981, 1982 the springs release also high concentrations of methane in the free gases emanating from the springs. Not only methane is abundant in these springs but also helium (average 1.1 %, Mastan 1987), the springs being

comparable to the extreme case of the Homorod mud volcano. The methane found in the Herculane gas-bearing springs, could have o geothermal origin (Welhan 1988 and Darling 1998). Further investigation are needed to better understand the link between the radioactivity and gas-geochemistry of the system.

Plotting the isotopic values of $\delta^{13}C\text{-}CH_4$ vs. the dissolved concentration of methane in the water samples, it can be observed that the majority of the samples are found below 2000 µg/L. Taking into consideration the articles of Warner et al. 2013, Molofsky et al. 2013, the background level could be <500 µg/L for the Romanian samples. The samples containing up to 1000 µg/l of methane could be considered as significant amounts of dissolved methane in the samples. Above 1000 µg/L of methane the gas content of the samples can be considered high, and for 3.4% of the samples as extreme concentrations.

For the microbial gases it can be observed that the samples containing very high amounts of methane are close to hydrocarbon reservoirs, or wells. For the thermogenic range the highest amounts of gases have an isotopic range of $\delta^{13}C\text{-}CH_4$ between -30 to -25‰. These gases are of pure thermogenic origin and could be considered as gas-bearing springs (Etiope 2015), which could possibly be linked directly to subsurface hydrocarbon reservoirs.

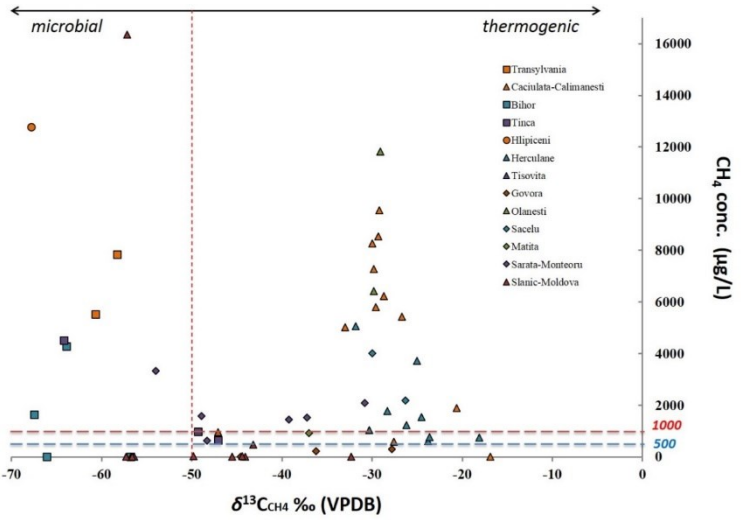

Figure 55 Plot shoving the relationship between CH_4 concentration and $\delta^{13}C$-CH_4 from the investigated springs.

3.4.7. Seeps vs. reservoirs

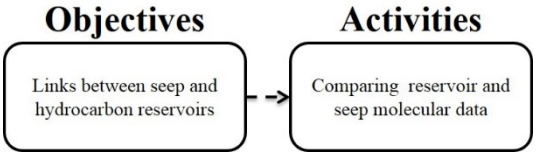

Based on the molecular composition of some reservoirs (for which isotopic data are not available), and on the molecular and isotopic compositions of related seeps we can evaluate the molecular fractionation of gas migration, from the reservoir to the surface, using the Bernard diagram ($C_1/(C_2+C_3)$ vs $\delta^{13}C_1$). Molecular fractionation is a secondary alteration of gas that can lead to misinterpretation of the origin of the gas when it is analysed at the surface or in shallower reservoirs; it is a sort of segregation process or ‘‘chromatographic effect’’ occurring during gas migration to the surface related to differential molecular adsorption on the solid grains of the mud, and differential solubility, so that seeping gas (at surface or trapped in shallower, near surface, pools) is dryer (higher C_1/C_{2+}) than the main, deeper reservoir gas (Etiope et al., 2009a). If this secondary alteration is not evaluated, many cases of dry gas (with relatively low C_{2+} contents) can be misinterpreted and erroneously attributed to microbial origin.

The association seep-reservoir in Romania was determined in 9 sites (Andreiasu, Bacau, Deleni, Praid, Sarmasel, Berca, Herculane, Slanic-Moldova and Govora). The results show that in the case of gas seeps (especially the everlasting fires) there is no appreciable molecular fractionation (the difference of the $C_1/(C_2+C_3)$ ratio between seep and reservoir is within ±100), see figure 115. Significant fractionation ($\Delta(C_1/C_2+C_3) > 100$) occurs for mud volcanoes and spring, see figure 116. In dry seeps the gas ascent mechanism is primarily a single-phase

system and less influenced by water or mud than in the mud volcanoes. We also observed that the molecular fractionation is inversely proportional to the gas flux. A clear example is offered by two seeps, connected to the same reservoir. The first the Deleni seeps: the stronger seep, with higher gas flux (~17 tons/year; Deleni 1) has a lower molecular fractionation value closer to that of the reservoir) respect to the weaker seep (~3 tons/year Deleni 2). This phenomenon was observed also for mud volcanoes: Paclele Mici shows a higher molecular fractionation due to lower flux, than Paclele Mari (~380 compared to ~730 tons/year) see figure 116. Paclele Mici mud volcano has a Bernard ratio resembling microbial gas ($(C_1/C_2+C_3) >1500$), but complete isotopic determination demonstrate its thermogenic origin. Taking into consideration the data from Filipescu & Huma from 1979, we can observe slight change of the molecular fractionation of Paclele Mici and Mari, possibly because of the decrease of the activity of the mud volcanoes over time.

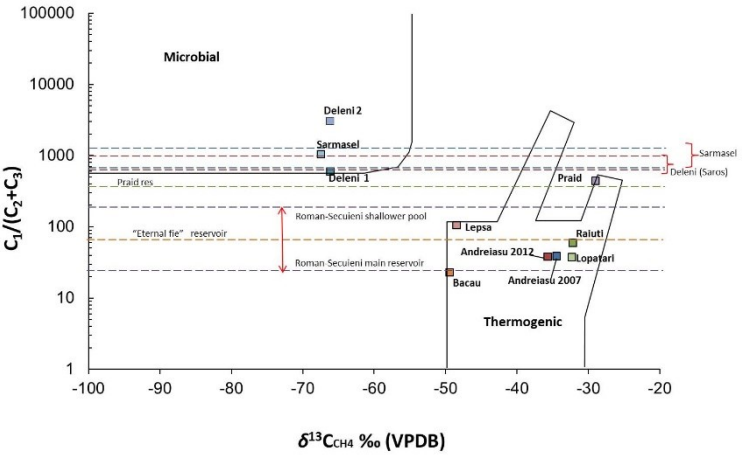

Figure 56 Bernard-diagram showing dry seep vs. reservoir. Reservoirs are shown as horizontal lines since ^{13}C are missing for Romania. Reservoir depth: Sarmasel: -200 until -1440 m; Deleni (Saros): -160 until -2125 m; Praid -2576 m; Romani-Secuieni -310 until -2179 m; "Everlasting" fires reservoir: -3484 until -3496 m. Data from Filipescu and Huma 1979.

In the case of Herculane we can observe that the gas composition is not as much fractionated as the reservoir. One possibility is that the gases could have a different origin than mentioned by Filipescu & Huma, this is why we have a difference between reservoir and the manifestation (seep). Comparing the molecular composition of gas from the Scorillo spring (Mastan et al. 1981, 1982 vs. present data), we can observe that the present data is more fractionated then mentioned in the previous research. This difference could be due to compositional change of the gas in time. If we compare the Herculane reservoir and the Neptun II gases, we observe again that the reservoir gases and the gases in the springs are different, being of different origin. By comparing the present day data with that from Mastan et al. 1981, 1982, we observe that there is almost no significant change in the fractionation of the gases from the Neptun II spring over time. One possibility is that the

"reservoir" mentioned by Filipescu & Huma, is a shallow pool of gas, possibly being produced by the decomposition of organic material from the shallow sediments reacting with the geothermal fluids.

The seep vs. reservoir characterization is also very good for finding the feeding reservoir of the seeps. A good example is the Bacau seep, where the reservoir is composed of a main deeper reservoir, and a few shallow pools (Filipescu and Huma 1979). In this instance the seeps is feed by the main reservoir because the Bernard-ratio is almost the same in the case of the seep/reservoir.

The Ferdinand 2 spring gas is very similar to the Govora deeper reservoir. There is a slight fractionation difference, being possibly caused by oxidation of the gases. The Ferdinand 2 spring is again a very good example of evaluating the "feeder" reservoir.

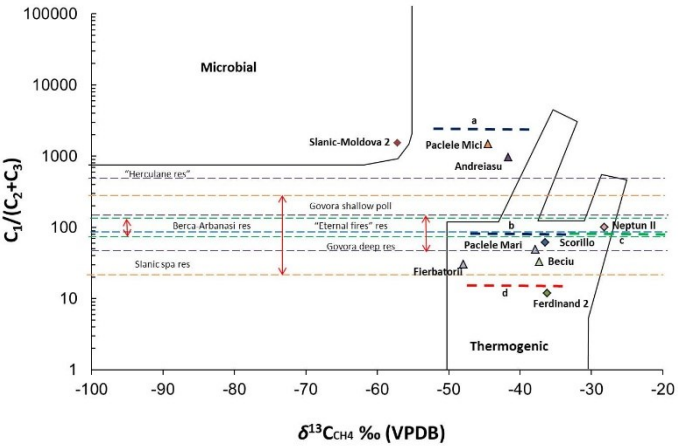

Figure 57 Bernard-diagram showing wet seeps vs. reservoir. Reservoirs are shown as horizontal lines. Reservoir depth for Berca-Arbanasi: -2601 until -3331 m; Herculane reservoir data between -298.6 m until -465 m; Slanic spa data between -1232 until -1288 m; Govora resrevoor between -2813 until -4488m. Line "a" represent the composition of Paclele Mici and line "b" Paclele Mari composition according to Filipescu & Huma 1979. Line "c" represents the composition of Neptun composition and line "d" the Scorillo spring, according to Mastan et al. 1981.

For the everlasting fires from the Carpathians Andreiasu, Raiuti and Lopatari are very similar, indicating that the 3 seeps coul be linked to the same reservoir,. We can also see that the Bernard-ration didn't change for the Andreiasu fire between 2007 and 2013. Andreiasu MV has the same source as the fires, but because the migration includes interaction with migrating water and sediments (mud volcanism), a higher fractionation takes places. This is normal for mud volcanoes, having a higher molecular fractionation than the reservoirs, as indicated in Etiope et al. 2009a. If not evaluated correctly this mud volcano could be considered microbial. Similar ''false'' microbial identifications may occur in other mud volcanoes and weak seeps, as well as in shallow gas reservoirs which are produced by slow

accumulation of gas migrating from a main deeper reservoir. High flux gas seeps are instead the best indicators of reservoir molecular composition, for example Sarmasel and Praid.

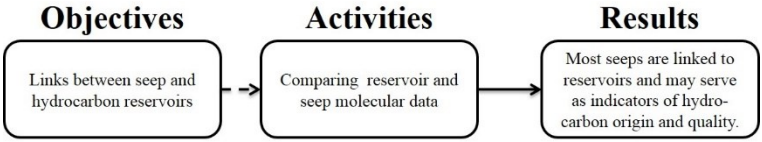

3.4.8. Radiometric measurements of the water samples

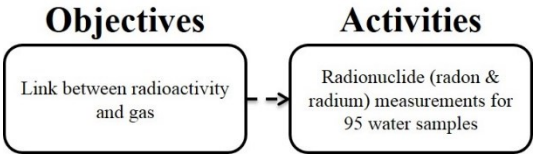

In 2012 a survey was carried out in which methane and radon flux was measured together with radon concentration in soil, from a gas seep found on a hydrocarbon reservoir in Transylvania (Frunzeti et al. 2012b). It was observed that the area of the gas seep close to the main vents had a higher radon flux, and also that radon concentration in the soil increased in correlation to the methane flux.

In order to evaluate a possible link between radioactivity and gas in water, radon and radium activity was also measured. The gases from the springs could act as a carrier gas for the radon; thereby the water could have a higher radon activity then the surrounding waters in the environment

Also in the case of mud volcanoes or gas-bearing spring, there is a possibility that we don't just have a higher radon activity but also a higher radium activity. Radium-226 is a radioactive metal; which can be transported through the solid phase (mud) and the water phase. For the purpose of evaluating, if there is any correlation between the radon/radium activity and hydrocarbon emissions, we performed a total of 95 water sample measurements, for determining radon and radium activity. Two water samples are from the Tisovita ophiolite.

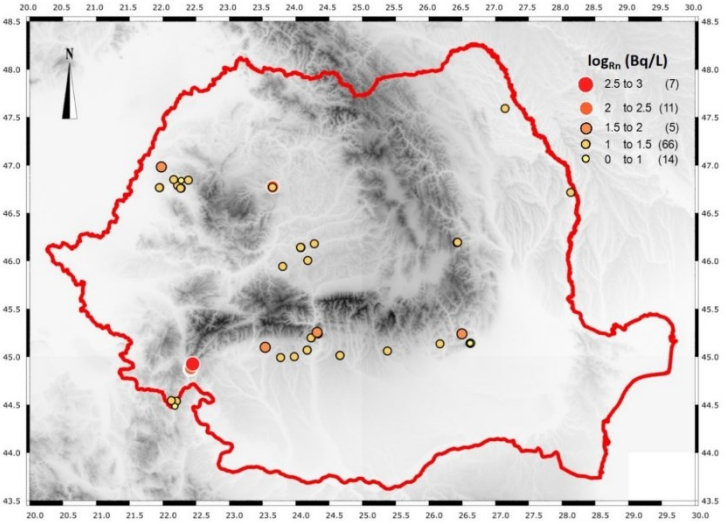

Figure 58 Dot-plot for the radon activity for the investigated springs. In the legend the values are in Bq/L logarithmic scale, values in brackets represent the number of seeps in each category.

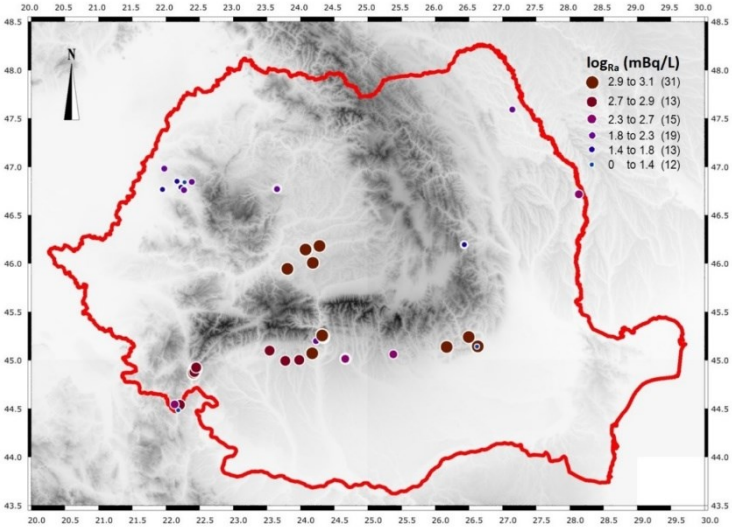

Figure 59 Dot-plot for the radium activity for the investigated springs. The legend the values are in mBq/L logarithmic scale, values in brackets represent the number of seeps in each category.

The dot-plot map for the radon activity, it can be observed that Herculane area has the highest radon activity of the investigated samples. Throughout the whole investigated area we can find smaller values in Sacelu, Caciulata-Calimanesti and Sarata-Monteoru. We have very low activity at Slanic-Moldova, Valcele, Someseni and the Bihor samples. In the case of radium the distribution is a bit more uniform. Two areas can distinguished, a high activity and a low activity area. The high activity is the southern region of the Transylvanian Basin continuing in the Carpathian Foredeep. In the Foredeep we have higher values in Sarata-Moneoru and Herculane. In the Foredeep we have also very low activity areas, like: Valcele, Caciulata-Calimanesti and Sacelu.

Cluster-analysis was performed on the springs, in order to verify if the sites could be categorized based on their radon activity. The cluster-analysis has been performed taking into consideration the Eucledian distances, and for linkage calculation Ward's method was used. It can be observe from figure 119, based on the phenom line (at a linkage distance of 1000), six groups can be observed and a total of 9 subgroups. Based on the tree diagram the majority of samples in each subgroup represent: subgroup A the Bihor samples, B – Slanic-Moldova, C-D-G Herculane samples, E – Sarata-Monteoru and F-H-I – Foredeep.

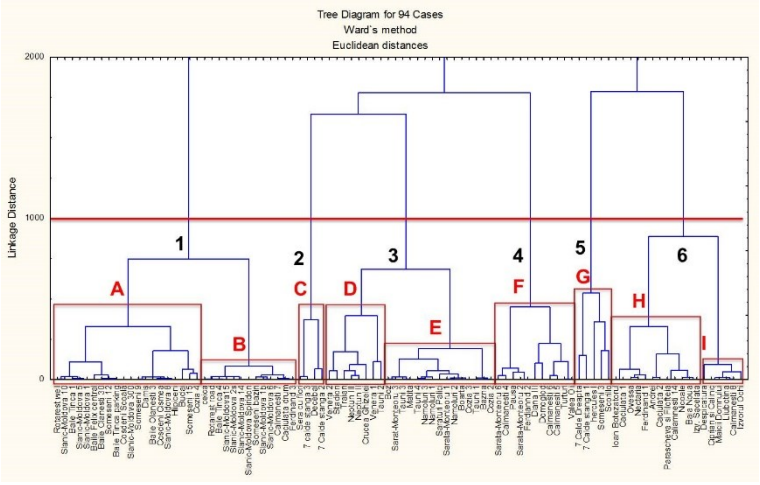

Figure 60 Tree diagram for Cluster-analysis for the radon activity. Groups: A – Bihor, B – Slanic-Moldova, C-D-G Herculane, E – Sarata-Monteoru, F-H-I Foredeep.

Based on the cluster analysis, we observed that the clusters are geological/geographical groups were the springs are found. It can be seen in the above cluster diagram that the Bihor samples contain one group, Slanic-Moldova samples another one, the Herculane samples 3 different group (based on their radon activity), and the Sarata-Monteoru water samples a separate group, while 3

individual groups represent the samples from the Carpathian Foredeep. The Transylvanian samples and the Moldavian samples are scattered in different groups.

No significant correlation was found between the radon and/or radium activity and concentration of dissolved gases.

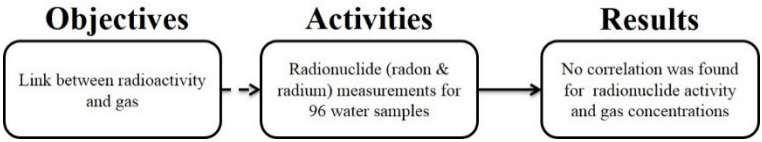

4. CONCLUSIONS

This thesis entitled: "Geogenic methane in petroliferous and geothermal areas in Romania: origin and emission to the atmosphere" had 6 main objectives.

The first objective was to assess the geographical distribution and mapping of the main hydrocarbon seeping areas with GIS. This objective has been performed based on an extensive literature survey but also on direct field investigation and exploration. A total of 141 sites were investigated. The result of the first objective is the HYSED-RO database, which is the first modern database for seepages in Romania. From the HYSED-RO database (609 seeps), the majority, 51% represent mud volcanoes, 21% gas-bearing seeps, 11% oil seeps, 10% gas seeps, 4% solid seeps and the rest of 4% unknown manifestations. The data-base is available here: www.hydrocarbonseepage.blogspot.ro. Further work must be performed for a better elaboration of the database. This would presume evaluating the uncertain seeps from the database, in order to verify if these seeps can be considered as seeps in sensu strictu, and to verify their activity. Some seeps could have disappeared.

The second objective of the thesis was to find possible relationships between the seepage areas and geological features (fault, lithology etc.). This task was performed using geo-spatial analysis following four methods: Fry-analysis, distance distribution, weight-of-evidence analysis and frequency ratio method. Based on the mentioned methods, we observed that on a local scale the occurrence of seeps are controlled by faults (<1 km), while on higher scale the seep occurrences are mainly controlled by folds (anticline axes). In order to verify in more detail the occurrence of seeps, more detailed geological/tectonical maps would be necessary

(lithological, more precise tectonic features, and if possible vertical profiles of the areas).

The third objective of the thesis was to evaluate the geological emissions to the atmosphere of methane, and the associated hydrocarbons (mainly ethane and propane) from the main petroliferous areas, and some selected geothermal provinces in Romania. Flux measurements were carried out on 39 sites. For the emission estimate of methane at country level additional 67 flux values were used from the literature. Following up-scaling procedures adopted in a wide literature, a total of 2.6 Gg methane / year were estimated for the Romanian territory. The geological emission of methane can be considered comparable with some man-made emissions (field burning of agricultural land, industrial processes) in Romania. For a better estimation on a country scale the previously measured seeps should be re-measured, but also the output of new or uncertain sites should be evaluated.

The fourth objective of the thesis was to evaluate the origin and post-genetic alteration of gas. In total 12 gas and 96 water samples were collected for molecular and isotopic analysis. In order to have a country scale view of the gas origin, 25 gas molecular and isotopic and 28 waters sample data (28 molecular and 19 isotopic) from the literature were also used. Based on the molecular and isotopic data the Transylvanian gases are mainly microbial; thermogenic methane can be found at the eastern edge of the Basin close to the Neogenic volcanism. The gases from the Carpathian Orogen are of thermogenic origin. Based on $\delta^{13}C\text{-}CO_2$ Andreiasu, Raiuti and Lepsa eternal flames show indication of biodegradation, probably related to shallow gas reservoirs.

For the first time also some source rocks are proposed for the seep gases, based on isotopic data. Two models were used: the Bernad & Faber model and the GOR model. Based on the two models Lopatarti and Raiuti gases originate from a type III kerogen, having a maturity of 1.0 to 1.6 %Ro for $\delta^{13}C_{ker}$ -26 to -28‰. The Andreiasu gas is more uncertain, being probably a mix between type II/III of higher maturity. Lepsa, is a type II, of lower maturity, and it is probably mixed with microbial gas. Pausa on first impression resembles Andreiasu in isotopic composition.

From the 96 water samples collected, for 3.6% of the samples have values above 10000 µg/L of methane: these can be considered actual expression of seepage (gas-bearing springs). Many other springs have very low CH_4 concentrations, and they should not be considered as seeps (the HYSED-RO database shall be revised in this respect).

The origin of methane in the springs resembles the microbial and thermogenic zonation found in the gas seeps and mud volcanoes. The Herculane gases would need a more detailed gas-geochemical survey in order to better understand the origin of the gases (isotopic analysis of methane), but also the origin of the high helium content of the free gases present in the system.

An interesting observation is that the Transylvanian gases (Sarmasel, Deleni, Tauni) have measurable amount of C_{2+} alkanes, which may imply that the gas is not totally microbial, as generally assumed. The presence of a deeper (thermogenic) petroleum system in Transylvania was, in fact, postulated by Popescu (1995), but it was never demonstrated. We also found some old literature talking about oil seeps in Transilvania. The presence of thermogenic hydrocarbons in deep

rocks in Transylvania would open new energy resource prospective. This aspect deserves further research.

On a country scale the comparison of the hydrocarbon isotopes with those of kerogen would be a new leap on finding the source rock from which the Romanian gases were formed.

This thesis has the largest data-set of methane isotopic values ever reported so far for the Romanian gases: a repository of a total of 123 isotopic values, out of which 74% are from the experimental work of the present thesis.

The fifth objective of the thesis was to investigate the link between surface seepage and hydrocarbon reservoirs. This was done by comparing available data on the reservoirs with those from the seep occurring above the reservoirs.

The comparison of reservoir vs. seep geochemistry suggests that most seeps are linked to reservoirs; gas is coming directly from reservoirs; therefore, many seeps may serve as indicators of subsurface hydrocarbon origin and quality. The association seep-reservoir in Romania was determined in 9 sites (Andreiasu, Bacau, Deleni, Praid, Sarmasel, Berca, Herculane, Slanic-Moldova and Govora). The results show that in the case of gas seeps (especially the everlasting fires, where gas flux is relevant) there is no appreciable molecular fractionation (the seep has the same C_1-C_2-C_3 composition of the reservoir). We also observed that the molecular fractionation (loss of C_2 and C_3 gases during gas migration) is inversely proportional to the gas flux. The seep vs. reservoir characterization is also very useful for finding

the feeding reservoir of the seeps. High flux gas seeps are then the best indicators of reservoir molecular composition (for example Sarmasel and Praid).

Further investigations regarding reservoir and seep geochemistry, should regard the isotopic analysis of gas from wells close to the seeps (as mentioned in Introduction isotopic data are so far available only for seeps).

The sixth objective of the thesis was to verify the eventual correlation between radioactivity and gas (it is known that hydrocarbon related fluids may be more radioactive respect to host rocks or other underground fluids). This part of the thesis was carried out by measuring the radon and radium activity in 98 water samples from different geological settings across Romania. Our measurements show no correlation between radionuclide activity and gas concentrations. The highest value of radon (a few hundred units of Bq/L) was found for the Herculane geothermal spa waters, where radioactivity is likely due to local uranium-rich igneous rocks. Future studies may verify a possible relationship between oil seeps and radioactivity.

The following scheme summarises objectives, activity, the main results and suggested future research, discussed in this thesis.

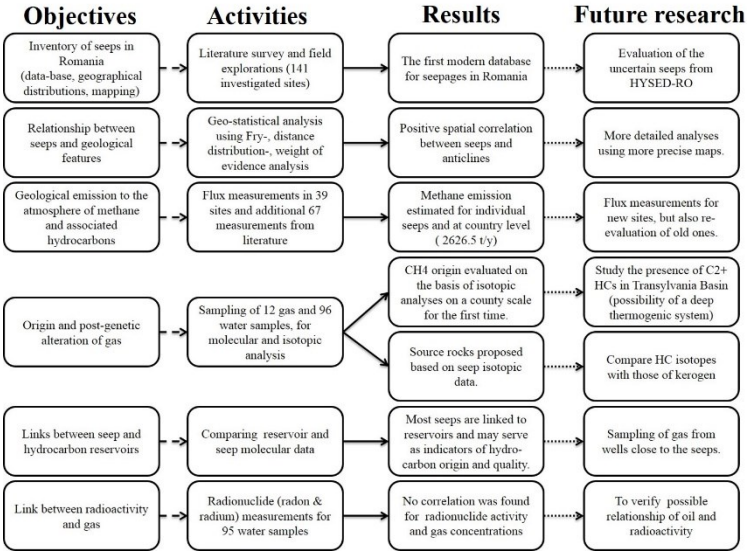

By combining the results acquired, it is possible to draw a general picture of the distribution and origin of natural gas in Romania.

Adding all the $\delta^{13}C$ data into a dot-plot map, we can observe that $\delta^{13}C$ enriched methane occurs in Transylvanian Basin towards the Neogenic Volcanic area, from the Paleogene Flysch towards the inner Foredeep, at the Bihor springs from east towards west (increasing heat flow), and finally from the Foredeep towards the Caciulata-Calimanesti and Sacelu-Gorj geothermal areas. Depletion of $\delta^{13}C$ from methane occurs from the Foredeep towards the Moldavian and Scythian Platforms.

Deuterium in methane is enriched in the Foredeep towards the geothermal areas, while from Paleogene Flysch it gets enriched towards the Inner Foredeep, and

starts to deplete towards the Outer Foredeep. In the Transylvanian Basin the deuterium ratios are stable.

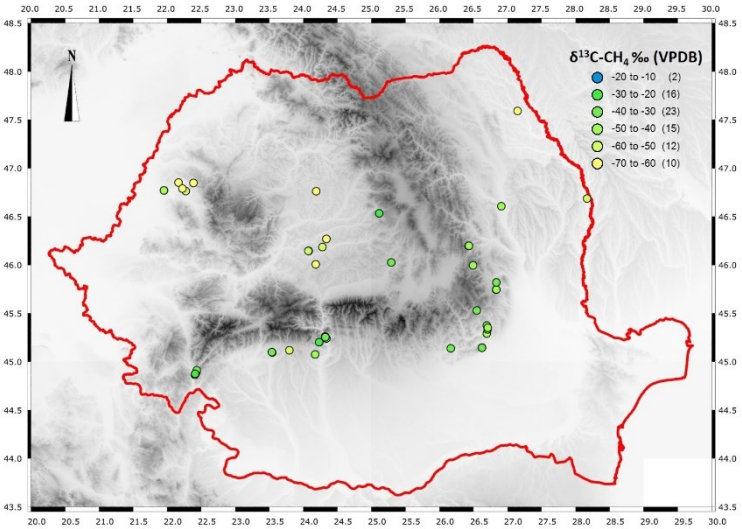

Figure 61 Dot-plot for the $\delta^{13}C$ in methane in all Romanian sampled gases.

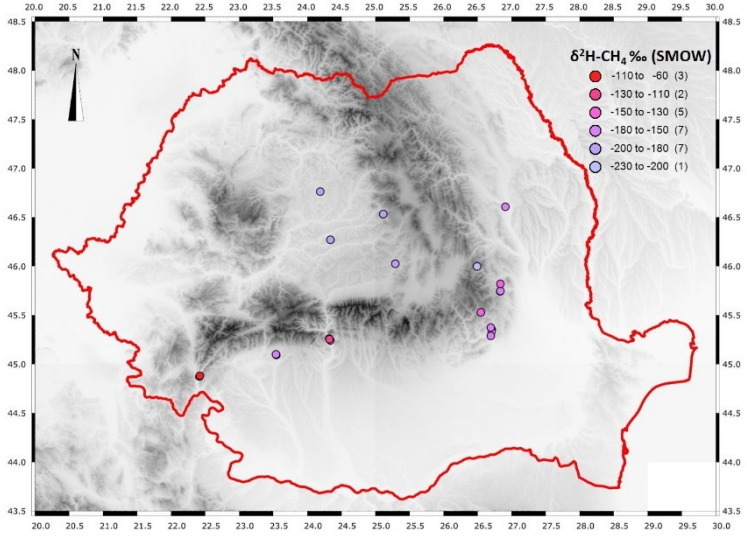

Figure 62 Dot-plot for the δ^2H in methane in all Romanian sampled gases.

The Petroleum Seepage System (PSS) was defined by Abrams 2005, as the interconnection of the sediments, tectonics (the migration paths), the hydrocarbon generation, and surface manifestations of the fluids. Based on the definition of Abrams 2005 and also on the data presented in the thesis, a total of 8 PSS could be defined (for the first time) in Romania. The Transylvanian Basin has two individual PSS: a predominantly microbial (in the western and central basin parts) and a predominantly thermogenic one (along the eastern basin margin). Both systems could be affected by other sources of hydrocarbons. The microbial one (the origin of gas is from a shallow petroleum system) could have minor inputs of thermogenic methane (deep petroleum system). While the thermogenic one may have been affected by the Neogenic Volcanism (example the origin of the Praid gases). In the

Moldavian and Scynthian Platforms we have two smaller PSS, another microbial one, and a southern predominantly thermogenic one.

In the Carpathian Basin, Bacau is a separate PSS, because it is found at the border of the Carpathian Foredeep and Moldavian Platform. The south eastern part of the Carpathian Foredeep contains one PSS, being the area with the highest output of gaseous hydrocarbons, but also the most mature ones. The area of Caciulata-Calimanesti until the Sacelu-Gorj area, and in the Herculane spa area, contains based on the origin, two separate thermogenic PSS. In these areas (Caciulata-Calimanesti, Sacelu-Gorj and Herculane) the gases could be a mix between thermogenic and also of abiotic type of methane (geothermal methane).

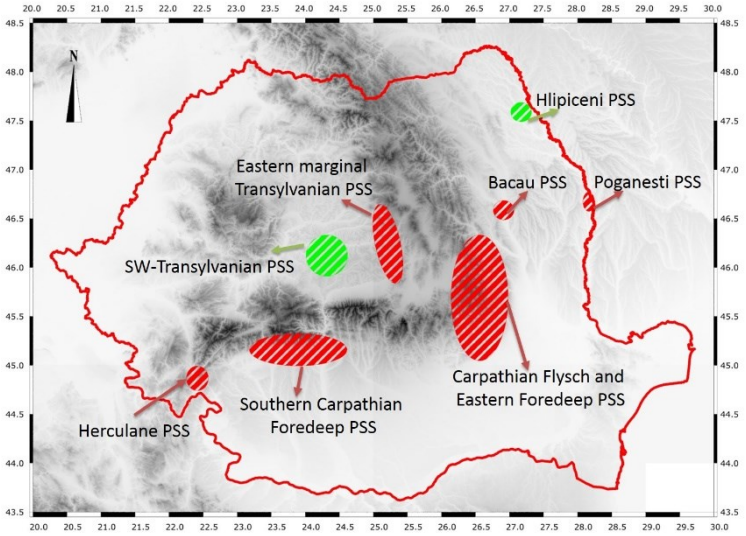

Figure 63 Map showing the eight petroleum seepage systems determined for the Romanian territory. Green areas represent the predominantly microbial, while red the predominantly thermogenic origin.

This is the first time that the seep gases from Romanian, have been evaluated for: origin, source rocks, secondary alteration processes (sources); relationship to tectonics (migration) and for total output of the gases (surface expressions) on a country scale. In other words it is the first time that for Romania the petroleum seepage systems were investigated in a holistic way from source to surface.

SELECTED REFERENCES

Abrams M.A., 2005, Significance of hydrocarbon seepage relative to petroleum generation and entrapment. Marine and Petroleum Geology, 22, 457–477.

Andrae C. J., 1853, Salzen von Reussen bei Hermannstadt und über die geol. Bescchaff enheit des Berges Büdös und seiner Umgenbung, Jahrb.d.k.k.geol. R.A.N, Viena, 169-170 (in german).

Andreescu M., Burst D., Demeterscu C., Ene M., Polonic G., 1989, On the geothermal regime of the Moesian Platform and Getic Depresion. Tectonophysiscs 164, 281-286.

Andrei A.S., Robeson M.S., Baricz A., Coman C., Muntean V., **Ionescu A**., Etiope G., Alexe M., Sicora C.I., Podar M., Banciu H.L., 2015, Contrasting taxonomic stratification of microbial communities in two hypersaline meromictic lakes, The ISME Journal in press.

Baciu C., Caracausi A., Etiope G., Italiano F., 2007, Mud volcanoes and methane seeps in Romania: main features and gas flux, Annals of Geophysics, 50/4, 501-511.

Baciu C., Etiope G., Cuna S., Spulber L., 2008, Methane seepage in an urban development area (Bacau, Romania): origin, extent and hazard. Geofluids 8,311-320.

Baciu C., Frunzeti N., **Ionescu A**., Etiope G., Costin D., Malos C., 2012, Geogenic gas emissions in Romania and their value for tourism, 12th International Multidisciplinary Scientific Geoconference, SGEM 2012, Conference Proceedings, 439-446.

Barbieri G., Cambuli P., 2009. The weight of evidence statistical method in landslide susceptibility mapping of the Rio Pardu Valley (Sardinia, Italy). 18th World IMACS/MODSIM Congress, Cairns, Australia 13–17 July 2009. http:// www.mssanz.org.au/modsim09/G3/barbieri.pdf .

Beca C., Prodan D., 1983, Geologia zacamintelor de hidrocarburi, Editura Didactica si Pedagogica, Bucuresti, 271 pp.

Berman M., 1977, Distance distribution associated with Poisson processes of geometric figures. Journal of Applied Probability, 14, 195-199.

Berman M., 1986, Testing for spatial association between a point process and another stochastic process. Applied Statistics, 35, 54-62.

Bernard B.B., Brooks J.M., Sackett W.M., 1978, Light hydrocarbons in recent Texas continental shelf and slope sediments. J Geophys Res 83, 4053-4061.

Berner U. & Faber E., 1996, Empirical carbon isotope/maturity relationships for gases from algal kerogens and terrigenous organic matter, based on dry, open-system pyrolysis. Org Geochem 24, 947-955.

Bonham-Carter G.F., Agterberg F.P., Wrigh D.F., 1989, Weights of evidence modeling: a new approach to mapping mineral potential. In: Agterberg F.P., Bonham-Carter G.F. (eds) Statistical applications in the earth sciences: Geol. Surv. of Canada, Paper, 89–9, 171-183.

Borcos M., Udubasa G., Sandulescu M., 1983, Harta substantelor minerale utile Republica Socialista Romania, (in Romanian).

BP, 2014, BP statistical review of world energy. http://www.bp.com/en/global/corporate/about-bp/energy-economics/statistical-review-of-world-energy.html , accessed on February 2015

Brown A., 2011, Identification of source carbon for microbial methane in unconventional gas reservoirs. American Association of Petroleum Geologists Bulletin 95, 1321-1338

Carranza E.J.M., 2009, Controls on mineral deposit occurrence inferred from analysis of their spatial pattern and spatial association with geological features. Ore Geology Reviews 35, 383-400.

Chung H.M., Gormly J.R., Squires R.M., 1988, Origin of gases hydrocarbons in subsurface environments: theoretical considerations of carbon isotope distribution. Chemical Geology 71, 97-104.

Cosma C., Moldovan M., Dicu T., Kovacs T., 2008, Radon in Water from Transylvania (Romania), Radiation Measurement 43, 1423-1428.

Darling W.G., 1998, Hydrothermal hydrocarbon gases: 1. Genesis and geothermometry. Applied Geochemsitry 13/7, 815-824.

Delichatsios M.A., 1990, Procedure for calculating the air entrainment into turbulent pool and jet fires. J Fire Prot Engin 2, 93-98.

Demetrescu C. & Andreescu M., 1994, On the thermal regime of some tectonic units in a continental collision environment in Romania. Tectonophysics, 230, 265-276.

Demetrescu C. & Polonic G., 1989, The evolution of the Pannonian Depression (Romanian sector) as derived from subsidence and heat flow data. Tectonophysics 164, 287-299.

Demetrescu C., 1982, Thermal structure of the crust and upper mantle of Romania. Tectonophysics 90, 123-135.

Dirks P.H.G.M & Berger L.R., 2013, Hominin-bearing caves and landscape dynamics in the Cradle of Humankind, South Africa. Journal of African Earth Sciences 78, 109-131.

Dirks P.H.G.M., Mikhailov A., Kuskov A., 2000. DotProc 1.3 Shareware.

Dolton G.L., 2006, Pannonian Basin Province, Central Europe (Province 4808)—Petroleum geology, total petroleum systems, and petroleum resource assessment: U.S. Geological Survey Bulletin 2204–B, 47 p.

Etiope G. & Ciccioli P., 2009, Earth's degassing - a missing ethane and propane source. Science vol. 323, 478

Etiope G. & **Ionescu A**., 2014, Low-temperature catalytic CO_2 hydrogenation with geological quantities of ruthenium: a possible abiotic CH_4 source in chromitite-rich serpentinized rocks. Geofluids, in press

Etiope G. & Klusman R.W., 2002, Geologic emissions of methane to the atmosphere. Chemosphere 49, 777-789

Etiope G. & Klusman R.W., 2010, Microseepage in drylands: flux and implications in the global atmospheric source/sink budget of methane. Glob Plan Change 72, 265-274.

Etiope G. & Schoell M., 2014, Abiotic gas: atypical but not rare. Elements 10, 291-296.

Etiope G. & Sherwood-Lollar B., 2013, Abiotic methane on Earth. Rev Geophys 51, 276-299.

Etiope G., 2015, Natural gas seepage: The Earth's hydrocarbon degassing. Springer International Publishing, 199 p.

Etiope G., Baciu C., Caracausi A., Italiano F., Cosma C., 2004, Gas flux to the atmosphere from mud volcanoes in eastern Romania. Terra Nova 16,179-184.

Etiope G., Baciu C., Schoell M., 2011a, Extreme methane deuterium, nitrogen and helium enrichment in natural gas from the Homorod seep (Romania). Chemical Geology 280, 89-96.

Etiope G., Christodoulou D., Kordella S., Marinaro G., Papatheodorou G., 2013, Offshore and onshore seepage of thermogenic gas at Katakolo Bay (Western Greece). Chemical Geology 339, 115-126.

Etiope G., Feyzullayev A., Baciu C.L., 2009b, Terrestrial methane seeps and mud volcanoes: a global perspective of gas origin. Mar Pet Geol 26, 333-344.

Etiope G., Feyzullayev A., Milkov A.V., Waseda A., Mizobe K., Sun C.H., 2009a, Evidence of subsurface anaerobic biodegradation of hydrocarbons and potential secondary methanogenesis in terrestrial mud volcanoes. Marine and Petroleum Geology 26, 1692-1703.

Etiope G., Martinelli G., 2009, "Pieve Santo Stefano" is not a mud volcano: comment on "Structural controls on a carbon dioxide-driven mud volcano field in the Northern Apennines" (by Bonini 2009). J Struct Geol 31, 1270-1271.

Etiope G., Nakada R., Tanaka K., Yoshida N., 2011c, Gas seepage from Tokamachi mud volcanoes, onshore Niigata Basin (Japan): origin, post-genetic alterations and CH_4-CO_2 fluxes. Appl Geochem 26, 348-359.

Etiope G., Schoell M., Hosgörmez H., 2011b, Abiotic methane flux from the Chimaera seep and Tekirova ophiolites (Turkey): Understanding gas exhalation from low temperature serpentinization and implications for Mars. Earth and Planetary Science Letters 310, 96-104.

Etiope G., Tsikouras B., Kordella S., Ifandi E., Christodoulou D., Papatheodorou G., 2013b, Methane flux and origin in the Othrys ophiolite hyperalkaline springs, Greece. Chem Geol 347, 161-174.

Filipescu, M.N. & Huma I., 1979, Geochimia gazelor naturale, Editura Academiei Republicii Socialiste Romania, 175 pp (in Romanian).

Flory, P. J., 1936, Molecular size distribution in linear condensation polymers, J. Amer. Chem. Soc., 58, 1877-1885.

Formolo M., 2010, The microbial production of methane and other volatile hydrocarbons. In: Kenneth N (ed) Handbook of hydrocarbon and lipid microbiology, Springer, New York. pp 113-126.

Frunzeti N., Baciu C., Etiope G., Pfanz H., 2012a, Geogenic emission of methane and carbon dioxide at Beciu mud volcano (Berca-Arbanasi hydrocarbon-bearing structure, Eastern Carpathians, Romania). Carpathian J Earth Environ Sci 7, 159-166.

Frunzeti N., Moldovan M., **Ionescu A**., Burghele B., Baciu C., Cosma C., Popita G., Stoian L.C., 2012b, Flux measurements of 222Rn and CH4 along with soil gas concentrations (222Rn, CO, NO2 and SO2) over a methane reservoir in Transylvania (Romania). FERAS, abstract.

Fry N., 1979, Random point distribution and strain measurements in rocks. Tectonophysics, 60, 89-105.

Ghosh S. & Carranza E.J.M., 2010, Spatial analysis of mutual fault/fracture and slope controls on rocksliding in Darjeeling Himalaya, India. Geomorphology 122, 1-24

Hosgormez H., Etiope G., Yalçın M.N., 2008, New evidence for a mixed inorganic and organic origin of the Olympic Chimaera fire (Turkey): a large onshore seepage of abiogenic gas. Geofluids 8, 263-275.

Ionescu A., Burrato P., Etiope G., Baciu C., 2014, HYSED-RO: a database of hydrocarbon seeps in Romania. Results from IDEI 2011 project PN-II-ID-PCE-2011-3-0537 "Geogenic emissions of greenhouse gases from geothermal and petroleum systems - Application to Romania".

Jeffrey A.W.A., Alimi H.M., Jenden P.D., 1991, Geochemistry of the Los Angeles Basin oil and gas systems. In: Biddle, K.T. (Ed.), Active Margin Basins. American Association of Petroleum Geologists Memoir, vol. 52, pp. 197-219.

Jenden P.D., Hilton D.R., Kaplan I.R., Craig H., 1993, Abiogenic hydrocarbons and mantle helium in oil and gas fields. In: Howell DG (ed) The future of energy gases (US geological

survey professional paper 1570). United States Government Printing Office, Washington, pp 31-56.

Jenden P.D., Kaplan I.R., Poreda R.J., Craig H., 1988, Origin of nitrogen-rich natural gases in the California Great Valley: Evidence from helium, carbon and nitrogen isotope ratios, Geochimica et Cosmochimica Acta Vol. 52, pp. 85l-861.

Kis B.M., 2013, Hydrogeochemistry of mineral waters from the eastern Carpathians - Transylvanian basin boundary, PhD thesis.

Knapp J.H, Knapp C.C., Raileanu V., Matenco L., Mocanu V., Dinu C., 2005, Crustal constraints on the origin of mantle seismicity in the Vrancea Zone, Romania: The case for active continental lithospheric delamination. Techtonophysics 410, 311-323.

Kotarba M.J., Curtis J.B., Lewan M.D., 2009, Comparison of natural gases accumulated in Oligocene strata with hydrous pyrolysis gases from Menilite Shales of the Polish Outer Carpathians. Organic Geochemistry 40 (2009) 769–783

Krezsek Cs., 2011, Petroleum Systems of Romania. Search and Discovery Article #10349.

Krezsek Cs., Filipescu S., Silye L., Matenco L., Doust H., 2010, Miocene facies associations and sedimentary evolution of the Southern Transylvanian Basin (Romania): Implications for hydrocarbon exploration. Mar. Petrol. Geol., 27, p. 191-214

Mastan I., Znamirovschi V., Cosma C., 1982a, The composition and origin of the emanated gases from Mehadica Valley Geothermal Source, St., Cerc/, Fiz., tom 34, nr 4, 347-350 (English abstract)

Mastan I., Znamirovschi V., Cosma C., 1982b, New data on the composition and origin of the natural gases emanated gases from Cerna valley and Mehadica Valley Geothermal Sources, St., Cerc/, Fiz., tom 34, nr 6, 579-585 (English abstract).

Mastan I., Znamirovschi V., Cosma C., Pop I., 1981, The composition and origin of the emanated gases from Cerna Valley Geothermal Sources, St., Cerc/, Fiz., tom 33, nr 6, 539-555 (English abstact)

Mastan, I. Helium in Geothermal Water Sources; Ph.D. Thesis, University Babes-Bolyai, Cluj-Napoca, Romania, 1987; pp. 34-35 (in Romanian).

McCollom T.M. & Seewald J.S., 2007 Abiotic synthesis of organic compounds in deep-sea hydrothermal environments. Chem Rev 107, 382-401.

McGenity T.J., 2010, Methanogens and Methanogenesis in Hypersaline Environments. Timmis K.N. (ed.), Handbook of Hydrocarbon and Lipid Microbiology

Milkov A.V., 2010, Methanogenic biodegradation of petroleum in the West Siberian Basin (Russia): Significance for formation of giant Cenomanian gas pools. AAPG Bulletin, v. 94, no. 10, pp. 1485-1541.

Milkov A.V., 2011, Worldwide distribution and significance of secondary microbial methane formed during petroleum biodegradation in conventional reservoirs. Org Geochem 42, 184-207

Miller J. B., Mack K. A., Dissly R., White J. W. C, Dlugokencky E. J., Tans P. P., 2002, Development of analytical methods and measurements of 13C/12C in atmospheric CH4 from the NOAA Climate Monitoring and Diagnostics Laboratory Global Air Sampling Network, J. Geophys. Res., 107(D13), 4178, doi:10.1029/2001JD000630.

Moldovan M., Cosma C., Encian I., Dicu T., 2009, Radium-226 concentration in Romanian bottled mineral water, Journal of Radioanalytical and Nuclear Chemistry, 279, p. 487-491.

Molin P., Fubeli G., Nocentini M., Sperini S., Ignat P., Grecu F., Dramis F., 2012, Interaction of mantle dynamics, crustal tectonics, and surface processes in the topography of the Romanian Carpathians: A geomorphological approach. Global and Planetary Change 90-91, 58-72.

Molofsky L.J., Connor J.A., Wylie A.S., Wagner T., Farhat S.K., 2013, Evaluation of methane sources in groundwater in Northeastern Pennsylvania. Groundwater, vol 51, no 3, 333-349

Morner N.A. & Etiope G., 2002, Carbon degassing from the lithosphere. Global Planet Change 33, 185-203.

Oh H.-J., Kim Y.-S., Choi J.-K., Park E., Lee S., 2011, GIS mapping of regional probabilistic groundwater potential in the area of Pohang City, Korea, Journal of Hydrology 399, 158-172.

Paraschiv D., 1984, On the natural degasification of the hydrocarbon-bearing deposits in Romania, An. Inst.Geol. Geofiz., LXIV, 215-220.

Pawlewicz M, 2007, Total Petroleum Systems of the Carpathian–Balkanian Basin Province of Romania and Bulgaria. U.S. Geological Survey Bulletin 2204–F, 17 p

Pawlewicz M., 2005, Transylvanian Composite Total Petroleum System of the Transylvanian Basin Province, Romania, Eastern Europe. U.S. Geological Survey Bulletin 2204–E, 10 p.

Pop C.I., 2014, Emisii geogene de metan in Platforma Moldoveneasca si Bazinul Transilvaniei, Babes-Bolyai University PhD thesis.

Pop C.I., **Ionescu A**., Baciu C., 2015, Methane seepage from geologic sources on the Moldavian Platform (Eastern Romania). Carpathian Journal of Earth and Environmental Sciences, February 2015, Vol. 10, No. 1, 203-210.

Popescu B.M., 1995, Romania's petroleum systems and their remaining potential. Petroleum Geoscience, Vol. 1, 337-350.

Popita G.-E., Frunzeti N., **Ionescu A**., Lazar A.L., Baciu C., Popovici A., Pop C., Faur V.C., Proorocu M., 2014, Evaluation of carbon dioxide and methane emission from Cluj-Napoca municipal landfill, Romania, accepted, Environmental Engineering and Management Journal

Povara I., Simion G., Marin C., 2008, Thermo-mineral waters from the Cerna Valley Basin (Romania), Studia Universitatis Babes-Bolyai, Geologia, 53(2), 41-54

Rowland H.A.L, Omoregie E.O., Millot R., Jimenez C., Mertens J., Baciu C., Hug S.J., Berg M., 2011, Geochemistry and arsenic behavior in groundwater resources of the Pannonian Basin (Hungary and Romania), Applied Geochemistry 26, 1-17.

Salati S., van Ruitenbeek F.J.A., Carranza E.J.M., van der Meer F.D., Tangestani M.H., 2013, Conceptual modeling of onshore hydrocarbon seep occurrence in the Dezful Embayment, SW Iran. Mar. Pet. Geol. 43, 102-120.

Sandulescu M., 1984, Geotectonica Romaniei. Editura Academiei Romane, Bucuresti, 336 pp.

Spulber L., Etiope G., Baciu C., Malos C., Vlad S.N., 2010, Methane emissions from natural gas seeps and mud volcanoes in Transylvania (Romania), Geofluids 10, 463-475.

Spulber L., 2010, Geogenic emissions of methane in Transylvania and theire environmental implications, PhD thesis, Babes-Bolyai University.

Tang Y., Perry J.K., Jenden P.D., Schoell M., 2000, Mathematical modeling of stable carbon isotope ratios in natural gases. Geochim Cosmochim Acta 64, 2673-2687

Taran Y.A., Kliger G.A., Sevastianov V.S., 2007, Carbon isotope effects in the open-system Fischer–Tropsch synthesis. Geochimica et Cosmochimica Acta 71, 4474-4487

Tazaz A.M., Bebout B.M., Kelley C.A., Poole J., Chanton J.P., 2012, Redefining the isotopic boundaries of biogenic methane: Methane from endoevaporites, Icarus, http://dx.doi.org/10.1016/j.icarus.2012.06.008, in press

Thampi K.R., Kiwi J., Gratzel M., 1987, Methanation and photo-methanation of carbon dioxide at room temperature and atmospheric pressure. Nature 327, 506-508.

Uruioc S., Masu S., Sinitean A., Albulescu M., 2012, Mud volcanoes from Banat region (Romania): Their environment impact. Carpathian Journal of Earth and Environmental Sciences, August 2012, Vol. 7, No. 3, p. 145-158.

US EIA, 2013. Technically recoverable shale oil and shale gas resources: an assessment of 137 shale formations in 41 countries outside the United States. US Department of Energy, Washington, 730 p.

USGS, 2002, Map Showing Geology, Oil and Gas Fields, and Geologic Provinces of Europe including Turkey.

Warner N.R., Kresse T.M., Hays P.D., Downa A., Karr J.D., Jackson R.B., Vengosh A., 2013, Geochemical and isotopic variations in shallow groundwater in areas of the Fayetteville Shale development, north-central Arkansas. Appl. Geochem.

Welhan J.A., 1988, Origins of methane in hydrothermal systems. Chemical Geology 71, 183-198.

Whiticar M.J. & Etiope G., 2014, Methane in land-based serpentinized peridotites: new discoveries and isotope surprises. AGU 2014 Fall Meeting Abstracts

Whiticar M.J., 1999, Carbon and hydrogen isotope systematics of bacterial formation and oxidation of methane. Chem Geol 161, 291-314.

Wynn J.G., Sumrall J.B., Onac B.P 2010, Sulfur isotopic composition and the source of dissolved sulphur species in thermos-mineral springs of the Cerna Valley, Romania, chemical geology 271, 31-43.

Zhu Y., Shi B., Fang C., 2000, The isotopic compositions of molecular nitrogen: implications on their origins in natural gas accumulations. Chem Geol 164, 321-330.